CHALMERS
UNIVERSITY OF TECHNOLOGY

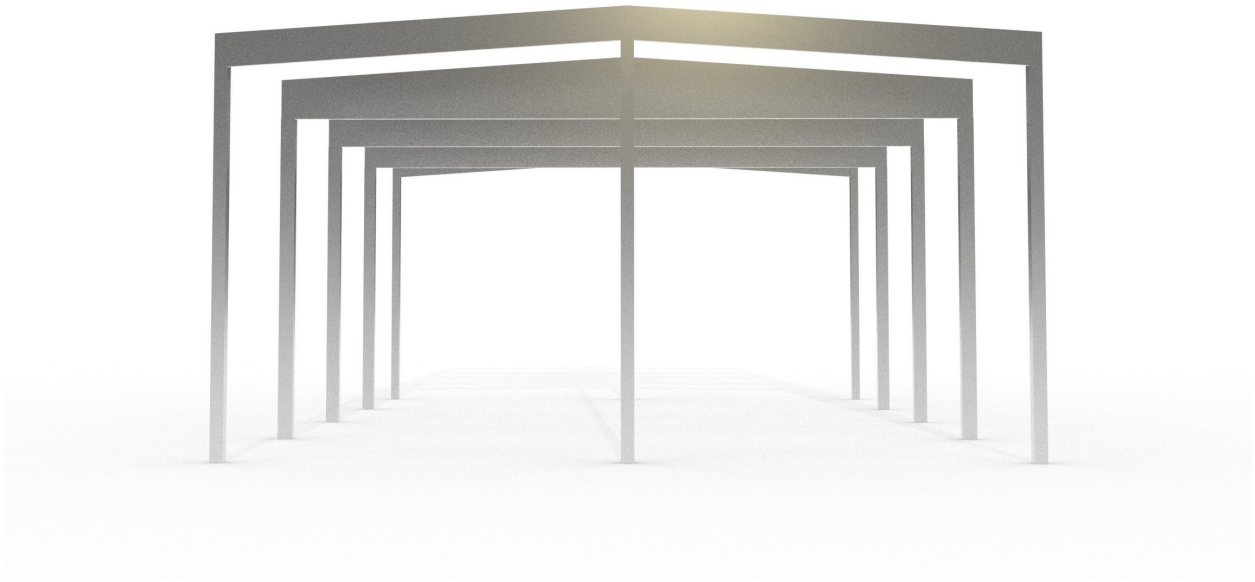

Optimization of Load-Bearing Structures with Respect to Environmental Impact

An implementation of an optimization tool for timber industrial buildings in early design stages based on parametric design

Master's thesis in Master Program Structural Engineering and Building Technology

WILMA ELM DAHLMAN
HANNA TYNELIUS

DEPARTMENT OF ARCHITECTURE AND CIVIL ENGINEERING
CHALMERS UNIVERSITY OF TECHNOLOGY
Gothenburg, Sweden 2023
www.chalmers.se

Master's thesis 2023

Optimization of Load-Bearing Structures with Respect to Environmental Impact

An implementation of an optimization tool for timber industrial buildings in early design stages based on parametric design

WILMA ELM DAHLMAN
HANNA TYNELIUS

CHALMERS
UNIVERSITY OF TECHNOLOGY

Department of Architecture and Civil Engineering
Research group for Architecture and Engineering
Chalmers University of Technology
Gothenburg, Sweden 2023

Optimization of Load-Bearing Structures with Respect to Environmental Impact
An implementation of an optimization tool for timber industrial buildings in early design stages based on parametric design
WILMA ELM DAHLMAN
HANNA TYNELIUS

Supervisors:
Niklas Johansson & Ruben Gustafsson, Ramboll Sweden AB.

Examiner:
Senior Lecturer Mats Ander, Research Group for Architecture and Engineering, Chalmers University of Technology.

Master's Thesis 2023
Department of Architecture and Civil Engineering
Research group for Architecture and Engineering
Chalmers University of Technology
SE-412 96 Gothenburg
Telephone +46 31 772 1000

Cover: Illustration of a timber industrial building

Typeset in LaTeX
Printed by Chalmers Reproservice
Gothenburg, Sweden 2023

Optimization of Load-Bearing Structures with Respect to Environmental Impact
An implementation of an optimization tool for timber industrial buildings in early design stages based on parametric design
WILMA ELM DAHLMAN
HANNA TYNELIUS
Department of Architecture and Civil Engineering
Chalmers University of Technology

Abstract

The Swedish government has set up national goals to reach net zero emissions from human activities by 2045. In 2020 the construction industry was responsible for 21 percent of the total green house gas emissions in Sweden. Hence, it has become of interest to investigate new methods of mitigating the environmental impact of new buildings. One alternative for such a method is parametric design, which enables effective evaluation of multiple design solutions. This thesis investigates how a parametric design tool can be utilized in the design of load-bearing structures in order to reduce the material usage, and thus the environmental footprint. The investigation is performed by implementing a tool with the aim of producing a first draft of an optimized load-bearing structure for a timber industrial building. The tool is developed in Grasshopper with Python scripting and the results are displayed in Rhinoceros 3D. Sizing optimization combined with topology optimization are the chosen optimization methods that are integrated in the tool. The outcome of the thesis indicates the possibility of a significant reduction of material usage in the load-bearing structures of two reference projects. In conclusion, the usage of parametric tools in the construction industry could be a valuable asset in the work towards reaching net zero emissions by 2045. Moreover, the implemented tool can be an encouragement to structural engineers in the construction industry to challenge today's way of building in order to design more sustainable buildings in the future.

Keywords: Parametric Design, Sizing Optimization, Topology Optimization, Timber Industrial Building, Glulam, Carbon Dioxide Equivalents, Sustainable Buildings, Grasshopper, Galapagos, Rhinoceros 3D.

Optimering av lastbärande strukturer med hänsyn till miljöpåverkan
En implementering av ett optimeringsverktyg för hallbyggnader i trä i tidigt designskede baserat på parametrisk design
WILMA ELM DAHLMAN
HANNA TYNELIUS
Institutionen för Arkitektur och Samhällsbyggnad
Chalmers tekniska högskola

Sammanfattning

Sveriges regering har satt upp nationella mål för att nå nettonollutsläpp orsakade av mänsklig aktivitet år 2045. Under 2020 stod byggbranschen för 21 procent av de totala utsläppen av växthusgaser i Sverige. På grund av detta har det blivit relevant att undersöka metoder för att mildra miljöpåverkan från nya byggnader. Ett alternativ för en sådan metod är parametrisk design, vilket möjliggör effektiv utvärdering av flera designlösningar. Studien undersöker hur ett parametriskt designverktyg kan användas vid konstruktion av stomsystem för att minska materialanvändningen och därmed miljöpåverkan. Undersökningen utförs genom att implementera ett verktyg med syfte att ta fram ett första utkast till en optimerad stomme för en hallbyggnad i trä. Verktyget är utvecklat i Grasshopper med kodning i Python och resultaten visas i Rhinoceros 3D. Storleksoptimering i kombination med topologioptimering är de valda optimeringsmetoderna som integreras i verktyget. Resultatet av studien indikerar möjligheten till en betydande minskning av materialanvändningen i bärande konstruktioner i två referensprojekt. Sammanfattningsvis kan användningen av parametriska verktyg i byggbranschen vara en värdefull tillgång i arbetet mot att nå nettonollutsläpp till 2045. Dessutom kan det implementerade verktyget vara en uppmuntran för konstruktörer i byggbranschen att utmana dagens sätt att bygga för att utforma mer hållbara byggnader i framtiden.

Nyckelord: Parametrisk design, storleksoptimering, topologioptimering, hallbyggnad i trä, limträ, koldioxidekvivalenter, hållbara byggnader, Grasshopper, Galapagos, Rhinoceros 3D.

Acknowledgements

This study has been carried out as a Master Thesis project, corresponding to 30 credits, within the master program of *Structural engineering and Building Technology* at Chalmers University of Technology. Furthermore, the thesis has been performed in a close collaboration with the Structural engineering group at Ramboll Gothenburg. The project has been executed in the spring of 2023.

We would like to express our deepest gratitude to our examiner and supervisor Mats Ander, Senior Lecturer at Chalmers University of Technology, for all guidance and commitment in the realizing this study. Moreover, we would like to give a tribute to the bachelor program of *Architecture and Engineering* for constantly encouraging the curiosity of learning and sparking the interest in parametric methods.

We would also like to give a special thanks to Ramboll that wanted to explore the chosen field of study with us. Especially, a thanks to our supervisors Niklas Johansson, Team leader at the Structural Engineering group at Ramboll, and Ruben Gustafsson, structural engineer at Ramboll, for all the time spent, guidance and support during the project. Moreover, we would like to thank our other colleagues at Ramboll for all the advice and fun moments as well as all insights and complementary documents that have contributed to the formation and reliability of the tool.

Lastly, we would both like to give our families a commendation for the constant support and encouragement during our five-years of education at Chalmers University of Technology.

Wilma Elm Dahlman and Hanna Tynelius, Gothenburg, June 2023

Contents

List of Figures

List of Tables

1
Introduction

This chapter presents the background of the thesis, together with the aim and thesis questions. Moreover, the methodology and limitations are introduced.

1.1 Background

Human activities have resulted in an increase of the greenhouse gas carbon dioxide of about 50 percent in the recent two hundred years [1]. This has resulted in global warming which in turn creates an unstable climate with several devastating ecological consequences. In 2020 the construction and building sector released 21 percent of the total greenhouse gas emissions in Sweden, where carbon dioxide stands for 70 percent of these emissions [2]. The Swedish government has set up national goals for limitations of carbon dioxide emissions. The target value for 2045 is to reach net zero for the anthropogenic emissions [3].

Boverket, the Swedish national board of housing, building and planning, has established new requirements which state that an environmental product declaration has to be submitted for new constructions that are built from 2022. To achieve an environmental improvement, Boverket suggests to introduce limit values for the carbon dioxide footprint of new constructions in 2027. This value should then be lowered in 2035 and 2043 in order to meet the national climate goal for 2045 [4].

The environmental footprint of a building can be evaluated through a system called environmental product declaration, EPD. This system divides the life of a building into different stages, distinguishing between product and construction stage, operational stage and end of life stage. There are several measures that can be taken in order to produce buildings with lower climate impact. In the product and construction stage it is possible to choose favourable alternatives for the structural system, material production methods, type and amount of building materials as well as transportation of raw materials and construction elements. In the operational stage the energy usage and heating of a building plays a significant role. When it comes to the end of life stage, renovation and re-usage of buildings as well as recycling of building parts and materials are susceptible to influence [5]. To gain an overall improvement it is of importance that each of the stakeholders takes action in their area of responsibility [6].

In the years between 1993 and 2020 significant improvements of the emissions from

the operational stage of buildings can be observed due to the increasing number of energy efficient buildings. However, the remaining emissions have been constant during this period [2]. In a report written by Malmqvist et al. (2018) several case studies were analysed and it was concluded that prior to the finalization of a building the construction process stage stands for 14 percent of the embodied greenhouse gas emissions whilst the product stage stands for the remaining 86 percent. Clients and designers are important stakeholders in the product stage [6]. Hence, they are of importance in the development of more efficient methods to decrease the emissions.

Since material manufacturing is a large part of the product stage the amount of building material is an important parameter to consider in the construction of new buildings with reduced carbon footprint. At an early stage in the building process, there are multiple opportunities to influence material usage. Construction projects are however often governed by narrow time frames and budgets, which makes it necessary to have efficient methods to evaluate and iterate structural designs.

An efficient way to perform optimization of structures is to develop a parametrically controlled model, which easily can be altered. This kind of model allows for multiple iterations to be evaluated in a short amount of time, making it possible to find the solution with the lowest material usage. It also results in a first draft of the load-bearing structure early in the design, which is not only favourable from an environmental perspective but also from an economical point of view, since it limits the risk of interdisciplinary collisions. Thus, it is relevant to develop tools for early stage design based on these kinds of parametric models.

1.2 Aim

The aim of this master thesis is to implement an efficient parametric tool for early stage design. The purpose is to encourage the use of new methods to design load-bearing structures. The aim of the tool is to produce a first draft of an optimized load-bearing structure for a timber industrial building with regard to material volume. Hence, the tool contributes to finding a reduced carbon footprint of the structure. The tool is developed in the software Rhinoceros 3D together with Grasshopper.

1.3 Objectives

To achieve the aim the following thesis questions are examined and answered.

- Is a parametric optimization tool useful in the early design stages?
- How can the results from the tool be used?
- What skills are required from the user?
- What structural system is most environmentally beneficial?
- Is the optimized result practically feasible?

1.4 Methodology

The working process is divided into the following steps:

- Literature study
- Evaluation of existing software
- Implementation of the tool
- Verification of the tool
- Evaluation of the results

The literature study is performed to gain an understanding of the chosen field of study. The study includes investigations of the demands and goals for the construction industry, life cycle assessment approach, optimization algorithm in parametric design and structural systems for timber industrial buildings.

Both commercial and in-house environmental assessment software are evaluated to determine what factors are relevant to implement in the optimization tool. Furthermore, the functionality of the optimization component Galapagos in Grasshopper are evaluated.

The tool is developed based on the knowledge gained from the literature study and the analysis of the software. Based on this, a flowchart for the tool is defined. The tool is developed using a parametric model generated in Rhinoceros 3D in combination with Grasshopper. The implementation is done in two steps, where the first consists of producing a code that generates an optimized structural system from user defined input. For this part, Grasshopper components combined with Python scripting are utilized. In the second step an additional optimization algorithm is integrated using Galapagos.

Verification of the structural system is made during the development of the tool. This is done by analysing the structural components in a commercial finite element software called FEM-design. The utilization rates of the structural components obtained from the tool are compared to the results of the finite element analysis to ensure reliable results. The load application is verified with comparisons to two reference projects.

The final step of the implementation of the tool is to evaluate its functionality and draw conclusions about its usability. Possibilities for further developments will be discussed.

1.5 Limitations

Considering the time frame of this project some limitations are needed. The implemented tool only produces one type of building, which is chosen to be an industrial building. The building material is limited to timber in the form of glulam stan-

dard dimensions. The layout of the structural system is limited to tapered beams or beams with constant cross section simply supported on columns. Since a large portion of the emissions arise in the product stage this is the area of focus for the tool. The implementation is limited to the structural system excluding the foundation. The calculations are based on beam theory and no finite element analysis is performed.

2
Theory

In this chapter relevant theory concerning the study is introduced. This theory regards the environmental aspects in the construction industry, the concept of optimization, parametric design, timber as construction material, industrial buildings and relevant loads.

2.1 Environmental Aspects in the Construction Industry

In the following subsections the environmental demands and requirements of the construction industry will be introduced. Both the current and future challenges relevant to this study will be investigated.

2.1.1 Demands and Requirements

The Swedish parliament has set up long term goals for the domestic emissions of carbon dioxide. These goals states that no later than the year of 2045 Sweden will reach net zero emission of greenhouse gases and achieve negative emissions onwards. Consequently, Boverket has been commissioned to establish the new demands and to introduce a course of action for the requirements set on the construction industry. In the year of 2022 and beyond, the contractors have the liability to provide an EPD, Environmental Product Declaration, for all new construction projects and hand in to Boverket, the Swedish national board of housing, building and planning [3].

2.1.1.1 Environmental Product Declaration

An *Environmental Product Declaration*, EPD, aims to demonstrate the environmental footprint of a product. An EPD needs to be third-party certified to ensure that the information is trustworthy. The declaration is based on *product category rules*, PCR, and a *life-cycle assessment*, LCA. The PCR includes guidelines, which specify choice of methods and acceptable limitations for the basis. The LCA is based on the guidelines that are given in the PCR, in order to ensure comparability between different products [7]. Furthermore, the PCR defines the functional unit that should be used in the life-cycle assessment calculations. The unit can for instance be a volume, a mass or an area [8].

In an environmental declaration of a building the environmental footprint is presented in kilograms carbon dioxide equivalents per area. *Carbon dioxide equivalents*, CO2e, is a measure that accounts for several greenhouse gases which contributes to the global warming to a varying extent. The area that is commonly used in the declarations of buildings is the gross area, in Sweden denoted *BTA*, or the heated area, in Sweden denoted A_{temp} [9].

A complete life-cycle assessment considers the entire life-span of a building, from cradle to grave. The different modules of a building's life-cycle can be seen in Figure 2.1. The life-cycle is divided into three main categories, *product- and construction stage*, A1-A5, the *operational stage*, B1-B7, and *end of life stage*, C1-C4. The *product stage*, A1-A3, involves supply of raw material, transportation and manufacturing. The *construction process stage*, A4-A5, concerns the transportation to the construction site and also installation processes. The operational stage involves all services needed during the entire life-span, such as usage, manufacturing, repair, energy and water consumption. The end of life stage includes all actions of the demolition of the building, such as recycling, transport and deposition [10].

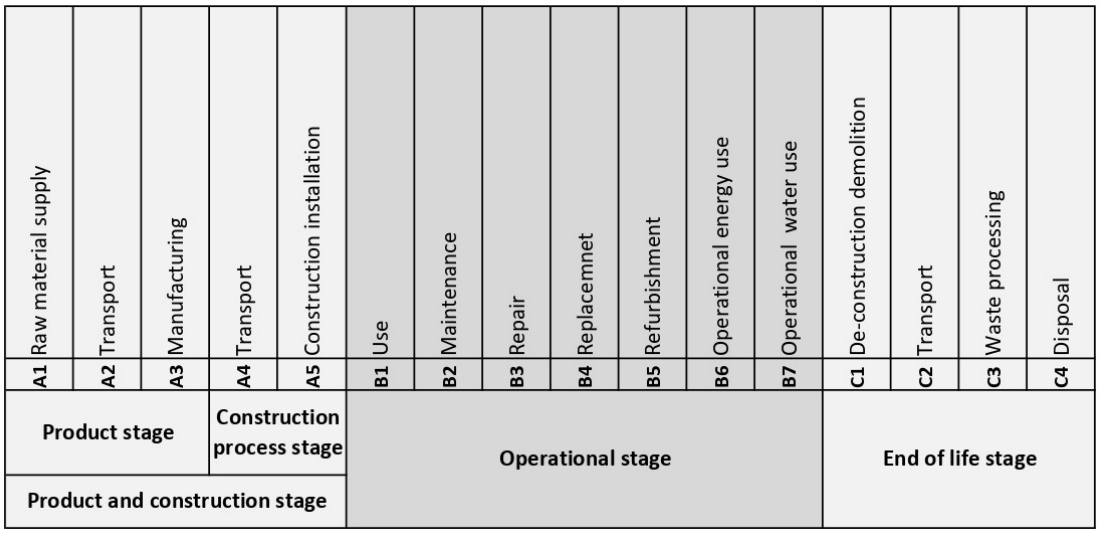

Figure 2.1: Modules in the life-cycle assessment. Figure redrawn after [10].

The life-cycle assessment calculations can either be based on generic climate data or on product specific data from EPD:s. However, the contractor has an obligation to communicate which parts of the building that are calculated based on generic data and which parts are calculated based on product specific data. Moreover, if generic data has been used it is required that the values are based on the national climate database set up by Boverket. The database is established based on Swedish circumstances [4].

2.1.1.2 Course of Action

The *course of action* established by Boverket, described in Figure 2.2, includes several rule adjustments concerning environmental declarations and limit values for the environmental footprint of new constructions. Before new requirements and limit values can take place in 2027, 2035 and 2043, Boverket needs to perform an evaluation of possible consequences for the stakeholders in the industry. Moreover, possible adjustments in the strategy needs to be investigated to be able to reach the national environmental milestones. This evaluation is planned to be finalized three year before the new step-wise requirements will be introduced [4]. The course of action facilitates a readjustment for the contractors as well as for other stakeholders in the industry and supports preparations for the green transition [3].

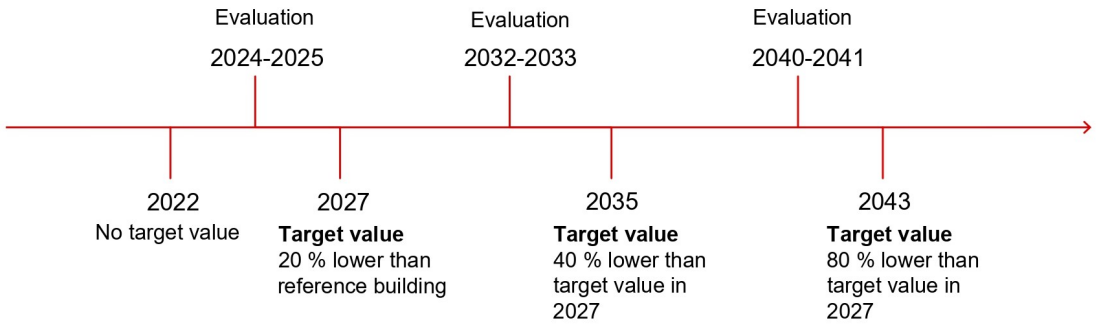

Figure 2.2: Overview of the course of action established by Boverket, showing target values of climate emissions from buildings. Figure redrawn after [4].

In the year of 2022 the first act of the new regulation by Boverket was enforced, which includes requirements of environmental certification for buildings being completed in the year 2022 and beyond. Thus, responsible contractors will be liable to submit an environmental product declaration, EPD, for all new constructions. The requirement from 2022 will initially be applied for apartment building and premises. The certificate will include the load-bearing system, internal walls and the envelope of the building. Furthermore, the life-cycle assessment will be limited to the product- and construction stage, A1-A5 [4].

The limit values are planned to be put into action in the year of 2027 and are based on a reference building. At that time, the environmental footprint in the product and construction stage, A1-A5, should have decreased with 20 percent in relation to the reference building. The demands for the environmental declaration will be expanded to a greater part of the life-cycle assessment, A1-A5, B2, B4, B6 and C1-C4. Moreover, the building elements that need to be included will also be extended to include the load-bearing system, internal walls, the envelope of the building, building installations and internal sheeting layers. The coming years, 2035 and 2043 the limit value will decrease to 40 percent and 80 percent respectivly based on the

limit value set in 2027 [4].

2.1.2 Current Situation

In the year of 2020, the greenhouse gas emissions from the construction industry accounted for 21 percent of the total domestic emissions [2]. In the years between 1993 and 2020, several improvements in the operational stage were made thanks to more energy efficient buildings and a higher usage of renewable energy sources. However, the product and construction stage has remained at a constant level during these years. Consequently, the product and construction stage now accounts for a greater part of the total greenhouse gas emissions during a building's life-cycle [8, 10].

The life-cycle assessment is needed to gain an understanding of the environmental footprint of today's construction industry. The expectation is that the different stakeholders will receive incentives to improve their methods. The impact of the modules in the life-cycle assessment varies greatly between different buildings. One reason is the choice of building materials. Another reason is that emissions from the operational stage varies highly depending on the choice of energy source and the buildings estimated life-span. Consequently, the emissions from the product and construction stage can vary between 25 percent and 70 percent of the total emissions during a life-span of 50 years. The product stage, A1-A3, accounts for about 84 percent of the greenhouse emissions from the product and construction stage, A1-A5. The construction installation stage, A5, accounts for about 13 percent and the transportation to the construction site, A4, accounts for the remaining 3 percent [8].

In the report written by Malmqvist et al. (2018), several case-studies are analysed and different stakeholder's responsibility and measures are discussed. In addition to reducing the impact from the operational energy usage, the importance of reducing the impact from the product and construction stage is identified as an important measure in the reduction of the emission of carbon dioxide equivalents. Particularly, the designer and its clients have the liability in the product stage, during which minimizing the amount of material and the choice of sustainable materials are two significant measures. In addition to this, the choice of a light-weight construction can reduce the amount of concrete in the foundation with up to 50 percent, which is beneficial for the reduction of the environmental footprint. The contractors have the main responsibility to ensure improvements at the construction site, the stages A4-A5, as well as during the demolition of the building or building parts. Furthermore, they have the responsibility of the purchasing of materials, preferably from local manufacturers, to reduce the transportation distances [6].

2.1.3 Challenges

The construction industry is facing several challenges in conjunction with the green transition. *The Smart Built Environment*, a strategic innovation program for the civil engineering sector, estimates that a 40 percent reduction of the environmental footprint is possible through digital development. Digital methods are not widely

used in the industry today even though methods and knowledge definitely are under development. In particular, it is a great challenge for smaller companies to implement the new digitalization processes. However, the new requirements from Boverket on environmental declaration will hopefully lead to an expanded usage of digital methods for climate calculation and that stakeholders will be encouraged to explore the possibilities of the new digital methods [4].

Building information modelling, BIM, is considered to be an effective method to compile the basis information for an environmental declaration. BIM involves the creation and management of a digital representation of a construction project throughout its entire life-cycle. This representation commonly contains both a 3D model and additional information regarding different aspects of the building [11]. Furthermore, BIM can contribute to an efficient way to compare and evaluate different design solutions at an early stage.

2.2 Optimization

Mathematical optimization is the theory of finding the optimal solution to a problem by obtaining the maximum or minimum value of one or several objective functions. Single-objective optimization means that the optimization is performed with regard to only one goal whilst multi-objective optimization is performed with regard to several goals. One sole solution to the optimization is identified for single-objective optimization. However, if the multi-objective optimization has conflicting goals one single optimal solution can not be obtained, but rather a collection of compromised solutions [12].

2.2.1 Structural Optimization

Christersen and Klarbring [13] describes optimization as making things the best. With this definition as a foundation, they conclude that structural optimization implies creating the structural system that can manage the assigned loads in the best possible way. The definition of the best way is however not explicitly described but a few examples are brought up in the literature. The best way can, according to Christersen and Klarbring [13], for example be to make the structure as stiff, as light or as insensitive to instability as possible. All these examples correspond to maximization or minimization problems which require certain constraints. An example of such a requirement is a limitation of the amount of material usage. Without a constraint to this the maximization of the stiffness can result in an optimization without a well-defined solution, as the structure can grow immensely stiffer when applying more material. Displacements, stresses and geometry are often governing and hence limited in problems treating structural optimization [13].

Structural optimization always includes an objective function called f, a design variable called x, and a state variable called y. A structural optimization problem can thereafter be formulated as following: *minimize f(x,y) with respect to x and y.* The

objective function is used to determine how good a suggested solution is in relation to the others. The goal of the optimization is generally to minimize or maximize this function. It is the design variable together with the state variable that governs the value of the objective function. The design variable controls the structural design. This value can be altered throughout the optimization in order to find the optimal solution. Lastly, the state variable represents how the assigned situation affects the structure [13].

Structural optimization is sorted into three different branches depending on the method that is used. The three methods are denominated as *sizing optimization*, *shape optimization* and *topology optimization* [14]. Sizing optimization is the main focus in this thesis but topology optimization is also treated.

2.2.1.1 Sizing Optimization

Sizing optimization is performed with respect to the dimensions of the individual structural elements in the structural system. In this case the overall dimensions and shape of the system is known and not altered. This is the simplest form of structural optimization [14].

2.2.1.2 Shape Optimization

The principle idea of shape optimization is to find the geometry of the structure with the best mechanical behaviour that meet the given constraints [15]. This is performed by modifying the boundary of the structural domain. By changing for example the shape of the domain stress concentrations can be avoided [16].

2.2.1.3 Topology Optimization

The most general form of structural optimization is topology optimization. In this form of structural optimization the most beneficial topology of the structure is sought [14]. This means that the optimal placement of material within the structural domain for a given set of conditions is determined [17]. The resulting structure provides the most favourable force paths through the material. The solution is generated by discretizing the structure into finite elements and removing the elements that are not necessary [16].

2.2.2 Different Algorithms

Optimization in general as well as structural optimization can be performed using several different algorithms. In this thesis an *evolutionary algorithm* is treated. This optimization method is stochastic which means that it includes elements of randomness [18, 19]. This random feature reduces the risk of the solution getting stuck in local maxima or minima and not finding the sought global minima or maxima, which is a common problem when using more simple optimization algorithms [20, 21]. The principle of local maxima and minima are illustrated in Figure 2.3.

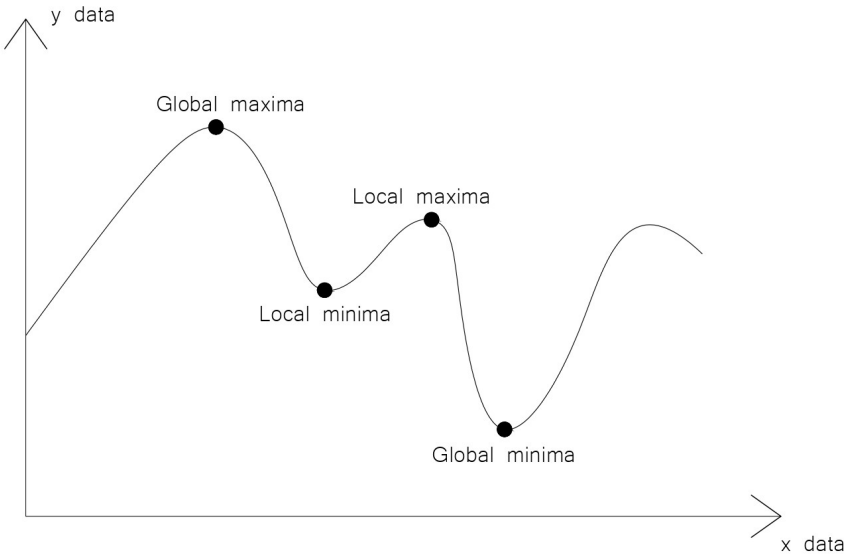

Figure 2.3: Illustration of local maxima and minima.

2.2.2.1 Evolutionary Algorithms

Evolutionary algorithms are mimicking the principle of natural evolution and are based on a population of individuals, in optimization more commonly referred to as solutions, that can exchange information with each other. First an initial population of solutions is randomly generated. All these solutions are evaluated and the best fitted ones are selected. These solutions are then crossed to make a new, improved population of solutions. Solutions are evaluated and new solutions are generated until a global optimum solution is found or a maximum number of generations is reached [18].

2.3 Parametric Design

Generating models based on a number of parameters with user-specified relationships between them is called parametric design. Changing the values of the parameters will make the model change interactively, without the user having to apply the changes directly to the model. In a non-parametric model a change in one part usually leads to required small alterations in other parts, which means that changes are harder to make and takes longer time to implement [22]. Adjustments in a parametric model are not limited to individual elements but is also applicable for global geometry changes of the model [23]. A global change could for example be changing the overall dimensions of a building which will cause the structural elements to adjust thereafter.

Parametric design has proven to be a useful tool in performing iterations and optimization in early stages due to its nature of quickly generating results. With this tool structural engineers can receive quick feedback on how a design works and make

alterations thereafter in an efficient manner [24].

2.3.1 Rhinoceros 3D

Rhinoceros 3D, or Rhino, is a free form modeling software developed by Robert McNeel & Associates. Geometries can be built up using points, curves, surfaces, solids and meshes [25]. Non-Uniform Rational B-Splines, commonly referred to as NURBS, are used to represent geometries in Rhino. The geometries can be standard geometrical objects as well as free-form objects. NURBS are described by mathematical expressions resulting in flexible and accurate shapes. An advantage with NURBS is that only small amounts of information is required to represent a geometrical shape [26].

2.3.2 Grasshopper

Rhinoceros 3D has a direct link to a graphical algorithm editor called *Grasshopper*, which opens in a separate window. This software is a visual programming environment which means that the programming can be performed by connecting predefined components to each other. Custom components can also be defined through either C# or Python scripting. The link between Rhino and Grasshopper allows the user to interactively see the model change in Rhino when components are connected in Grasshopper. There are several ways to utilize the parametric setup of a Grasshopper model to perform optimization. Two tools that can be utilized are the built-in components Galapagos and Octopus. Galapagos performs single-objective optimization whilst Octopus performs multiple-objective optimization. This master thesis treats single-objective optimization and hence Octopus will not be used.

2.3.2.1 Galapagos

The optimization in Galapagos can be performed using two different algorithms. The two alternatives are an evolutionary solver, the principles of which are explained in Chapter 2.2.2.1, and a simulating annealing solver, which is not treated in this thesis. The evolutionary solver is generally recommended but for cases with a large number of degrees of freedom the annealing solver may be preferable [27].

As for the usage of Galapagos, it requires a genome and a fitness as input in order to run. The genome is one or several parameters that can be altered to affect the fitness and the fitness is the value that should be optimized. Since Galapagos performs single-objective optimization, only one fitness value can be provided. There are multiple adjustable parameters inside Galapagos, which are controlled by the user. The fitness value can be chosen to be either maximized or minimized and a run-time limit can be applied. This limit causes the optimization to stop if it consumes to much time without finalizing. A threshold is not required but can be set. This defines the value of the fitness and the optimization will stop if a fitness with the threshold is found [27]. These settings apply to both solvers.

There are also settings which apply to the specific algorithms. For the evolutionary solver the max stagnant, population size and initial boost should be chosen. Inbreeding and maintain are also adjustable parameters for the evolutionary solver. The max stagnant controls how many generations that can be generated without gaining a better solution before the solver stops. Population is the amount of options that are tested before the optimization moves on to the next generation. The initial boost controls the size of the population in the first generation of solutions. Inbreeding is a freedom factor which manages the similarity of the genes that are bred. A positive value means similar genes whilst a negative value will give different genes. Lastly, maintain governs how many cross-overs that should be done in each generation.

2.4 Timber as a Construction Material

Sweden has a long history of building in timber and has one of the greatest sawmill and wood industries in the world [28]. The industry develops rapidly with several new technologies for material treatment as well as different production techniques. The modern timber industry has extended the possibilities of timber as a building material. Hence, it has become possible to build everything from small houses to more extensive buildings, such as stadiums and multi-storage buildings. Timber as a building material has several advantages, such as environmental aspects and structural benefits [29]. As the demands for sustainable buildings increase, also the request for timber constructions has increased in the recent years [28].

2.4.1 Structural Properties

Timber is a biological and natural material that comes with geometrical dissimilarities, which affect its structural behaviour. Furthermore, timber is an *anisotropic material*and a *hygroscopic material*, which also affect its structural behaviour. Therefore, the strength and stiffness properties of timber specimens are often sorted by a non-destructive strength test in order to ensure the quality of the structural behaviour. Moreover, the varying strength properties are taken into account with several measures that are specific for timber elements, such as *load duration classes*, *service classes*, *partial coefficients* and load application angle in relation the fibers of the timber [30].

The load duration classes consider the time period of load application. When a timber specimen is subjected to a constant load over time *creep* occurs, which is a reduction of the strength capacity. The load duration classes are divided into five cumulative time-periods, which can be seen in Table 2.1. In a design the creep is taken into account by applying a strength modification factor, k_{mod} [30].

Table 2.1: *Load duration classes*

Load-duartion class	Cumulative duration	Example of load
Permanent	$>$ 10 years	Dead-weight
Long-term	0.5 - 10 years	Stored goods
Medium-term	1 week - 6 months	Snow load, imposed load
Short-term	$<$ 1 week	Wind load
Instantaneous	-	Accidental load, wind gusts

The modification factor is also characterized by service classes that reflects the hygroscopic properties of timber. A hygroscopic material is a material that absorbs moisture from the surrounding environment, which also influences the strength and stiffness properties of the timber. The moisture content is affected by the relative humidity and temperature of the air. The service classes are divided into three categories, service class 1, service class 2 and service class 3, which can be seen below [30].

- **Service class 1** - The surrounding environment is about 20 degrees and has a relative humidity that does not exceed 65 percent more than a few weeks a year. Consequently, the average moisture content in the wood does not exceed 12 percent. The service class is characterized by heated and ventilated environments with protected elements [30].

- **Service class 2** - The surrounding environment is about 20 degrees and has a relative humidity that does not exceed 85 percent more than a few weeks a year. Consequently, the average moisture content in the wood does not exceed 20 percent. Usually, the service class is used for environments which are not constantly heated and with elements protected from precipitation [30].

- **Service class 3** - The surrounding environment leads to an average moisture content that exceeds 20 percent in the wood. The service class is often used when construction is not protected from precipitation or is in direct contact with the ground [30].

In design of timber constructions the great variation of geometric imperfections and the uncertainties of strength and stiffness properties needs to be considered. This is done by using several partial coefficients specific for design of structural timber elements, such as factors considering size effects, insatiability effects and creep effects [30]. The modification factors that are relevant in this thesis project are further explained in Chapter 2.5.3.

An anisotropic building material is a material that has different properties in different directions. This is due to the tube shaped structure of wood. Hence, the loading direction is an important factor to consider when designing timber constructions. The timber has a longitudinal direction parallel to the grains and a radial and a tangential direction, both perpendicular to the grains. This is illustrated in Figure 2.4. There is a significant difference in strength in directions parallel and perpen-

dicular to the grains. The difference between the tangential and radial direction is however often disregarded [30].

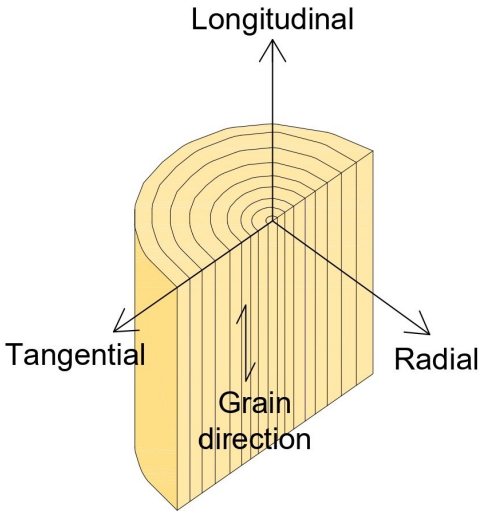

Figure 2.4: Directions in timber. Figure redrawn after [31].

2.4.2 Advantages and Disadvantages

Historically, timber has mostly been used in smaller constructions such as single family houses and lower residential buildings. The limitation to smaller buildings was due to fire safety regulations. From 1874 to 1994 the Swedish regulations stated that timber buildings were limited to a maximum height of two stories [32, 29]. With new techniques and production methods timber is these days not more of a fire-hazard than other building materials. Timber can even be beneficial compared to steel elements in a fire. This because timber is considered to have a calculable strength capacity when charring occurs in the wood. Steel elements need to be protected from fire to ensure the load carrying capacity [29]. In 1994 the regulations containing amongst other things requirements regarding the number of stories for buildings made from combustible building materials were abolished. They were instead exchanged with usage based requirements called Boverkets Byggregler, BBR [32].

Timber is a light-weight material and has a relatively high strength in proportion to its weight. This, comes with several environmental benefits. In Malmqvist T. et al. (2018), it is concluded that timber constructions have a lower carbon footprint than steel constructions when considering the product- and construction stage. Moreover, it can be seen in a case study that a light-weight structure can reduce the amount of concrete in the foundation with about 50 percent. Thus, the case study shows a total reduction of embodied greenhouse gas emission of about 50 percent when the synergy of a light-weight timber structure and a reduction of concrete material in the foundation was achieved compared to a concrete and steel structure [6].

Furthermore, the accessibility of wood is also important to consider from the en-

vironmental perspective. In the report written by Malmqvist T. et al. (2018), it is shown in several case studies that timber structures with over-sea transportation may have greater carbon footprint emissions, in module A4, compared to other building materials. However, it is concluded that for the summarized result in the product and construction stage, A1-A5, it is still beneficial with timber constructions [6].

Moreover, timber is a bio-based material which stores carbon due to the photosynthesis of trees. It is the only renewable building material which does this[33]. Compared to other building materials, timber is thus environmentally beneficial when considering the product- and construction stages, A1-A5. However, the end of life stage, C1-C4, plays a significant role since combustion and decomposition re-releases the carbon to the atmosphere. Thus, it is of importance to have a sustainable timber production which embraces the re-planting of trees. Re-planting of trees actually enables resumption of carbon dioxide during the life-cycle of the building in order to compensate for the released carbon when demolishing timber structures [34].

Whilst timber is considered to have several environmental advantages, as described above, it also has disadvantages in terms of fulfilling several functional requirements. For instance, timber has a low noise insulation ability, which can force constructions with coarser structural elements and noise insulation in form of air gaps in walls and joists. These air gaps are filled with insulation and can in turn pose a fire-hazard which needs to be managed. Other drawbacks are that timber is sensitive to moisture and vibrations [29].

2.4.3 Glulam

Timber is a building material that can be used in several different forms. One of these is glued laminated timber, denoted glulam, which is a refined timber product suitable for demanding timber constructions [35]. Glulam is produced by gluing several wood laminates together to form one stiff and strong solid structural element. The wood laminates consist of finger jointed sawn boards in which the fibres of the wood are parallel with the axial direction of the element. Lamellas with thicknesses of 45 mm and widths of up to 215 mm are commonly used in Sweden [30]. A few dimensions of glulam beams and columns are stock products, which generally are available at glulam manufacturers. In addition to this, the manufacturing assortment also includes a large number of additional standard dimensions that can be produced [36]. One or more glulam elements can be glued together beside each other to form an element with a width of more than 215 mm [30]. Relative to its weight, glulam is one of the strongest building materials. Glulam has a higher mean capacity as well as a smaller dispersion of strengths than structural timber, which is illustrated in Figure 2.5 [36].

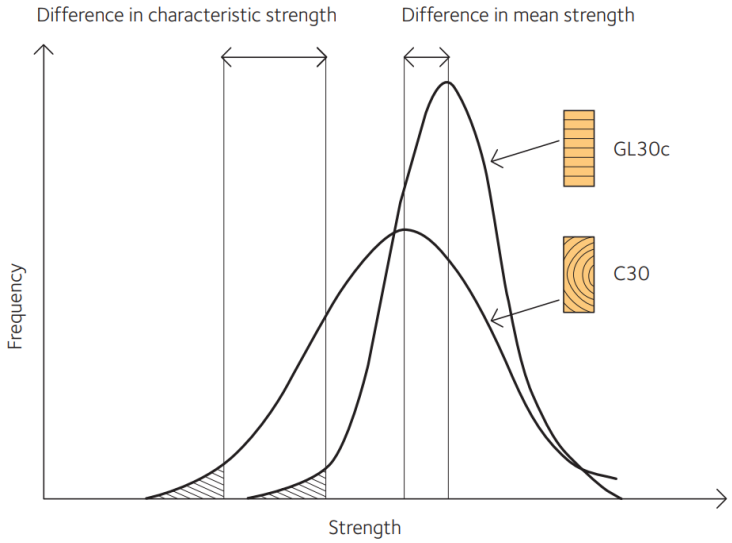

Figure 2.5: Strength of glulam compared to structural timber [30].

One significant advantage of glulam compared to structural timber is that it is easily custom made according to the requirements of a specific project. Elements can be curved or produced with varying cross sectional heights and lengths. The length of a glulam element is governed by the transportation and is normally limited to around 30 meters. Frames and arcs can also be produced in glulam. To decrease the instantaneous deflection of a glulam beam it can be made with a small pre-camber. This implies that it is produced with a small curvature upward, which counteracts parts of the vertical deflection. Glulam constructions in Sweden are to be executed, dimensioned and controlled according to the regulations SS-EN 1995-1-1 and SS-EN 1995-1-2, together with Boverkets konstruktionsregler and EKS11 [36].

2.4.3.1 Strength Classes in Sweden

The strength of the lamellas in a glulam element can vary in one element. One common way to construct a glulam element is to use lamellas of higher strength in the outmost layers as these will have the highest stresses, as seen in Figure 2.6. Lower strengths can then be used in the inner layers where the stresses are lower. This type of layout results in higher utilization of the material and is called combined glulam, which is denoted with a c. For the combined glulam the strength class is called GL30c in Sweden, were 30 indicates the bending strength parallel to the fibres in megapascals. The layers of higher strengths must in this strength class be at least 17 percent of the height of the cross section. Is is also possible to produce glulam with the same strength in all lamellas and the strength class for these is called GL30h, where h stands for homogenous. Both combined and homogenous glulam can be split sawn and are these elements are sorted into the classes GL28cs and GL28hs, where s stands for split. [37].

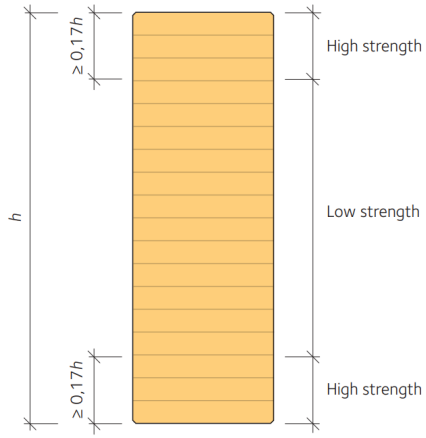

Figure 2.6: A combined glulam cross section [30].

2.4.3.2 Production

In Sweden glulam is typically made from spruce, but production with pine also occurs. The production of glulam does not vary much and is quite similar for all manufacturers. The timber lamellas are produced at a sawmill, where they are also generally dried and sorted by strength before they are delivered for further processing. In order for the glued connection to gain a good strength the timber should have a moisture ratio of 5-16 percent during the gluing process. In addition to this accepted range two adjacent lamellas should not have a difference in moisture ratio of more than 5 percent. The lamellas are firstly finger jointed to create longer elements of around 30 to 40 meters. After the glue in the finger joints have hardened the jointed lamellas are planed. They are then stacked and glued together to form either combined or homogeneous glulam elements, according to the principles described in Chapter 2.4.3.1. The outer lamellas are always placed with the core outwards. The inner lamellas are placed with the core facing the same way as each other. This helps decrease the inner stresses in the final product [35].

2.4.3.3 Environmental Aspects of Glulam

As stated in Chapter 2.4.2 timber has environmental advantages compared to other building materials. Furthermore, the production of glulam is energy efficient. Residual products such as sawdust are used to produce energy that is needed during the drying process of the timber. The timber itself is reusable and recyclable, whilst the glue is a non-renewable product. The amount of glue is however less than one percent of the total weight of the product making the negative impact of the glue on the final product negligible. Glulam does not only have a small negative environmental impact, but also has the favourable effect as it binds more than 700 kg carbon dioxide per cubic meter [36]. The climate data base provided by Boverket, which is described in Chapter 2.1.1.1, states a value of 0.133 carbon dioxide equivalents per kilo material for glulam. The value assumes a usage of fossile energy during production and is to a high extent governed by this assumption.

2.5 Industrial Buildings

Industrial buildings are frequently occurring structures that have a wide area of usage, such as different kinds of halls for sport activities, storage spaces and logistic centers. These activities often requires large open spaces and therefor influence the design of the structure. The design of the roof beams highly varies depending on the width of the building and if the field of usage allows for column placement in the open area. However, in some cases the area of usage limits the placement of the columns to only the exterior walls, which leads to constructions with longer spans. The building is usually a one story building, where spans typically varies between 10 to 30 meters, which have a significant impact on the choice of the primary load-bearing structure [38].

In this thesis the considered building is an industrial building where the load-bearing structure is constructed with timber elements. In the following sub-chapters common structural systems that are relevant in this study will be presented. Furthermore, the loads applied on an industrial building will be introduced.

2.5.1 Structural Systems

A timber industrial building can be constructed using several different structural systems [39]. A common timber system consists of beams simply supported on glulam columns, where the beams can be for example glulam beams with constant cross section or tapered glulam beams. The beams with constant cross section can be placed horizontally to create a flat roof or in an angle to create a single pitched roof whereas the tapered beams always result in a duo pitched roof. The spacing of the columns can vary between different cases but generally follows standard module dimensions. This allows for the usage of module wall and roof elements with standard measurements.

2.5.1.1 Structural Stability

The structural system has to be designed to withstand both vertical and horizontal loads. The vertical loads are transferred from the roof beams to the columns and eventually to the ground. The structural system has to be braced in order to handle the horizontal forces. The horizontal forces can cause lateral displacement in two directions as well as torsional displacement, as seen in Figure 2.7 [30]. To handle these three effects the bracing has to be applied in at least three walls. The direction of the walls must never meet in one point and at least two of the walls should not be parallel to each-other [35]. Some kind of bracing is also required in the roof to distribute the horizontal forces to the bracing in the walls which in turn will transfer the load to the ground [30]. The bracing can be achieved by a few different methods. Two common methods are to either insert diagonals or to utilize diaphragm action in stiff surface elements [35]. A non-braced beam-column system, and hence a mechanism, is shown in a) in Figure 2.8 whilst the stabilizing effect of these two solutions can be seen in b) and c).

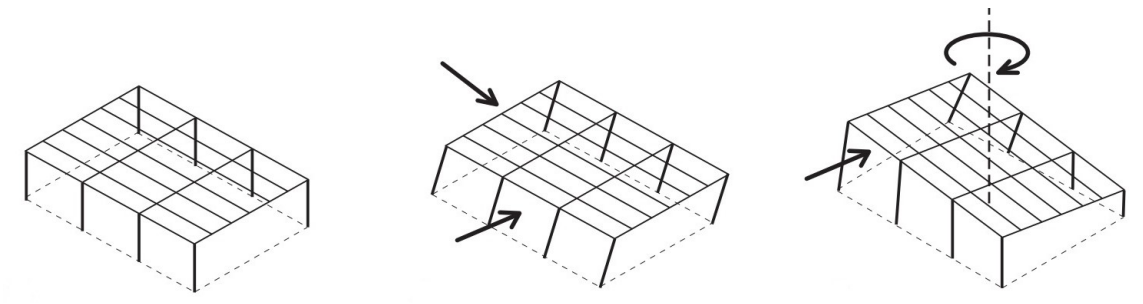

(a) Structural system with no applied lateral forces.

(b) Structural system exposed to centrally applied horizontal forces.

(c) Structural system exposed to non-centrally applied horizontal forces.

Figure 2.7: The effects of horizontal forces on a non-braced building [30].

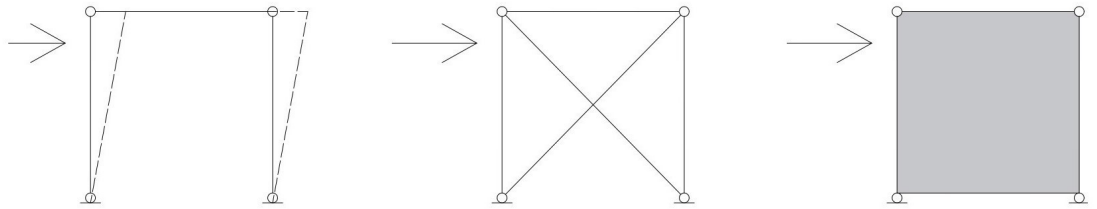

(a) System without bracing.

(b) System braced with diagonals.

(c) System braced with diaphragm action.

Figure 2.8: Illustration of different kind of bracing. Figure redrawn after [40].

To be able to transfer the horizontal forces from the roof to the ground via the bracing the beams also have to be stabilized. An example of how this bracing can look is shown in Figure 2.9 [35].

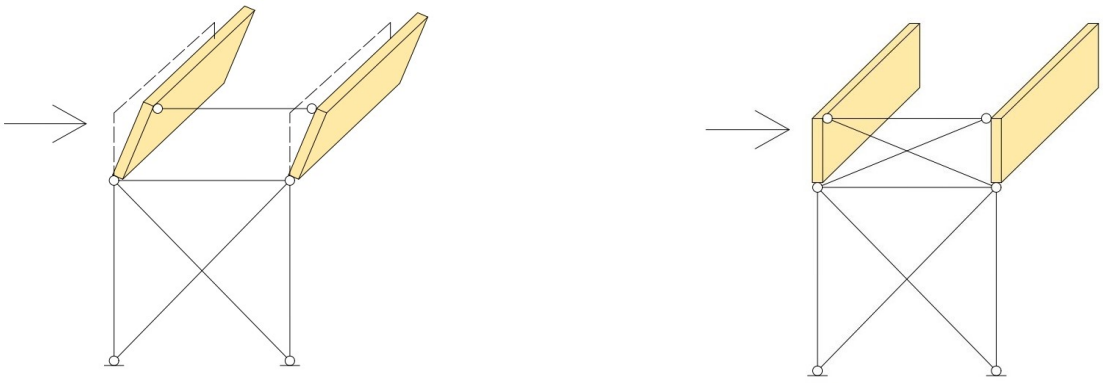

(a) Non-braced beams

(b) Braced beams

Figure 2.9: Illustration of the effect of bracing of roof beams. Figure redrawn after [40].

2.5.1.2 Glulam Beam with Constant Cross Section

The most common structural system for timber industrial buildings consists of beams with constant cross section, simply supported on one column in each end [36]. The principal layout of this system can be seen in Figure 2.10. This beam has to be dimensioned for the bending moment, shear force, lateral torsional buckling and deflection that occurs due to the vertical forces that are applied. Another effect that has to be taken into account is the compression perpendicular to the fibres at the connection between the column and the beam [30].

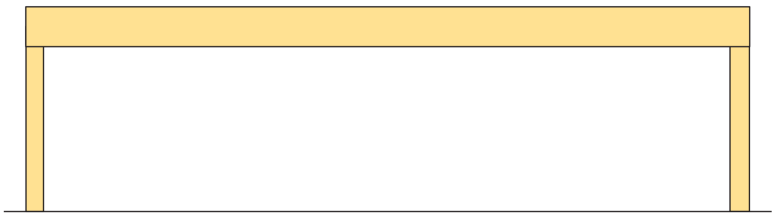

Figure 2.10: Glulam beam with constant cross section, simply supported on glulam columns [36].

2.5.1.3 Tapered Glulam Beam

An alternative to the beam with constant cross section is the tapered beam, which can be seen in Figure 2.11. This beam has a varying cross sectional height, which is done to distribute material according to the bending moment distribution. As the maximum bending moment occurs in the middle of the span, so does the highest beam height. The bending moment decreases towards the end of the span and hence, so does the cross sectional height. This beam is commonly simply supported on glulam columns. The dimensions of the tapered beam are chosen to withstand the same load effects as the beam described in chapter 2.5.1.2. The tapered beam has a critical section located at approximately the quarter point of the beam. The maximum bending stresses do not occur at the place of the highest moment but rather at this critical section [35]. These beams should also be dimensioned to withstand the tension that occurs at the apex and stresses that occurs at the tapered edge [30].

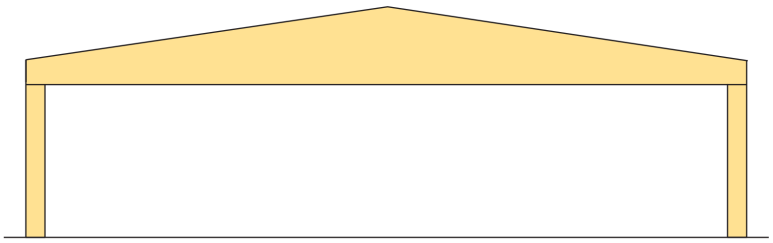

Figure 2.11: Tapered glulam beam, simply supported on glulam columns [36].

2.5.1.4 Glulam Column

The beams described in chapter 2.5.1.2 and 2.5.1.3 commonly both rest on glulam columns. These columns are dimensioned to withstand the normal force that occurs due to the vertical reaction forces from the beams as well as the bending moment and shear force that occurs due to horizontal forces on the wall. The column must also be able to withstand the interaction between the normal force and the bending moment. When dimensioning the columns buckling is an important mode of failure that has to be taken into account [30].

2.5.2 Loads

The dimensioning loads for a one story industrial building are self weight, snow load and wind load [36]. Self-weight is classified as a permanent fixed load, whilst both snow load and wind load are variable fixed loads [41, 40, 42]. The vertical loads are in this case the self-weight, snow load and wind load on the roof, whilst the horizontal loads consists of the wind loads on the walls.

2.5.2.1 Self-weight

Self weight is calculated according to in SS-EN 1991-1-1. As stated in chapter 5.1 in SS-EN 1991-1-1 the self weight includes both the structure itself and non-structural elements. For a structural member the characteristic self-weight is directly dependant on the size of the cross-section and the density of the material and is for an element with constant cross-section calculated according to Equation 2.1.

$$g_k = \rho_k \cdot A_{cs} \cdot g \tag{2.1}$$

where

g_k - Self-weight [N/m].
ρ_k - The characteristic density of the material [kg/m^3].
A_{cs} - The area of the cross section [m^2].
g - The acceleration due to gravity [N/kg].

2.5.2.2 Snow Load

Snow load on the roof of the building is calculated according to SS-EN 1991-1-3 and Equation 2.2 below.

$$s = \mu_i \cdot C_e \cdot C_t \cdot s_k \tag{2.2}$$

where

s - Snow load [N/m^2]
μ_i - Snow load shape coefficient depending on the shape of the roof and the risk of snow accumulation due to wind, sliding and snow falling from abutting roofs according to SS-EN 1991-1-3, 5.3.2 [-].

C_e - Exposure coefficient depending on the wind exposure on the site [-].
C_t - Thermal coefficient depending on energy losses through the roof [-].
s_k - Characteristic value of snow on the ground at the relevant site according to EKS11 [kN/m^2].

2.5.2.3 Wind Load

Wind load is calculated according to SS-EN 1991-1-4. The external wind pressure is calculated according to Equation 2.3 and the internal wind pressure is calculated according to Equation 2.4.

$$w_e = q_p(z) \cdot c_{pe} \tag{2.3}$$

$$w_i = q_p(z) \cdot c_{pi} \tag{2.4}$$

where

w_e - External wind pressure [N/m^2]
w_i - Internal wind pressure [N/m^2]
$q_p(z)$ - Peak velocity pressure depending on the reference height z [N/m^2].
z - Reference height for the wind load [m].
c_{pe} - Shape factor for external load according to SS-EN 1991-1-4, 7.2 [-].
c_{pi} - Shape factor for internal load according to SS-EN 1991-1-4, 7.2.9 [-].

The peak velocity pressure is calculated according to Equation 2.5.

$$q_p(z) = c_e(z) \cdot q_b \tag{2.5}$$

Where

$c_e(z)$ - Exposure factor [-].
q_b - Basic velocity pressure [N/m2].

The basic velocity pressure is calculated according to Equation 2.6.

$$q_b = \frac{1}{2} \cdot \rho_{air} \cdot v_b^2 \tag{2.6}$$

Where

ρ_{air} - Air density [kg/m^3].
v_b - Basic wind velocity at the relevant site according to EKS11 [m/s].

The exposure factor is calculated according to Equation 2.7.

$$c_e(z) = \left(k_r \cdot ln\left(\frac{z}{z_0}\right)\right)^2 \cdot \left(1 + \frac{2 \cdot k_p}{ln\left(\frac{z}{z_0}\right)}\right) \tag{2.7}$$

Where

k_r - Terrain factor depending on the roughness length z0 [-].
k_p - Peak factor according to EKS 11 6.3.1(1) 9 § [-].
z - Reference height for the wind load [m].
z_0 - Roughness length according to SS-EN 1991-1-4, 4.2.3, Table 4.1 [m].

The roughness length depends on the terrain category at the sight. The terrain category is divided into five groups with different exposure to wind these are described in SS-EN 1991-1-4, A1. The terrain factor, k_r, is calculated according to Equation 2.8.

$$k_r = 0.19 \cdot \left(\frac{z_0}{0.05}\right)^{0.07} \tag{2.8}$$

The net pressure on a wall or roof element is the sum of the internal and the external wind pressure. Positive wind pressure is defined as acting towards a surface whilst negative wind pressure is defined as acting away from a surface, as seen in Figure 2.12 [42].

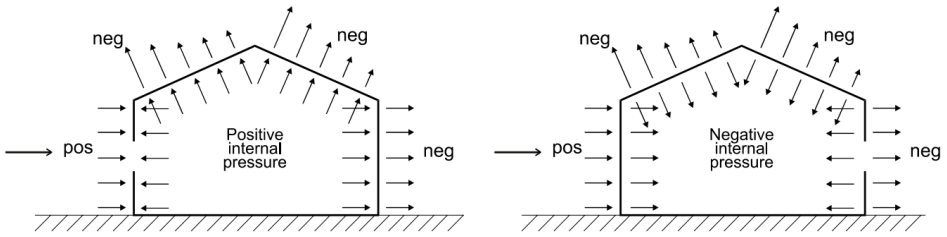

Figure 2.12: Illustration of positive and negative wind pressure [42].

2.5.3 Design Values for Material Properties

When designing timber structures there are some partial coefficients and modification factors that need to be considered. The design value of a property, X_d, can generally be expressed according to Equation 2.9

$$X_d = \eta \cdot \frac{X_k}{\gamma_m} \tag{2.9}$$

Where

η - Modification factor taking effects of volume, moisture, temperature and other relevant parameters into account.
X_k - The characteristic value of the property.
γ_m - Partial coefficient taking effects of the possibility of unfavourable deviation of a characteristic material property into account.

Relevant modification factors and partial coefficients are listed below.

- $\mathbf{k}_{mod}$ - Strength reduction factor that takes building material, service class and load duration class into account. The service class concerns the temperature and relative humidity in the environment and is further described in SS-EN-1995-1-1, 2.3.1.3. The duration class concerns the loading time and is explained in EN 1995-1-1, 2.3.1.2. The factor is chosen according to SS-EN 1995-1-1, 3.1.3, Table 3.1.
- $\mathbf{k}_{def}$ - Deformation factor used to calculate the final modulus of elasticity taking moisture effects on deformation into account. The factor depends on the building material and service class and is chosen according to SS-EN 1995-1-1, 3.1.4, Table 3.2.
- $\mathbf{k}_{h}$ - Factor to increase the bending and tension strength for members with a cross-sectional height of less than 600 mm.
- $\mathbf{k}_{crit}$ - Bending moment strength reduction factor to take lateral torsional buckling into account.
- $\mathbf{k}_{c}$ - Compression strength reduction factor to take instability and buckling into account.
- $\mathbf{k}_{cr}$ - Shear strength reduction factor to take the influence of cracks into account.
- $\mathbf{k}_{m}$ - Reduction factor for interaction with bending moments in both directions. The factor is set to 0.7 for rectangular cross-sections and 1.0 for other types of cross-sections.
- $\mathbf{k}_{r}$ - Bending strength reduction factor taking the effect of curved lamellas into account. The factor is set to 1 for tapered beams.
- $\mathbf{k}_{m,\alpha}$ - Strength reduction factor taking the effect of stresses parallel with the tapered edge into account. Applicable for tapered beams.
- $\mathbf{k}_{vol}$ - Volume factor used to adjust the tension strength perpendicular to the grains at the apex. Applicable for tapered, curved and boomerang beams.
- $\mathbf{k}_{dis}$ - Factor used to increase the tension strength perpendicular to the grains at the apex taking the effect of stress distribution at the apex into account. Applicable for tapered, curved and boomerang beams.
- $\mathbf{k}_{c,90}$ - Compression strength modification factor taking the load application situation into account. Chosen according to SS-EN 1995-1-1, 6.1.5.
- γ_{M} - Partial reduction coefficient for materials in ultimate limit state. For glulam the factor is set to 1.25 according to SS-EN-1995-1-1, 2.4.1.

2.5.4 Load Combinations

In accordance with SS-EN 1990 a building should be designed to fulfil requirements in both serviceability limit state and ultimate limit state. The relevant load cases treated in this thesis are described in Chapter 2.5.4.1 and 2.5.4.2 below.

2.5.4.1 Serviceability Limit State

Serviceability limit state, SLS, concerns the functionality of the building, the comfort of the users of the building as well as the appearance of how the construction works.

Equation 2.10 shows the equation for the characteristic load combination and 2.11 show the equation for the quasi-permanent load combination.

$$\Sigma G_{k,i} + Q_{k,1} + \Sigma(\Psi_{0,i} \cdot Q_{k,i}) \tag{2.10}$$

$$\Sigma G_{k,i} + \Sigma(\Psi_{2,i} \cdot Q_{k,i}) \tag{2.11}$$

Where

$G_{k,i}$ - Permanent actions.
$Q_{k,1}$ - Leading variable action.
$Q_{k,i}$ - Accompanying variable actions.
$\Psi_{0,i}$ and $\Psi_{2,i}$ - Reduction factors for loading situations with multiple variable loads. The factors are chosen according to SS-EN 1990, A1, Table A1.1 and EKS11.

2.5.4.2 Ultimate Limit State

Ultimate limit state, ULS, considers the safety of the users of the building and the safety of the building itself. ULS considers the states prior to structural collapse but is for simplicity defined as the state of actual collapse.

Equation 2.12 shows the equation for the load combinations in ULS.

$$\gamma_d \cdot (\Sigma(\gamma_G \cdot G_{k,i}) + \gamma_Q \cdot Q_{k,1} + \Sigma(\gamma_Q \cdot \Psi_{0,i} \cdot Q_{k,i})) \tag{2.12}$$

Where

G_k - Permanent actions.
$Q_{k,1}$ - Leading variable action.
$Q_{k,i}$ - Accompanying variable actions.
$\Psi_{0,i}$ - Reduction factor for loading situations with multiple variable loads. The factor is chosen according to SS-EN 1990, A1, Table A1.1 and EKS11.
γ_d - Partial coefficient to take the safety class into account. The factor is chosen according to EKS11.
γ_G - Load combination factor for the permanent actions.
γ_Q - Load combination factor for the variable actions.

The load combination factors depends on if the load is unfavorable or favourable for the specific design situation and are chosen according to table 2.2.

Table 2.2: *Load combination factors ULS*

	Permanent action, γ_G	Variable action, γ_Q
Unfavourable	1.2	1.5
Favourable	0.9	0

3
Method

In the method, the foundation for the tool and how the development of the tool has been performed is presented. Furthermore, the verification of the generated results is explained.

3.1 Foundation for the Tool

As a foundation for the creation of the tool a survey of which similar software already exists was made as well as an investigation of which optimization method would be suitable. Limitations for the tool were also clearly stated before the tool was developed.

3.1.1 Existing Environmental Software

The survey of existing software was made to investigate both how carbon dioxide equivalents per square meter building is evaluated and treated today and how parametric design is used in structural design today. The aim was to gain an understanding of how an additional tool could be constructed in order to create a contribution to the existing software.

One of the in-house software that was investigated was a software called *FENIX*. FENIX is developed in Grasshopper and the results are displayed in Rhinoceros. The software is applicable for several kind of buildings, such as multi-storey buildings as well as one-story buildings. The intention of the software is to enable closer cooperation between architects and engineers and function as a support for design decisions in the project planning phase. It gives architects a quick estimation of the amount of space the load-bearing structures occupies. Moreover, the software evaluates several solutions and their consequences from an environmental point of view in an early design stage [43].

The second in-house software that was analysed is called *Conceptualize*. This software aims to evaluate the carbon dioxide equivalents for few different structures and building materials for the same building volume and number of storeys. The software uses climate data from Boverkets climate database.

The commercial software that was investigated was a software called *One Click LCA*. One Click LCA is a software that enables life-cycle assessment calculations

as well as calculations of carbon dioxide emissions, with the aim of reducing the environmental footprint of buildings. One Click LCA can be integrated with several different design tools in order to export climate data and perform LCA-calculations. For instance the software is customized to be used in the Rhinoceros environment with Grasshopper.

With regard to this, a supplementary tool can be defined as a tool which has an optimization oriented approach regarding carbon dioxide equivalents. A tool that aims to give a first draft of an optimized load-bearing structure in an early design stage. The tool is aimed to be used by structural engineers in their field of work rather than by architects in dialog with clients.

3.1.2 Choice of Optimization Method

The optimization incorporated in the tool was performed in two separate parts. The primary optimization regards the choice of cross sections for the structural elements. This kind of structural optimization is called sizing optimization and is described further in Chapter 2.2.1.1. It is performed using a custom algorithm which evaluates a finite number of structural solutions and eventually chooses the best one, in this case the most material efficient.

Moreover, the spacing of the columns as well as the beam type can be optimized using the tool. This is an optimization of the entire structural system rather than of individual elements, making the categorization of the type of structural optimization less obvious. This optimization does however originate from the total volume of the building. The tool determines the most efficient beam type as well as placement of columns and beams, and hence the most efficient material distribution in the predefined space, making it into a kind of topology optimization. Topology optimization is further described in Chapter 2.2.1.3. When it comes to the choice of optimization algorithm for the topology optimization the selection was firstly narrowed down to the algorithms that are integrated in Grasshopper in the form of a pre-programmed component. This component is called Galapagos and is described in Chapter 2.3.2.1. Due to the finite amount of possible solutions, and hence low degree of freedom in the optimization problem the evolutionary algorithm was chosen. This algorithm is described in Chapter 2.2.2.1.

3.2 Tool Development

The optimization tool was developed in the parametric software Grasshopper. The 3D-model was created using standard components which are available in Grasshopper with dimensions for the structural elements derived from a custom component. The custom component is programmed in the Python language to perform structural calculations based on Eurocode with the aim of finding the most suitable cross sections for the structural elements. The structural elements of the two structural systems and how they are referred to in the optimization tool can be seen in Figure 3.1.

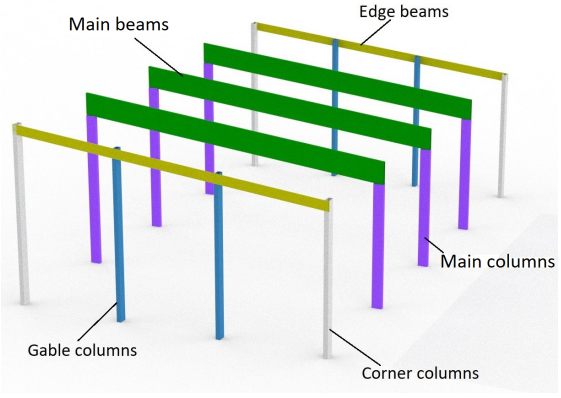

(a) System 1 - Beam with constant cross section.

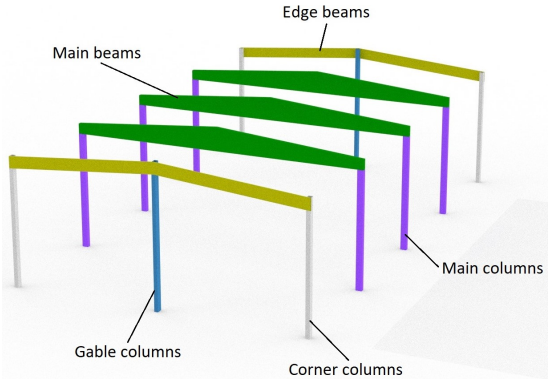

(b) System 2 - Tapered beam.

Figure 3.1: Structural elements in the structural systems.

The development of the tool was made in several steps. Firstly, the custom component was initiated by scripting a structural dimensioning algorithm of a system with roof beams with constant cross section. A 3D-model for the system was then produced. The structural capacity of this initial system was then verified before a system with tapered beams was implemented in a similar manner. An additional feature of the environmental impact of the type of roof construction used was also implemented. Lastly, the topology optimization algorithm was integrated and the tool was finalized.

3.2.1 Input and Output

The input data used in the tool can be divided into user-defined input data and internalized data. The user-defined input data is sorted into five categories. Table 3.1 shows a summary of the user-defined input data and what values it can take.

Table 3.1: *Possible values for the user-defined input data of the tool*

Geometry/dimensions	Width [m]	5 - 30
	Length [m]	10 - 50
	Height [m]	2 - 10
	Roof angle [°]	0 - 15
Structural system	Column spacing [m]	1 - 6
	Beam type [-]	1 - 2
Loading circumstances	Terrain category [-]	0 - 4
	Service class [-]	1 - 3
	Characteristic snow value [kN/m^2]	1.0 - 5.5
	Basic wind velocity [m/s]	21 - 26
	Approximate roof weight [kg/m^2]	10 - 100
	Exposure [-]	*
	Intended use of building [-]	**
Maximum utilization rates	ULS [%]	0 - 100
	SLS [%]	0 - 100
	Compression perpendicular to the grain [%]	0 - 100
Other	Include effect of roof type [-]	***
	View model [-]	Yes/No

* Windswept topography, normal topography or sheltered topography.
** Industry, school/store etc, animal stable or machine hall.
*** No, only steel roof, only timber roof or both steel and timber roof.

The height specified by the user is defined as the lowest free height indoors. The roof angle specified is altered by the custom component in the tool for the tapered beam in order to produce a more material efficient beam. The value can change by ±2 degrees. Column-spacing describes the center-to-center distance of the columns along the length of the building, i.e. between the main columns. The columns are always spaced evenly, which means that if the building length is not a multiple of the specified spacing another spacing will be chosen by the tool. This new spacing is based on the specified spacing but will be adjusted to the closest value which provides equal gaps between the columns. The gable columns are spaced evenly along the gable of the building with a predefined spacing of around six meters. This spacing varies somewhat and depends on the span length. The principle of how this spacing varies is in the same way as for the columns on the long side based on how the spacing is related to the side length of the building. The system with tapered beams always has a gable column in the middle of the gable and hence always an odd number of gable columns, whereas the other system can have both odd and even numbers of gable columns.

The beam type is chosen based on a numeric value, where 1 represents a glulam beam with constant cross section and 2 represents a tapered beam. The input category concerning the structural system can either be specified by the user or function as adjustable optimization data, which is described further in Chapter 3.2.2. The maximum utilization rates regulates how the stresses compares to the capacities of the elements and the specified utilization rates will not be exceeded. Different values

can be specified for the ultimate limit state, the serviceability state and the compression perpendicular to the fibres in the beam-column connection. *Include effect of roof type* controls if the carbon dioxide equivalents of the roof construction should be included or not. This is described further in Chapter 3.2.4. All user-defined input is explained further in Appendix A.

The internalized data contains a list of standard glulam dimensions and their corresponding strength class and relevant material data. Furthermore, the internalized data contains data concerning the type of roof construction, standard dimensions for structural timber for the purlins and load tables for the steel plates. All this data is imported from multiple excel sheets which is internalized in the Grasshopper environment. An extract of these excel sheets can be found in Appendix B. For each standard glulam dimension the sheet contains the following data:

- Width of the cross section b, [m].
- Height of the cross section h, [m].
- Characteristic shear strength f_{vk}, [Pa].
- Characteristic bending strength f_{mk}, [Pa].
- Characteristic compression strength parallel to grain f_{c0k}, [Pa].
- Characteristic compression strength perpendicular to grain f_{c90k}, [Pa].
- Characteristic tension strength perpendicular to grain f_{t90k}, [Pa].
- Mean elastic modulus E_{mean}, [Pa].
- Elastic modulus $E_{0.05}$, [Pa].
- Mean shear modulus G_{mean}, [Pa].
- Shear modulus $G_{0.05}$, [Pa].
- Mean density ρ_{mean}, [kg/m^3].
- Characteristic density ρ_k, [kg/m^3].

The internalized data concerning the roof construction consist of two excel sheets. The sheet about standard dimensions of structural timber consist of the height and width of the cross section. The second sheet contains load tables of the steel plates. The tables are categorized by the magnitude of the snow load, span, thickness of the steel panel, weight of the roof plate and the name of the roof types.

The output of the optimization tool is a 3D-model of the chosen structural system as well as information about the individual structural elements. The type of beam is clearly stated together with the dimensions of each element and the chosen center-to-center distance. For the main columns it is stated if a strengthened connection between the beam and the column is required to withstand the compression perpendicular to the fibres in the beams. The volume of glulam used for the structural system is specified together with the carbon dioxide equivalents per square meter building. If the user chose to include the effect of the roof type a short summary of the roof construction will be shown. Two examples of the output is shown in Figure 3.2 and 3.3.

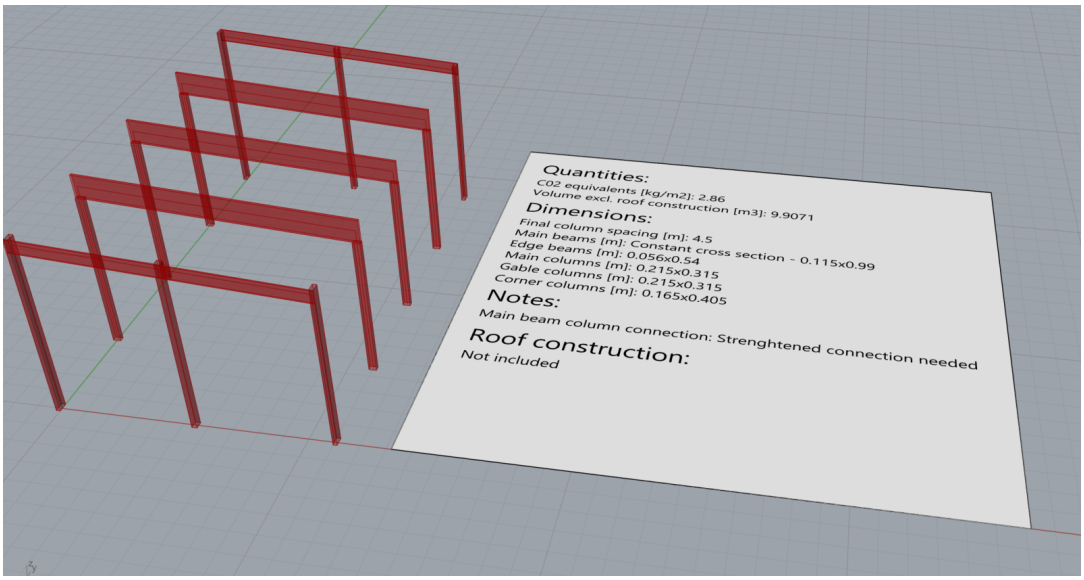

Figure 3.2: Output from the tool for a system with beams with constant cross section.

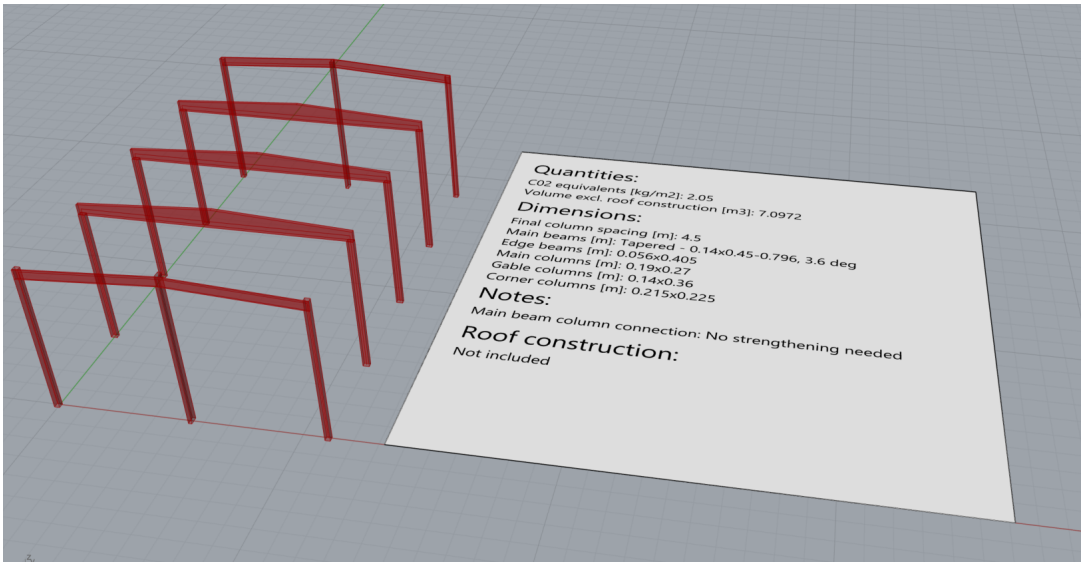

Figure 3.3: Output from the tool for a system with tapered beams.

3.2.2 Flowchart of the Custom Sizing Component

Figure 3.4 shows the flowchart for the generation of the dimensions of the structural members, which is scripted in a custom Python component in Grasshopper. The component has the internalized data as well as the user-defined data as input. These input categories are described further in Chapter 3.2.1. The component generates a sizing of the different structural members described in Figure 3.1. Furthermore, the component will compute the total volume of the final structure as well as the carbon dioxide equivalents per square meter building.

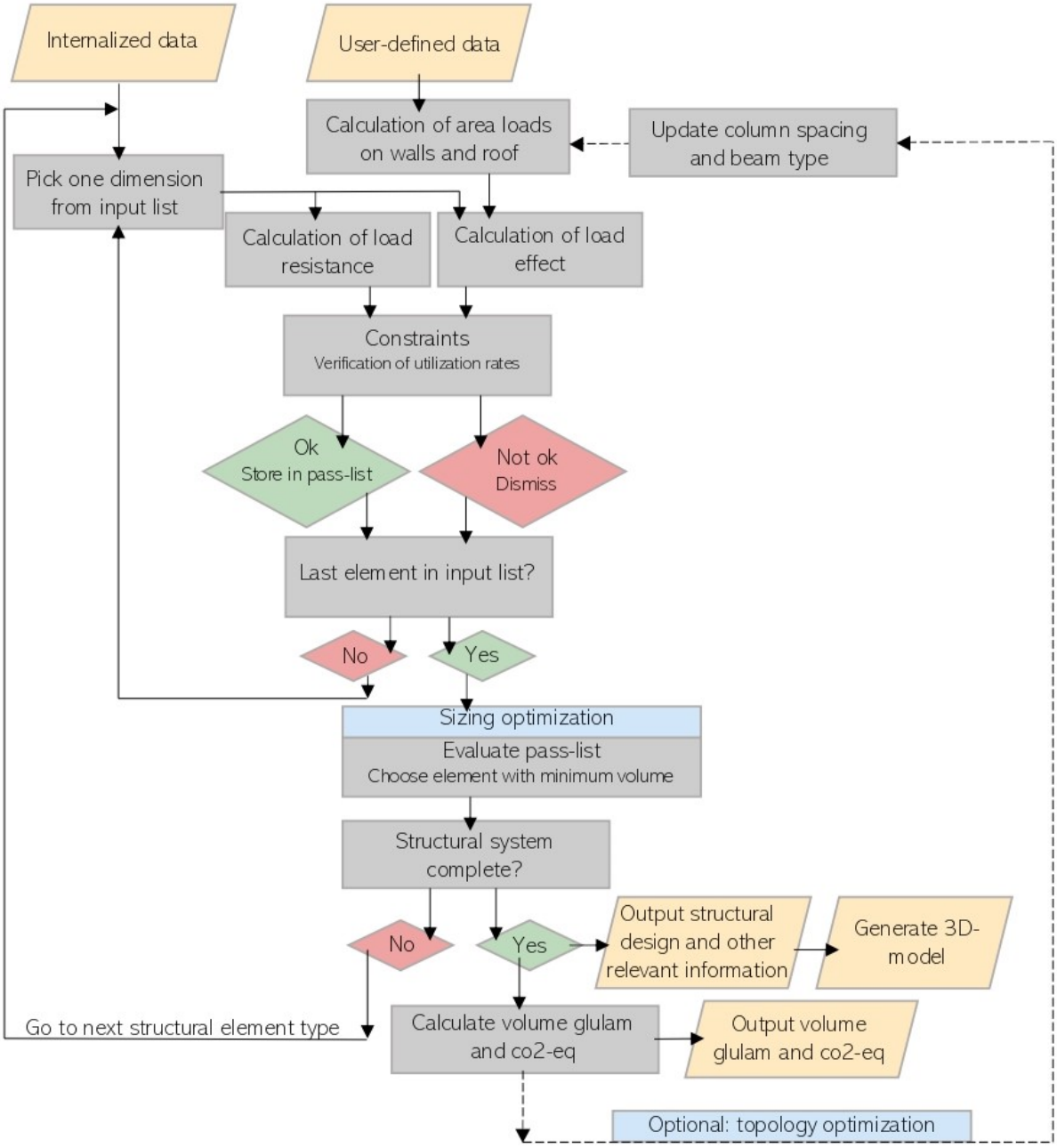

Figure 3.4: Flowchart for the optimization.

The optimization tool contains two kinds of optimizations, where one is always performed and one is optional. The main optimization, which is always performed, is a sizing optimization of the structural members. The secondary optimization, which is optional, is a topology optimization that adjusts the column spacing and beam type to find the most optimized structural system with regard to carbon dioxide equivalents per square meter building. The topology optimization should not be performed if the user has specific requirements of the column spacing and beam type, as the topology optimization may change these. If the user wishes to perform the topology optimization the user-defined input in the category *structural system* does not have to be defined. The optimization algorithm will choose these

values after the optimization is run. To generate a structure with both sizing and topology optimization the user has to provide the required input data and start the optimization algorithm. Thereafter the optimization runs until an optimal solution has been found and the user is provided with an optimized structural system. If the user however only wishes to perform the sizing optimization the system will be generated instantly based on the user-defined input data without having to start an optimization algorithm.

Firstly, the calculations of the distributed area loads on the roof and walls are carried out, such as the dead-weight of the roof construction, the wind load and the snow load. Thereafter, the sizing of the different structural members is executed. The sizing is performed element by element. It starts out with the main beams, followed by the edge beams, main columns, gable columns and lastly the corner columns. The beams are dimensioned before the columns in order to find the total load from the complete roof structure including the weight of the beam, which will act on and effect the size of the columns. For each sizing of all structural members, the calculations loops through the standard dimensions of glulam members with related material properties and calculates the load effect and resistance of each cross section. The load effect includes calculations of several load combinations that involves self-weight, snow load and wind load. The resistance is calculated based on the material properties and cross section dimensions. Each structural member is then controlled for relevant constraints and is saved in a list if all criteria are passed. If any criterion is not fulfilled the dimension will be dismissed. The constraints for each element are explained further in Chapter 3.2.3. An evaluation is made of all stored cross sections and the cross section with minimum volume is chosen before the algorithm moves on to the next structural element. If the input results in a situation where non of the provided standard dimension can withstand the loads, the component will not perform the dimensioning of the rest of the structural elements and the only output will be that no structural system fulfils the requirements. This situation is illustrated in Figure 3.5.

The only exception to the flowchart is if the compression perpendicular to the grain in the beams is larger than the capacity. This depends on the contact area between the column and the beam and hence on the cross sectional height of the column. If this is the case a check will be made to see if switching to a slightly wider beam but keeping the smaller column will give smaller volume than keeping the beam and switching to a larger column. This is explained further in Chapter 3.2.3.3.

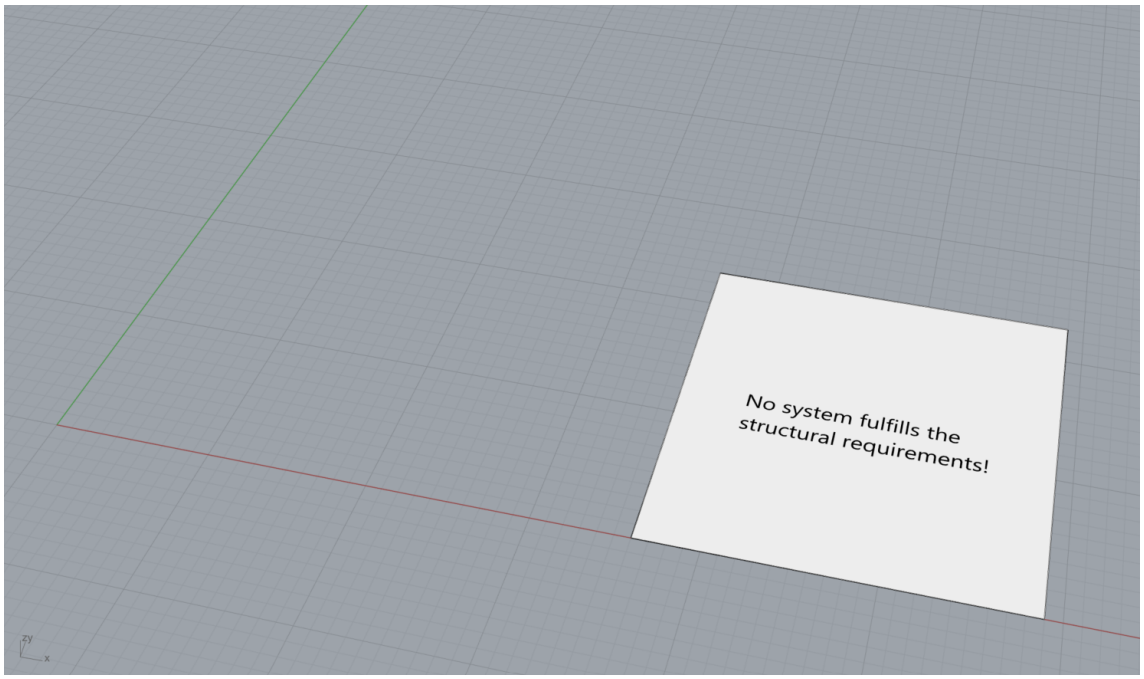

Figure 3.5: The output when one or more structural elements cannot withstand the applied loads.

3.2.3 Structural Models and Constraints

In the following subsections the structural models will be presented for the structural elements. The constraints and assumptions that are used in the design of members will be further described.

3.2.3.1 Beam with Constant Cross Section

Figure 3.6 shows the structural model that is used for designing the beams with constant cross section, both the edge and the main beams. The beams are considered to be simply supported. The loads that act on the beam are self-weight, snow load and wind load. The self weight includes the weight of the beam and weight of the roof construction including the secondary load-bearing structure, insulation and sheeting layers. The distributed loads, $q_{d,1}$ and $q_{d,2}$ are calculated according Chapter 2.5.4. Their distribution depends on the sizes of the wind zones, according to SS-EN 1991-1-4. The safety class is chosen to class 3, since this is the most conservative one. The loads are re-calculated to act perpendicular to the surface. The design includes constraints both in the ultimate limit state and serviceability limit state.

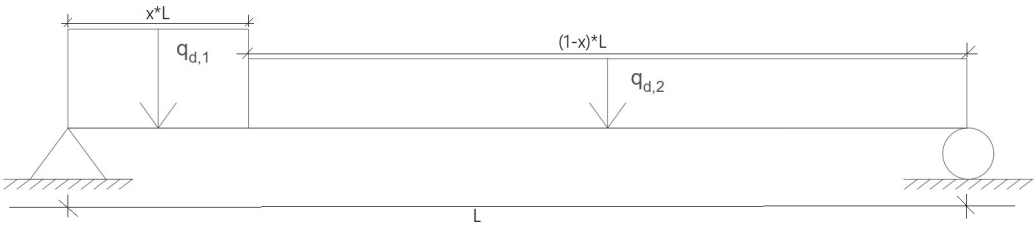

Figure 3.6: Structural model for beams with constant cross section. The size of x depends on the sizes of the wind zones, according to SS-EN 1991-1-4.

3.2.3.1.1 Design in Ultimate Limit State

The design of the beams in ultimate limit state is governed by bending moment, shear force and compression stress perpendicular to the grain, according to Equation 3.1, Equation 3.5 and 3.19.

The moment capacity of the cross section for the main and edge beams is verified to fulfill the constraint in Equation 3.1.

$$M_{Ed} \leq f_{md} \cdot W_y \cdot k_{crit} \tag{3.1}$$

where

M_{Ed} - Design load effect from bending moment [Nm].
f_{md} - Dimensioning bending strength [Pa].
W_y - Section modulus about the strong axis y [m^3].
k_{crit} - Factor considering lateral torsional buckling [-].

The factor considering lateral torsional buckling is calculated according Equation 3.2. If an element is restrained against lateral torsional buckling the factor is set to one.

$$k_{crit} = \begin{cases} 1.0 & \text{for } \lambda_{rel,m} \leq 0.75 \\ 1.56 - 0.75 \cdot \lambda_{rel,m} & \text{for } 0.75 < \lambda_{rel,m} \leq 1.4 \\ \frac{1}{\lambda_{rel,m}^2} & \text{for } 1.4 < \lambda_{rel,m} \end{cases} \tag{3.2}$$

where

$\lambda_{rel,m}$ - Relative slenderness ratio in bending [-].

The relative slenderness ratio is calculated according to Equation 3.3.

$$\lambda_{rel,m} = \sqrt{\frac{f_{md}}{\sigma_{m,crit}}} \tag{3.3}$$

where

$\sigma_{m,crit}$ - Critical bending stress [Pa].

The critical bending stress is calculated according to Equation 3.4.

$$\sigma_{m,crit} = \frac{\pi\sqrt{E_{0.05} \cdot I_z \cdot G_{0.05} \cdot I_{tor}}}{l_{ef} \cdot W_y} \tag{3.4}$$

where

$E_{0.05}$ - 5th percentile value of modulus of elasticity [Pa].
$G_{0.05}$ - 5th percentile value of shear modulus [Pa].
I_z - Second moment of inertia about the weak axis z [m^4].
I_{tor} - Torsional moment of inertia [m^4].
l_{ef} - Effective length depending on support conditions and load configuration [m].

The effective length is calculated according to EN 1995-1-1_2004 6.3.3. The value is based on simply supported boundary conditions and a uniformly distributed load, both for the edge and main beams. Moreover, the length is decreased by 0.5·h due to load application at the tension edge of the beams. The torsional moment of inertia is calculated based on an interpolation curve that is established from data points according to Appendix E.

The shear capacity of both the main beams and edge beams is controlled according to Equation 3.5.

$$V_{Ed} \leq \frac{f_{vd} \cdot A \cdot k_{cr}}{1.5} \tag{3.5}$$

where

V_{Ed} - Design load effect from shear force [N].
f_{vd} - Design shear strength [Pa].
A - Area of the cross section [m^2].
k_{cr} - Reduction factor considering influence of cracks [-].

$$k_{cr} = min \begin{cases} \frac{3.0}{f_{vk}} \\ 1.0 \end{cases} \tag{3.6}$$

3.2.3.1.2 Design in Serviceability Limit State

The design of the beams in serviceability limit state is governed by the instantaneous deflection limit and the final deflection limit. The deflection limits are based on the

area of usage for the building, which is specified by the user.

The constraint for the instantaneous deflection is controlled according to Equation 3.7, with characteristic load combinations, according Chapter 2.5.4. The beams are assumed to be fabricated with a precambering. Consequently, the instantaneous deflection caused by the self-weight of the beam is neglected and the deflection limit is reduced by the factor $\frac{1}{1.5}$, as seen in Equation 3.7 and Equation 3.8.

$$w_{inst,q} \leq \frac{l}{X \cdot 1.5} \tag{3.7}$$

where

$w_{inst,q}$ - Total instantaneous deflection for variable load [m].
l - Length of the span [m].
X - Value based on the area of usage [-].

The constraints for the final deflection is controlled according Equation 3.8, with quasi-permanent load combinations according to Chapter 2.5.4.

$$w_{inst,g} \cdot k_{def} + w_{inst,q} \cdot (1 + \psi_2 \cdot k_{def}) \leq \frac{l}{X \cdot 1.5} \tag{3.8}$$

where

$w_{inst,g}$ - Total instantaneous deflection for permanent load [m].
k_{def} - Deformation factor [-].
ψ_2 - Reduction factor [-].
X - Value based on the area of usage [-].

3.2.3.2 Tapered Beam

The structural model that is used for the design of the tapered beam is shown in Figure 3.7. The beam is considered to be simply supported. The loads that act on the beam are self-weight, snow load and wind load. The loads are simplified to a uniformly distributed load, q_d, that is considered to act vertically. The load combinations are calculated according to Chapter 2.5.4. The loads are re-calculated to act vertically. The design contains constraints in both ultimate limit state and serviceability limit state.

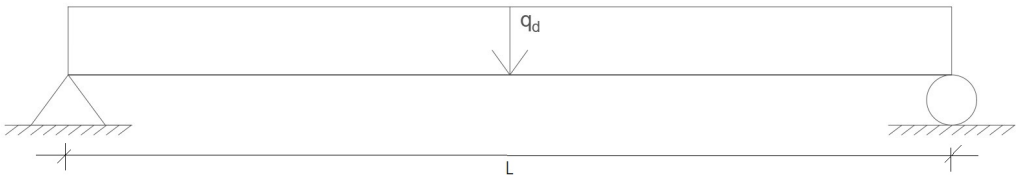

Figure 3.7: Structural model for the tapered beam.

3.2.3.2.1 Design in Ultimate Limit State

The design in ultimate limit state is governed by bending moment, shear force, compression stress perpendicular to the grain and tension stress perpendicular to the grain. The constraint for the shear force is controlled according to Equation 3.5 and the compression stress perpendicular to the grain is controlled according to Equation 3.19.

The bending moment is controlled both in the critical section and at the apex, according to Equation 3.9 and Equation 3.10.

$$M_{Ed,0} \leq f_{md} \cdot W_{y,0} \cdot k_{m,\alpha} \cdot k_{crit} \tag{3.9}$$

$$M_{Ed,ap} \cdot k_l \leq f_{md} \cdot W_{y,ap} \cdot k_{crit} \cdot k_r \tag{3.10}$$

where

$M_{Ed,0}$ - Design load effect in critical section [Nm].
$M_{Ed,ap}$ - Design load effect at the apex [Nm].
f_{md} - Dimensioning bending strength [Pa].
$W_{y,0}$ - Section modulus about the strong axis y, in critical section [m^3].
$W_{y,ap}$ - Section modulus about the strong axis y, at the apex [m^3].
$k_{m,\alpha}$ - Factor considering the tapered edge [-].
k_{crit} - Factor considering lateral torsional buckling [-], Equation 3.2.
k_l - Correction factor [-].
k_r - Modification factor considering the lamination curvature [-].

The modification factor, k_r, is equal to one for tapered beams. The factor considering the tapered edge is calculated according to Equation 3.11.

$$k_{m,\alpha} = \begin{cases} \frac{1}{\sqrt{1+(\frac{f_{m,d}}{0.75 \cdot f_{v,d}} \cdot tan\alpha)^2+(\frac{f_{m,d}}{f_{t,90,d}} \cdot tan^2\alpha)^2}} & \text{for tensile stresses at the tapered edge} \\ \frac{1}{\sqrt{1+(\frac{f_{m,d}}{1.5 \cdot f_{v,d}} \cdot tan\alpha)^2+(\frac{f_{m,d}}{f_{c,90,d}} \cdot tan^2\alpha)^2}} & \text{for compressive stresses at the tapered edge} \end{cases} \tag{3.11}$$

where

f_{md} - Dimensioning bending strength [Pa].
f_{vd} - Dimensioning shear strength [Pa].
$f_{t,90d}$ - Dimensioning tension strength perpendicular to the grain [Pa].
$f_{c,90d}$ - Dimensioning compression strength perpendicular to the grain [Pa].
α - Inclination of the tapered edge [°].

The correction factor, k_l, is calculated according Equation 3.12.

$$k_l = 1 + 1.4 \cdot tan\alpha + 5.4 \cdot tan^2\alpha \tag{3.12}$$

where
α - Inclination at the apex-zone [°].

The constraint for the tension perpendicular to the grain at the apex is verified by Equation 3.13.

$$M_{Ed,ap} \leq \frac{f_{t,90d} \cdot W_{y,ap} \cdot k_{dis} \cdot k_{vol}}{k_p} \tag{3.13}$$

where

$M_{Ed,ap}$ - Load effect at the apex [Nm].
$f_{t,90d}$ - Dimensioning tension strength perpendicular the the grain [Pa].
$W_{y,ap}$ - Section modulus about the strong axis y, at the apex [m^3].
k_{dis} - Modification factor that accounts for stress distribution in the apex zone [-].
k_{vol} - Volume factor [-].
k_p - Correction factor [-].

The modification factor, k_{dis}, is set to 1.4 for tapered beams. The volume factor, k_{vol}, is calculated by Equation 3.14.

$$k_{vol} = \left(\frac{V_0}{V}\right)^{0.2} \tag{3.14}$$

where

V_0 - Reference volume of 0.01 [m^3].
V - The stressed volume in the apex zone hence not greater than $\frac{2}{3}$ of the total volume [m^3].
The correction factor, k_p, is calculated according to Equation 3.15.

$$k_p = 0.2 \cdot tan(\alpha_{ap}) \tag{3.15}$$

where

α_{ap} - Angle of the tapered edge [°].

3.2.3.2.2 Design in Serviceability Limit State

The design of the tapered beam in serviceability limit state is based on similar principles as for the beam with constant cross section. For instance, the tapered beam is also assumed to be fabricated with a precambering. However, the constraints for the instantaneous deflection and the final deflection for a tapered beam are checked according to Equation 3.16 and Equation 3.17. The instantaneous deflection is controlled for the characteristic load combination and the final deflection is controlled for the quasi-permanent load combination.

$$w_{inst} = w_{inst,q} \cdot k_m \leq \frac{l}{X \cdot 1.5} \tag{3.16}$$

where

w_{inst} - Total instantaneous deflection [m].
$w_{inst,q}$ - Total instantaneous deflection for variable load [m].
k_m - Modification factor [-].
X - Value based on the area of usage [-].
l - Length of the span [m].

$$w_{fin} = w_{inst,g} \cdot k_{def} \cdot k_m + w_{inst,q} \cdot (1 + \psi_2 \cdot k_{def}) \cdot k_m \leq \frac{l}{X \cdot 1.5} \tag{3.17}$$

where

w_{fin} - Total final deflection [m].
$w_{inst,g}$ - Instantaneous deflection for permanent load [m].
$w_{inst,q}$ - Instantaneous deflection for variable load [m].
k_{def} - Deformation factor [-].
k_m - Modification factor [-].
ψ_2 - Reduction factor [-].
l - Length of the span [m].
X - Value based on the area of usage [-].

The modification factor, k_m, is calculated according to Equation 3.18.

$$k_m = \left(\frac{h}{h_{ap}}\right)^3 \cdot \frac{1}{0.15 + 0.85 \cdot \frac{h}{h_{ap}}} \tag{3.18}$$

where

h - The edge cross section height [m].
h_{ap} - The cross section height at the apex [m].

3.2.3.3 Columns

Figure 3.8 shows the structural model for the three different column elements - main columns and gable columns, Figure 3.8a, as well as corner columns, Figure 3.8b. The columns are assumed to have a pinned connection at the bottom and a horizontal vertical support at the top. The weight of the roof construction, the snow and wind load which act on the roof results in a point load, P_{roof}, applied on top of the column. The cross-bracing results in another point load, P_{brace} , which is also applied on the top of the column. The self-weight of the column together with the point load result in a compressive normal force in the column. The main and gable columns have uniformly distributed wind loads, $q_{d,y}$. The corner column has two uniformly distributed wind loads, $q_{d,y}$ and $q_{d,z}$, applied in two different directions. The load combinations are calculated according to Chapter 2.5.4. The design involves constraints in the ultimate limit state.

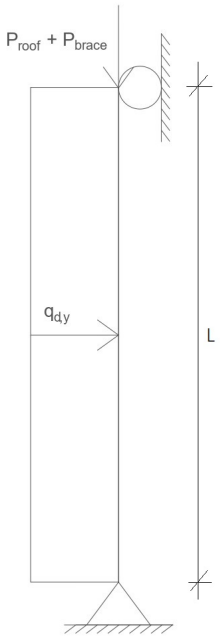

(a) Structural model for main and gable columns.

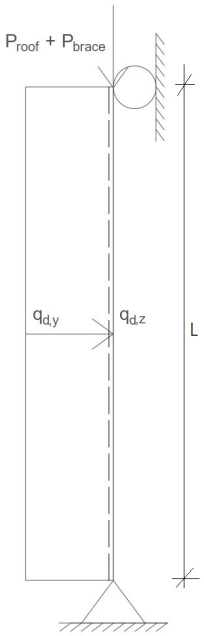

(b) Structural model for corner columns.

Figure 3.8: Structural model for corner columns.

The compressive force perpendicular to the grain in both the main beams and edge beams is controlled at the two supports, according to Equation 3.19. This is a verification of the beams but it is highly dependant on the contact area between the column and the beam and can hence not be checked until after the beam size is chosen and paired with a column height. If the constraint is not fulfilled for the main beam an additional verification is made for a strengthened connection, according to Chapter 3.2.3.4. The edge beams have a slightly different connection to the columns than the main beams. They are partially screwed into the side of the columns and partially resting on the top of them. This causes some of the applied force to be handled by a screwed connection at all times, thus lowering N_{c90Ed}. This connection is further explained in Chapter 3.2.3.5.

$$N_{c90Ed} \leq f_{c90d} \cdot h_c \cdot b \cdot k_{c90} \tag{3.19}$$

where

N_{c90Ed} - Design load effect from compression perpendicular to the grain [N].
f_{c90d} - Dimensioning compression strength perpendicular to grain [Pa].
h_c - Height of the column [m].
b - Width of the beam [m].
k_{c90} - Factor considering load configuration and degree of compressive deformation [-].

If the check for the compression perpendicular too the grains in the beam is not fulfilled after the connection is strengthened the tool will calculate how wide the beam has to be in order to fulfil the demands. The list with the approved beams will then be evaluated again and the beam with the smallest volume which has a width that is equal to or larger than the calculated lowest value will be chosen. The tool will then perform all the other relevant checks and evaluate which combination of approved beam and column will give the lowest volume.

3.2.3.3.1 Design in Ultimate Limit State

The constraints that are verified in the ultimate limit state are governed by normal force, shear force and combined axial compression and bending.

The axial compression is verified by Equation 3.20 for all three column types.

$$N_{Ed} \leq f_{c,0d} \cdot A \cdot k_c \tag{3.20}$$

where

N_{Ed} - Design load effect from normal force [N].
$f_{c,0d}$ - Dimensioning compressive strength parallel to the grain [Pa].
A - Area of the cross section [m^2].

k_c - Modification factor that accounts for instability effects [-].

The modification factor that considers instability effects is calculated according to Equation 3.21. If the columns are considered to be braced against buckling the factor k_c is set to one.

$$k_c = \frac{1}{k + \sqrt{k^2 - \lambda_{rel}^2}} for 0.3 \leq \lambda_{rel} \tag{3.21}$$

where

$k = 0.5 \cdot (1 + \beta_c \cdot (\lambda_{rel} - 0.3) + \lambda_{rel}^2)$, where $\beta_c = 0.1$ for glulam
λ_{rel} - Relative slenderness [-].

The relative slenderness is calculated according to Equation 3.22.

$$\lambda_{rel} = \frac{l_e}{\pi \cdot \sqrt{\frac{I}{A}}} \cdot \sqrt{\frac{f_{c,0k}}{E_{0,05}}} \tag{3.22}$$

where

l_e - Buckling length [m].
I - Moment of inertia [m^3].
A - Area of the cross section [m^2].
$f_{c,0k}$ - Characteristic compression strength parallel to the grain [Pa].
$E_{0.05}$ - 5th percentile value of modulus of elasticity [Pa].

All three columns types, main columns, gable columns and corner columns, are verified for shear force by Equation 3.23.

$$V_{Ed} \leq \frac{f_{vd} \cdot A \cdot k_{cr}}{1.5} \tag{3.23}$$

where

V_{Ed} - Design load effect from shear force [N].
f_{vd} - Design shear strength [Pa].
A - Area of the cross section [m^2].
k_{cr} - Reduction factor considering influence of cracks [-], Equation 3.6.

The combined axial compression and bending without risk for buckling, i.e. when $\lambda_{rel} \leq 0.3$, need to fulfill the requirements in Equation 3.24 and Equation 3.27. The two constraints are controlled for all three column types. Additionally, for the main and gable columns that only have one uniformly distributed wind load which acts in the y-direction, the load effect in the z-direction is set to zero.

$$\frac{M_{y,Ed}}{M_{y,Rd}} + \cdot k_m \cdot \frac{M_{z,Ed}}{M_{z,Rd}} + \left(\frac{N_{c,0Ed}}{N_{c,0Rd}}\right)^2 \leq 1 \tag{3.24}$$

$$k_m \cdot \frac{M_{y,Ed}}{M_{y,Rd}} + \cdot \frac{M_{z,Ed}}{M_{z,Rd}} + \left(\frac{N_{c,0Ed}}{N_{c,0Rd}}\right)^2 \leq 1 \tag{3.25}$$

where

$M_{y,Ed}$,$M_{z,Ed}$ - Design load effect of moment about the y- and z-axis [Nm].
$M_{y,Rd}$,$M_{z,Rd}$ - Design load capacity of moment about the y- and z-axis [Nm].
$N_{c,0Ed}$ - Design load effect of normal force [N].
$N_{c,0Rd}$ - Design load capacity of normal force [N].
k_m - Modification factor, k_m=0.7 for beams with rectangular cross section [-].

If there is a risk of buckling, i.e when $\lambda_{rel} \geq 0.3$, the effect from the interaction of axial load and moment needs to fulfill the requirements in Equation 3.26 and Equation 3.27. The constraints are verified for both the main and gable columns.

$$\frac{M_{y,Ed}}{M_{y,Rd}} + \cdot k_m \cdot \frac{M_{z,Ed}}{M_{z,Rd}} + \frac{N_{c,0Ed}}{k_{c.y} \cdot N_{c,0Rd}} \leq 1 \tag{3.26}$$

$$k_m \cdot \frac{M_{y,Ed}}{M_{y,Rd}} + \cdot \frac{M_{z,Ed}}{M_{z,Rd}} + \frac{N_{c,0Ed}}{k_{c.z} \cdot N_{c,0Rd}} \leq 1 \tag{3.27}$$

where

$M_{y,Ed}$,$M_{z,Ed}$ - Design load effect of moment about the y- and z-axis [Nm].
$M_{y,Rd}$,$M_{z,Rd}$ - Design load capacity of moment about the y- and z-axis [Nm].
$N_{c,0Ed}$ - Design load effect of normal force [N].
$N_{c,0Rd}$ - Design load capacity of normal force [N].
k_m - Modification factor [-].
$k_{c,y}$,$k_{c,z}$ - Modification factor that accounts for instability effects [-], Equation 3.21.

The constraints that consider the effect of lateral torsional buckling and the combined effect of axial load and bending is verified with Equation 3.28 and Equation 3.29.

$$\left(\frac{M_{y,Ed}}{k_{crit} \cdot M_{y,Rd}}\right)^2 + \frac{N_{c,0Ed}}{k_{c.z} \cdot N_{c,0Rd}} \leq 1 \tag{3.28}$$

$$\frac{M_{y,Ed}}{k_{crit} \cdot M_{y,Rd}} \leq 1 \tag{3.29}$$

where

$M_{y,Ed}$ - Design load effect of moment about the y-axis [Nm].
$M_{y,Rd}$- Design load capacity of moment about the y-axis [Nm].
$N_{c,0Ed}$ - Design load effect of normal force [N].
$N_{c,0Rd}$ - Design load capacity of normal force [N].

k_{crit} - Modification factor considering lateral torsional buckling [-], Equation 3.2.
$k_{c,y}$,$k_{c,z}$ - Modification factor that accounts for instability effects [-], Equation 3.21.

3.2.3.4 Strengthening of Connection

If the constraint for compression perpendicular to the grain of the beams, which is described in Equation 3.19, is not fulfilled a rough verification of the possibility of strengthening the connection between the beam and the column is done. This check is only applied on the connection between the main beams and main columns. The strengthening is performed by inserting a steel plate between the column and the beam and fastening it to the beam with four self-drilling wood screw. The principle of the applied strengthening method is illustrated in figure 3.9.

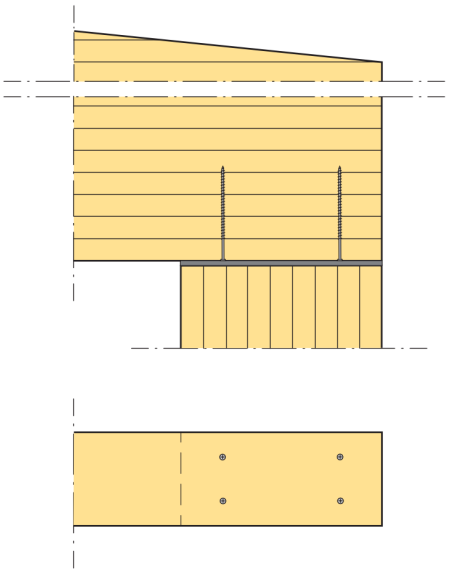

Figure 3.9: Strengthening of connection between beam and column [44].

Firstly the largest possible screw dimension which fits the contact area of the connection is chosen. The requirement set is to not exceed the minimum edge distances provided in SS-EN 1995-1-1:2004, 8.7.2. If no screw fits the contact area the connection cannot be strengthened according to this method and the tool rejects the solution. For the connections that need strengthening and where strengthening is possible a minimum thickness of the plate is calculated. If this thickness exceeds 20 mm the tool rejects the solution. If the solution is not rejected the capacity of the wooden screws is calculated as the minimum of the buckling capacity of the screws and the capacity for penetration perpendicular to the grains of beam. The buckling capacity if calculated according to Equation 3.30 and the penetration capacity is calculated according to Equation 3.36.

$$R_{kl,k} = k_c \cdot \left(\frac{\pi \cdot d_m^2}{4} \right) \cdot f_{y,k} \tag{3.30}$$

where

$R_{kl,k}$ - Buckling capacity of screws [N].
k_c - Reduction factor for buckling [-].
d_m - Inner thread diameter [m].
$f_{y,k}$ - Yield strength of the screw [N/m^2].

The reduction factor for buckling is calculated according to Equation 3.31.

$$k_c = \begin{cases} 1 & \text{for } \lambda_{rel} \leq 0.2 \\ \left(k + \sqrt{k^2 - \lambda_{rel}^2}\right)^{-1} & \text{for } \lambda_{rel} > 0.2 \end{cases} \tag{3.31}$$

where
λ_{rel} - Relative slenderness ratio [-].
k = 0.5 $(1 + 0.49 \cdot (\lambda_{rel} - 0.2) + \lambda_{rel}^2)$

The relative slenderness ratio is calculated according to Equation 3.32.

$$\lambda_{rel} = \frac{N_{pl}}{N_{cr}} \tag{3.32}$$

where

N_{pl} - Capacity related to yielding of the screw [N].
N_{cr} - Capacity related to buckling of the screw [N].

The capacity related to yielding of the screw and the capacity related to buckling of the screw are calculated according to Equation 3.33 and 3.34, respectively.

$$N_{pl} = \frac{\pi \cdot d_m^2}{4} \cdot f_{y,k} \tag{3.33}$$

where

d_m - Inner thread diameter [m].
$f_{y,k}$ - Yield strength of the screw [N/m^2].

$$N_{cr} = \sqrt{c_h \cdot E_s \cdot I_s} \tag{3.34}$$

where

c_h - Factor for horizontal stiffness.
E_s - Modulus of elasticity for the screw [N/m^2].
I_s - Moment of inertia for the screw [m^4].

The factor for horizontal stiffness is calculated according to Equation 3.35.

$$c_h = (0.19 + 0.012 \cdot d) \cdot \rho_k \tag{3.35}$$

where

d - Outer thread diameter [m].
ρ_k - Characteristic density of the beam [kg/m^3].

$$F_{ax,k,Rk} = \frac{f_{ax,k} \cdot d \cdot l_{ef} \cdot k_d}{1.2 \cdot cos^2(\alpha) + sin(\alpha)} \tag{3.36}$$

where

$F_{ax,k,Rk}$ - Capacity for penetration perpendicular to the grains of beam [N].
$f_{ax,k}$ - Characteristic withdrawal strength perpendicular to the grain [N/mm^2].
d - Outer thread diameter [mm].
l_{ef} - Length of the threaded part of the screw [mm].
α - Angle between the screw axis and grain direction with $\alpha \geq 30°$ [°].
$k_d = min \begin{cases} \frac{d}{8} \\ 1 \end{cases}$ [-].

The characteristic withdrawal strength perpendicular to the grain is calculated according to Equation 3.37

$$f_{ax,k} = 0.52 \cdot d^{-0.5} \cdot l_{ef}^{-0.1} \cdot \rho_k^{0.8} \tag{3.37}$$

where

d - Outer thread diameter [mm].
l_{ef} - Length of the threaded part of the screw [mm].
ρ_k - Characteristic density of the timber in the beam [kg/m^3].

The characteristic capacity of the strengthened connection is calculated according to Equation 3.38 and the dimensioning capacity is calculated according to the method described in Chapter 2.5.3.

$$R_{90,k} = min \begin{cases} k_{c90} \cdot b_b \cdot l_{ef,1} \cdot f_{c90k} + n \cdot R_k \\ b_b \cdot l_{ef,2} \cdot f_{c90k} \end{cases} \tag{3.38}$$

where

$R_{90,k}$ - Characteristic capacity of the strengthened connection [N].
k_{c90} - Magnification factor = 1.75 [-].
b_b - Width of the beam [m].

f_{c90k} - Characteristic compression strength perpendicular to the grains [Pa].
n - Number of screws [-].
R_k - Capacity of the wooden screws [N].
$l_{ef,1}$ - Effective length 1, see Figure 3.10 [m].
$l_{ef,2}$ - Effective length 2, see Figure 3.10 [m].

The effective lengths $l_{ef,1}$ and $l_{ef,2}$ are caluculated according to Equation 3.39 and 3.40, respectively.

$$l_{ef,1} = l_{sup} + 0.030 \tag{3.39}$$

where

l_{sup} - Length of the support, see Figure 3.10 [m].

$$l_{ef,2} = l_{sup} + 0.25 \cdot l_{ef} \cdot e^{3.3 \cdot \frac{l_{lef}}{h_b}} \tag{3.40}$$

where

l_{sup} - Length of the support, see Figure 3.10 [m].
l_{ef} - Length of the threaded part of the screw [m].
h_b - Height of the beam [m].

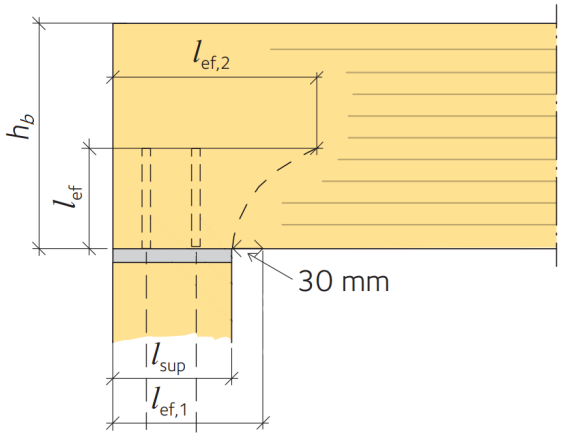

Figure 3.10: Illustration of effective lengths in strengthened connection [44].

If the new strengthened capacity gives a utilization rate of less than 100 percent for the compression perpendicular to the grains of the beam the solution is accepted and the tool will notify the user if a strengthening is needed. This check functions as a rough estimation and the information that is output regarding the strengthening of

the connection is limited to only if it is needed or not and does not include specific measurements and dimensions.

3.2.3.5 Connection Edge Beam

The connection between the edge beams and the gable columns follows the same principle as the connection between the edge beams and the corner columns. The beam is placed on a notch in the column and is partially screwed to and partially resting on the column. The principle is illustrated in Figure 3.11. The verification for the part of the connection that causes compression perpendicular to the grains in the beam is described in Chapter 3.2.3.3. The characteristic capacity of the screwed part of the connection is calculated according to Equation 3.41 and the dimensioning capacity is calculated according to the method described in Chapter 2.5.3.

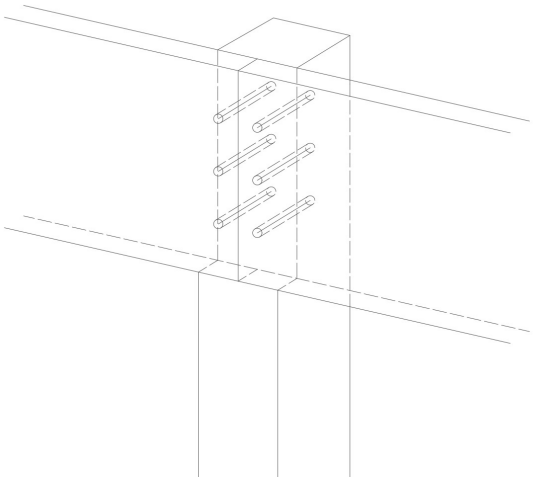

Figure 3.11: Illustration of the principle of the beam-column connection for the edge beams.

$$F_{v,Rk} = n{\cdot}min \begin{cases} f_{h,1,k} \cdot t_1 \cdot d \\ f_{h,2,k} \cdot t_2 \cdot d \\ \frac{f_{h,1,k} \cdot t_1 \cdot d}{1+\beta} \left(\sqrt{\beta + 2 \cdot \beta^2 \cdot \left(1 + \frac{t_2}{t_1} + \left(\frac{t_2}{t_1}\right)^2\right) + \beta^3 \cdot \left(\frac{t_2}{t_1}\right)^2} - \beta \left(1 + \frac{t_2}{t_1}\right) \right) \\ 1.05 \cdot \frac{f_{h,1,k} \cdot t_1 \cdot d}{2+\beta} \left(\sqrt{2 \cdot \beta \cdot (1+\beta) + \frac{4 \cdot \beta \cdot (2+\beta) \cdot M_{y,Rk}}{f_{h,1,k} \cdot d \cdot t_1^2}} - \beta \right) \\ 1.05 \cdot \frac{f_{h,1,k} \cdot t_2 \cdot d}{2+\beta} \left(\sqrt{2 \cdot \beta^2 \cdot (1+\beta) + \frac{4 \cdot \beta \cdot (1+2 \cdot \beta) \cdot M_{y,Rk}}{f_{h,1,k} \cdot d \cdot t_2^2}} - \beta \right) \\ 1.15 \cdot \sqrt{\frac{2 \cdot \beta}{1+\beta}} \cdot \sqrt{2 \cdot M_{y,Rk} \cdot f_{h,1,k} \cdot d} \end{cases} \tag{3.41}$$

where

n - Number of screws in connection [-].
$f_{h,i,k}$ - Characteristic embedment strength in timber member i [MPa].

t_i - Thickness of member i [mm].
d - Diameter of fastener[mm].
β - Ratio between the embedment strengths of the two members [-].
$M_{y,Rk}$ - Characteristic yield moment in the fastener [Nmm].

The screws are always placed in two columns with a varying number of rows. The maximum number of screws are eight in each column, making it a total of 16 screws. The number of screws are however regulated in order to not exceed the minimum edge distances provided in SS-EN 1995-1-1:2004, 8.7.

The characteristic embedment strength is calculated according to Equation 3.43.

$$f_{h,k} = \frac{0.082 \cdot (1 - 0.01 \cdot d) \cdot \rho_k}{k_{90} \cdot sin^2(\alpha) + cos^2(\alpha)} \tag{3.42}$$

where
d - Diameter of fastener[mm].
ρ_k - Density of the timber member [kg/m^3].
α - Load angle to the grain [°].

The characteristic yield moment in the fastener is calculated according to Equation 3.42.

$$M_{y,Rk} = 0.3 \cdot f_u \cdot d^{2.6} \tag{3.43}$$

where
f_u - Characteristic tensile strength of the fastener [MPa].
d - Diameter of fastener[mm].

The factor k_{90} is calculated according to Equation 3.44.

$$k_{90} = \begin{cases} 1.35 + 0.015 \cdot d \text{ for softwood} \\ 1.30 + 0.015 \cdot d \text{ for LVL} \\ 0.90 + 0.015 \cdot d \text{ for hardwood} \end{cases} \tag{3.44}$$

where
d - Diameter of fastener[mm].

3.2.4 Roof System

The user has the option to include the carbon dioxide equivalents from the roof construction or only evaluate the carbon dioxide equivalents from the main structural system described in Figure 3.1. This is regulated in the input called *Include effect*

of roof type. This input category only regulates if the carbon dioxide equivalents from the roof should be included in the calculation of total carbon dioxide equivalents or not and an approximate weight of the roof construction is hence always included when dimensioning the main structural elements. The two roof types that are treated in this thesis are a steel sheet roof and a timber roof made up from purlins and a plywood cover. The two types of roof systems and how they are dimensioned are explained in the sections below.

If the user specifies that the effect of roof type should not be included none of the calculations regrading roof type will be performed. If the user specifies to only include one of the roof types only the calculation corresponding to that roof type will be executed. Should the user specify to include the effect of both roof types the tool will determine suitable dimensions for both and choose the roof type that results in the lowest carbon dioxide equivalents per square meter building. If the roof type cannot fulfil the requirements of the specified building the only output will be the that no structural system fulfils the requirements. In the case where both roof types are included and only one roof type can fulfil the requirements the tool will automatically choose this one.

3.2.4.1 Timber Roof

The timber roof consists of continuous purlins with a plywood roof cover. The purlins have a spacing of 1200 mm and the plywood sheets are of the dimension 1200x2400, which means that one sheet covers two spans. The purlins form a gerber system with endbays with joints.

First the plywood thickness is dimensioned. The plywood is assumed to be class F25. The minimum thickness is calculated according to Equation 3.45.

$$t > \sqrt{\frac{6 \cdot M_{Ed}}{f_{md}}} \tag{3.45}$$

where
M_{Ed} - Design load effect of moment [Nm].
f_{md} - Dimensioning bending of the plywood [mm].

The tool will then choose the smallest plywood thickness that is larger than the minimum value from a list of thicknesses. The provided thicknesses ranges from 9 mm to 24 mm in steps of 3 mm. If the minimum plywood thickness that is required is above 24 mm, the roof type cannot fulfil the requirements and the timber roof cannot be created.

If a suitable plywood thickness is chosen the purlins are dimensioned. These are assumed to be made of structural timber of the class C24. The purlins are subjected bi-axial bending due the inclination of the roof. This is illustrated in Figure 3.12.

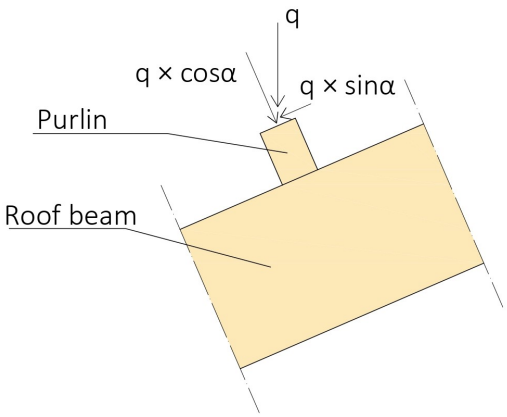

Figure 3.12: Illustration of bi-axial bending in purlins.

Given the bi-axial bending the purlins have to withstand the requirements in Equation 3.46 and 3.47.

$$\frac{M_{y,Ed}}{M_{y,Rd}} + k_m \cdot \frac{M_{z,Ed}}{M_{z,Rd}} \leq 1 \tag{3.46}$$

$$k_m \cdot \frac{M_{y,Ed}}{M_{y,Rd}} + \frac{M_{z,Ed}}{M_{z,Rd}} \leq 1 \tag{3.47}$$

where
$M_{y,Ed}$,$M_{z,Ed}$ - Design load effect of moment about the y- and z-axis [Nm].
$M_{y,Rd}$,$M_{z,Rd}$ - Design load capacity of moment about the y- and z-axis [Nm].
k_m - Modification factor, k_m=0.7 for rectangular cross sections [-].

The shear force acting on the purlins is verified with Equation 3.48.

$$V_{Ed} \leq \frac{f_{vd} \cdot A \cdot k_{cr}}{1.5} \tag{3.48}$$

where

V_{Ed} - Design load effect from shear force [N].
f_{vd} - Design shear strength [Pa].
A - Area of the cross section [m^2].
k_{cr} - Reduction factor considering influence of cracks [-].

Lastly, the deflection of the purlins is verified according to Equation 3.49.

$$w \leq \frac{l}{X} \tag{3.49}$$

where

w - Total deflection [m].
l - Length of the span of the purlins [m].
X - Value based on the area of usage [-].

The carbon dioxide equivalents for plywood is according to Boverket's climate database 0.358 kg/m^3. The corresponding number for structural timber is 0.069 kg/m^3. These values are integrated into the tool for evaluation of the contribution from the roof.

3.2.4.2 Steel Roof

The choice of steel roof is based on load tables from Ruukki Construction, which is a supplier of steel products. The products that are implemented are T70-57L-1058, T130-75L-930 and T153-40L-840, which all are insulated steel roofs. Ruukki Construction provides load tables of the maximum span length for each of their roof products for a specified snow load. Before being imported into the tool the tables are imported into an excel sheet and sorted by the different magnitudes of snow load. The data from the load tables is reduced to only include the product with the smallest volume for each maximum span length. The excel sheet con be found Appendix B.

The tool recognizes which part of the excel sheet is applicable for the specified snow load and only analyzes that part of the data. The spacing of the main beams is compared to the maximum spacing for each roof type, starting with the product with the smallest volume. If the roof type with the smallest volume has a maximum spacing which is smaller than the spacing in the project the tool moves on to the next roof type. The procedure continues like this until a product with a maximum spacing which is larger than the spacing in the project is found. The tool then selects this roof type and outputs relevant information about the product. The carbon dioxide equivalents for steel products, according to Boverket's climate database, are 2.6 kg/m^3, which is integrated in the tool. If no product fulfils the requirements the steel roof cannot be created.

3.2.5 3D Model

The 3D-model was generated using built-in components in Grasshopper together with the dimensions derived from the custom sizing component. In the modelling the components *stream gate* and *stream filter* were used to regulate which of the two structural systems were created. First a rectangle was made based on the specified building width and length. Points were created along the edges of the rectangle, showing the placement of the starting points of the columns. Similar points were created where the columns should end and lines were drawn to represent the columns as well as the beams.

The main columns and edge columns could be created directly along these lines whereas the rest of the lines had to be altered before the structural elements could be created. The lines for the main beams had to be extended by half the cross sectional height of the main columns in order to align the beams with the outer wall. The same adjustment was made for the lines for the edge beams. These lines were also moved slightly upwards in order to align the upper edges of the main beams. Lastly the lines for the edge beams were moved horizontally to align with the outer side of the gable columns and create the connection described in Chapter 3.2.3.5. The lines for the corner and gable columns were extended in order to reach up to the upper side of the beams. The lines and points for the corner columns were moved so that all columns would align along their outer edge. The magnitude of the movement in each direction was hence dependant on the height of the corner columns in comparison to the cross sectional height of the main columns and edge columns respectively.

All elements, except for the tapered beams, were then created by extruding a rectangles along the lines. The rectangles had the dimensions of the respective elements, which were output from the custom sizing component. All columns were made by extruding the rectangle centrally around their respective lines, whereas the beams were created with the line in the lower edge of the element. The tapered beams had to be made with a slightly different method as their cross sections are varying. These beams were modelled with the lines used to model the beams with constant cross section as a foundation. The end points of the lines were raised to the height at the end of the tapered beam. One point was then created in the middle of the beam line and rained to the apex height. The original end points and the three raised points were connected to form the boundary of the tapered beam. The shape was then extruded with the thickness of the beam. The corner and gable columns were trimmed where the edge beams intersect with them to create the connection between the two.

Lastly a wire frame model was created. This model was based on the lines that were created in the initial stage of the modelling process but were adjusted to be placed in the centre of each element, with the exception of the corner columns. These lines are placed at their original position, and the placement they had before they were moved to align with the outer edge of the columns. The wire frame line for the tapered beam is placed in the middle of the lowest cross section. An illustration of the wire frame model inside the model of the structural elements can be seen in Figure 3.13.

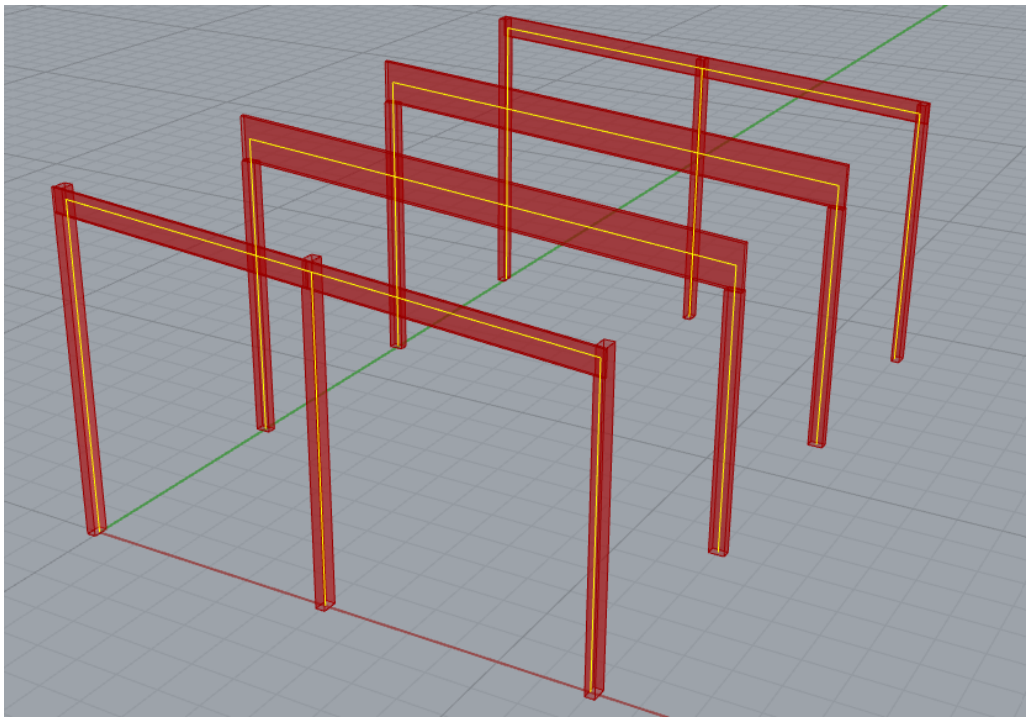

Figure 3.13: Illustration of the wire frame model inside the model of the structural elements. The wire frame is in yellow and the model of the structural elements is in red.

3.2.6 Assumptions and Simplifications in the Tool

The optimization tool is intended to be used as a preliminary design tool early in design processes and does not provide a final design. It is however based on thorough calculations on the basis of Eurocode and EKS11 and not rough estimations. It gives an indication of what dimensions are suitable and which beam type and column spacing gives the most favourable material usage. A number of simplifications and assumptions have been made and these are presented below for each element type.

3.2.6.1 Global System

In a global context, the roof structure is assumed to have a diaphragm action. Additionally, the tool presupposes that the building has four sets of cross braces, one in each wall, as illustrated in Figure 3.14. If the generated system includes gable columns the cross braces in the gables are fastened in these and the principle of the bracing is shown in Figure 3.14b and Figure 3.14a. However, if the generated system does not include gable columns the cross bracing in the gables is done according to Figure 3.14c. Nevertheless, the dimensioning of the cross braces is not considered in the tool. Another global assumption is that all load combination calculations are done for the safety class 3 for all element types.

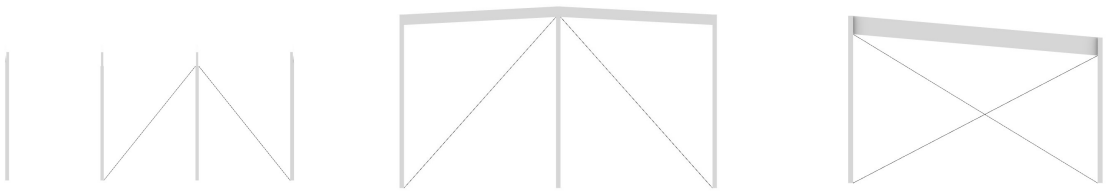

(a) Long side.

(b) Short side - with a gable column.

(c) Short side - without gable column.

Figure 3.14: Illustration of cross braces in walls.

3.2.6.2 Main Beam - Constant Cross Section

The top edges of the main beams are assumed to be fastened to the roof and hence restrained against lateral torsional buckling. The bottom edge is not assumed to be fastened to the roof and hence not restrained against lateral torsion. The axial load induced in the beams from horizontal wind load is neglected. In Equation 3.4, the applied load is for simplicity considered to be uniformly distributed, and the loads are assumed to act on the top of the beam.

Furthermore, the main beam is considered to be fabricated with a precambering which affects the deflection limits in the serviceability limit state, the consequences of which can be seen in Chapter 3.2.3.1.2. Moreover, wind zone H is for simplicity assumed to act over the whole beam as a uniformed distributed load when calculating the deflection. This decision was made since the majority of the beam is in the wind zone H.

3.2.6.3 Main Beam - Tapered

In the structural model for the tapered beam the loads are simplified to a uniformly distributed load which acts vertically. Moreover, the snow load and wind load, which depend on the roof angle, are not re-calculated when the tool evaluates several solutions with a varying roof inclination of ± 2 degrees. The effect of the change in load magnitude for this is considered to be negligible.

Similar to the beam with constant cross section, the tapered beam is considered to be restraint for lateral torsional buckling at the top edge but not the bottom edge. Moreover, the axial load induced in the beams from horizontal wind load is neglected. In Equation 3.4, the load is assumed to be applied on the top edge of the beams. When calculating the dimensioning bending strength the size effect is not considered.

The tapered beam is also consider to be fabricated with an precambering which affects the deflection limits, both the instantaneous and final deflection limit, as seen in 3.2.3.2.2. The snow load used in the calculations for serviceability limit state is set to the maximum snow load out of the two different ones that applies for duo pitched roofs.

3.2.6.4 Edge Beam

In the verification of the moment capacity, Equation 3.1, the edge beams are assumed to be restrained against lateral torsional buckling both in the top and bottom edge. Similar to the other beams the axial load is considered to be negligible.

Regarding the constraints in the serviceability limit state, the edge beams are considered to be fabricated with precambering. Thus, the instantaneous deflection from the permanent load is neglected. In the calculation for the deflection the applied wind load is assumed to be in wind zone H. If the structural system with the tapered beam is generated the edge beam is dimensioned for the side with the largest snow load.

3.2.6.5 Main Column

The permanent load from the self-weight of the column is assumed to act on the top of the column, which is a conservative presumption. The height used to dimension the columns is based on the highest main column that occurs in the system. The main columns are assumed to be braced against buckling in the weak direction, the z-direction, by the wall elements. Furthermore, the edge of the columns that is aligned with the wall is considered to be restrained against lateral torsional buckling. The other edge is assumed not to be braced against lateral torsional buckling.

3.2.6.6 Gable Column

Similar to the main column the self-weight of the gable column is considered to act on the top of column. The calculations of the gable columns are based on the highest possible height of gable columns that occurs in the structural system.

The gable column is assumed to be braced against buckling in the weak-direction, i.e. the z-direction. The column edge that is connected to the wall is considered to be restrained against lateral torsional buckling. The other edge is assumed not to be braced against lateral torsional buckling.

3.2.6.7 Corner Column

The corner columns are assumed to have the same application of its self-weight as the main and corner columns. They are dimensioned for the highest possible column in the system. Furthermore, the corner columns are assumed to be braced against buckling, in both z- and y-direction. They are also fully restrained for lateral torsional buckling and thus the modification factor.

3.3 Verification of Structural System

In order to ensure that the structural calculations in the tool are reliable two types of verifications were made. The first verification was made in a finite element analysis software in order to verify the utilization rates that are calculated in the tool. The

second verification was based on case studies in order to ensure that the applied loads in the tool are correct.

3.3.1 Load Effects and Resistances

A verification of the calculation of the load effects and the resistances was made in the finite element software FEM-design. All structural elements were modelled in FEM-design according to the same structural models and load magnitude as used in the tool. The constraints, relevant for each element, were verified by comparing the utilization rates that are generated by the tool with the utilization rates from FEM-design. This verification was made for a building with the input values displayed in Table 3.2. It was made for both beam types. The results from the verification of the utilization rates can be found in Table 4.12 to Table 4.17.

Table 3.2: *Input values used in the verification of the utilization rates*

Geometry/dimensions	Width [m]	18
	Length [m]	42
	Height [m]	6
	Roof angle [°]	3.6
Structural system	Column spacing [m]	6
	Beam type [-]	1 and 2
Loading circumstances	Terrain category [-]	0
	Service class [-]	1
	Characteristic snow value [kN/m^2]	1.5
	Basic wind velocity [m/s]	25
	Approximate roof weight [kg/m^2]	30
	Exposure [-]	Normal
	Intended use of building [-]	Industry
Maximum utilization rates	ULS [%]	100
	SLS [%]	100
	Compression perpendicular to the grain [%]	100
Other	Include effect of roof type [-]	No
	View model [-]	Yes

3.3.2 Applied Loads

A verification was made to ensure that the loads that are used for the dimensioning of the structural elements in the tool are reasonable. This verification was made using two reference projects, one of which had tapered beams and the other had beams with constant cross sections. The verification was made by setting the input of the tool to match respective reference project. The built-in sizing optimization in the tool was then inactivated and the dimensions of the structural elements from the reference projects were put in instead. The loads that act on each element in the calculation files from the reference project were then compared to the loads that were generated for the same structure in the tool. The results of the comparison

can be seen in Table 4.18 for reference project 1 with tapered beams and Table 4.19 for reference project 2 with beams with constant cross section.

4
Results

The aim of the thesis was to implement an efficient parametric tool for early stage design. Hence, the results involves the tool itself and the achievements from the tool. The optimization tool was implemented successfully and generates structural systems as intended. This chapter presents the efficiency of the tool in the form of case studies. Furthermore, the verification of the tool is presented. A user manual of the tool can be found in Appendix A.

4.1 Case Study 1

Reference project 1 is a system with tapered beams simply supported on columns. The results from the optimization performed by the tool for only sizing optimization as well as for sizing optimization combined with topology optimization are presented below. In order to get a compatible comparison the highest utilization rate used in the reference project of 87 percent was also used in the tool. No effect of roof type was used, which means that an approximate roof weight was included in the dimensioning of the structural elements but the carbon dioxide equivalents that the roof construction will add was not evaluated. Drawings of the project as well as relevant loading circumstances can be found in Appendix C.

4.1.1 Only Sizing Optimization

The original dimensions compared to the dimensions chosen by the tool when only sizing optimization is performed can be seen in Table 4.1. Figure 4.1 shows illustrations of how the structural systems in this case compare to each other.

Table 4.1: *The dimensions [mm] of the structural elements for the original design and the optimized design*

	Original design	Optimized design
Main beams	215x539-1260 (7°)	115x990-1504 (5°)
Edge beams	215x450	66x540
Main columns	215x315	190x315
Gable columns	215x360	190x315
Corner columns	315x215	215x270

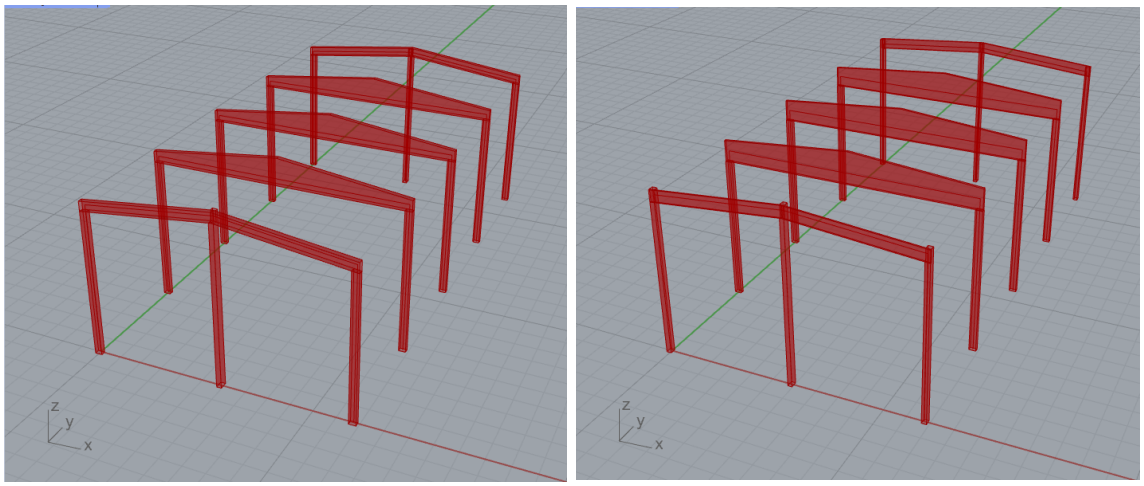

(a) Reference project 1 - original design. **(b)** Reference project 1 - optimized design.

Figure 4.1: Difference in structural system before and after the optimization for reference project 1.

The material per structural element as well as the total material usage for the system is presented in Table 4.2 for both the original design and the optimized design.

Table 4.2: *The material usage [m^3] for the original design and the optimized design*

	Original design	Optimized design	Difference [%]
Main beams	3x2.308	3x1.720	-25
Edge beams	4x0.588	4x0.216	-63
Main columns	6x0.454	6x0.401	-12
Gable columns	2x0.574	2x0.432	-25
Corner columns	4x0.460	4x0.415	-10
Total	**14.988**	**10.954**	**-27**

4.1.2 Sizing Optimization and Topology Optimization

The cross sectional dimensions, column spacing and beam type of the original system compared to the system chosen by the tool when sizing optimization combined with topology optimization is performed can be seen in Table 4.3. Figure 4.2 shows illustrations of how the structural systems in this case compare to each other.

Table 4.3: *The dimensions [mm] of the structural elements, column spacing [mm] and beam type [-] for the original design and the optimized design*

	Original design	Optimized design
Main beams	215x539-1260 (7°)	140x1080-1594 (5°)
Edge beams	215x450	90x495
Main columns	215x315	215x315
Gable columns	215x360	215x315
Corner columns	315x215	215x315
Column spacing	5500	7330
Beam type	Tapered	Tapered

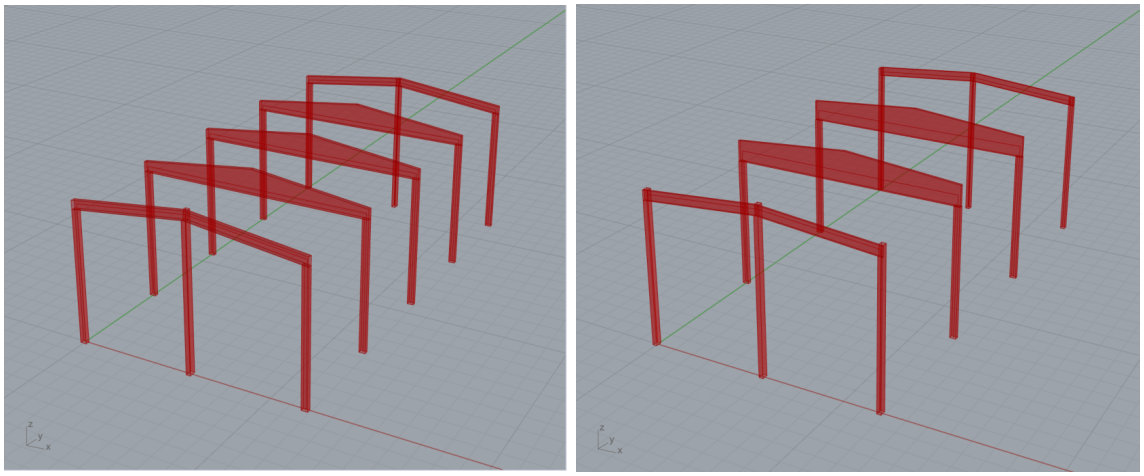

(a) Reference project 1 - original design. **(b)** Reference project 1 - optimized design.

Figure 4.2: Difference in structural system before and after the optimization for reference project 1.

The material per structural element as well as the total material usage for the system is presented in Table 4.4 for both the original design and the optimized design.

Table 4.4: *The material usage [m^3] for the original design and the optimized design*

	Original design	Optimized design	Difference [%]
Main beams	3x2.308	2x2.247	-35
Edge beams	4x0.588	4x0.270	-54
Main columns	6x0.454	4x0.454	-33
Gable columns	2x0.574	2x0.489	-15
Corner columns	4x0.460	4x0.93	+7
Total	**14.988**	**10.340**	**-31**

4.2 Case Study 2

Reference project 2 is a system with beams with constant cross section simply supported on columns. This system in the reference project does not have any gable columns. The results from the optimization performed by the tool for only sizing optimization as well as for sizing optimization combined with topology optimization are presented below. In order to get a compatible comparison the highest utilization rate used in the reference project of 77 percent was also used in the tool. No effect of roof type was used, which means that an approximate roof weight was included in the dimensioning of the structural elements but the carbon dioxide equivalents that the roof construction will add was not evaluated. Drawings of the project as well as relevant loading circumstances can be found in Appendix C.

4.2.1 Only Sizing Optimization

The original dimensions compared to the dimensions chosen by the tool when only sizing optimization is performed can be seen in Table 4.5. Figure 4.3 shows illustrations of how the structural systems in this case compare to each other.

Table 4.5: *The dimensions [mm] of the structural elements for the original design and the optimized design*

	Original design	Optimized design
Main beams	165x450	78x765
Edge beams	165x450	66x540
Main columns	165x180	140x180
Gable columns	-	-
Corner columns	180x165	140x180

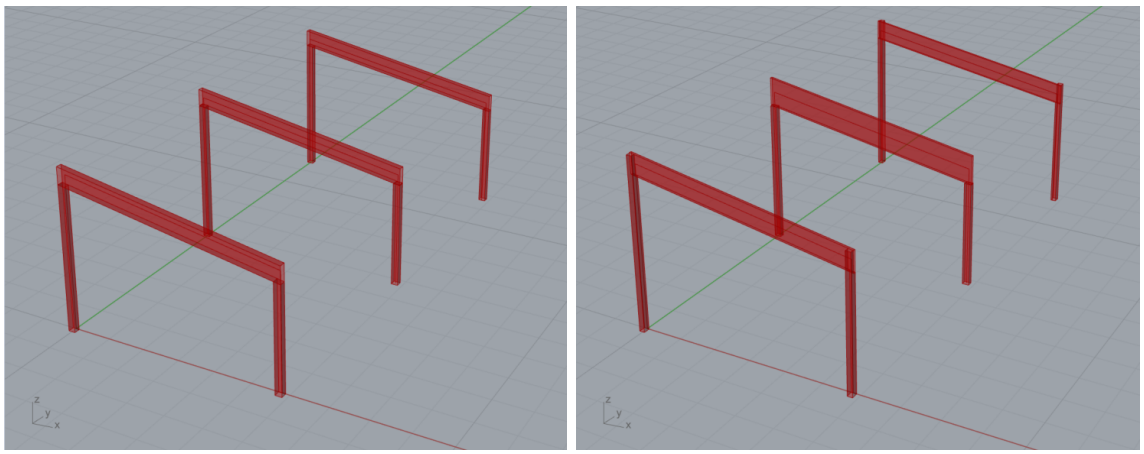

(a) Reference project 2 - original design. **(b)** Reference project 2 - optimized design.

Figure 4.3: Difference in structural system before and after the optimization for reference project 2.

The material per structural element as well as the total material usage for the system is presented in Table 4.6 for both the original design and the optimized design.

Table 4.6: *The material usage [m^3] for the original design and the optimized design*

	Original design	Optimized design	Difference [%]
Main beams	1x0.415	1x0.362	-20
Edge beams	2x0.451	2x0.216	-52
Main columns short side	1x0.084	1x0.072	-14
Main columns long side	1x0.115	1x0.097	-16
Gable columns	0x0	0x0	0
Corner columns short side	2x0.084	2x0.077	-10
Corner columns short side	2x0.115	2x0.103	-32
Total	**1.950**	**1.323**	**-32**

4.2.2 Sizing Optimization and Topology Optimization

The cross sectional dimensions, column spacing and beam type of the original system compared to the system chosen by the tool when sizing optimization combined with topology optimization is performed can be seen in Table 4.7. Figure 4.4 shows illustrations of how the structural systems in this case compare to each other.

Table 4.7: *The dimensions [mm] of the structural elements, column spacing [mm] and beam type [-] for the original design and the optimized design*

	Original design	Optimized design
Main beams	165x450 (10°)	90x765-1173 (8°)
Edge beams	165x450	42x405
Main columns	165x180	90x225
Gable columns	-	140x115
Corner columns	180x165	165x90
Column spacing	5800	5800
Beam type	Constant cross section	Tapered

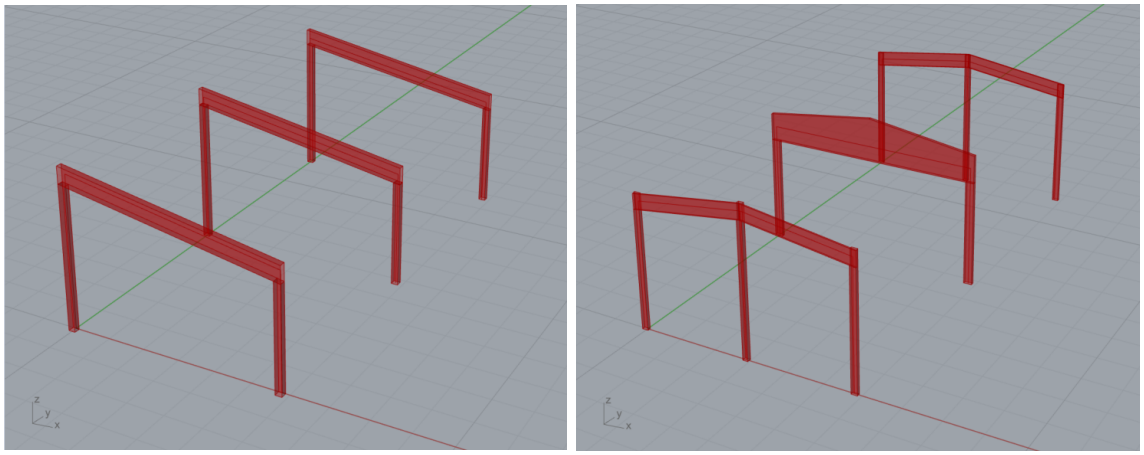

(a) Reference project 2 - original design. **(b)** Reference project 2 - optimized design.

Figure 4.4: Difference in structural system before and after the optimization for reference project 2.

The material per structural element as well as the total material usage for the system is presented in Table 4.8 for both the original design and the optimized design.

Table 4.8: *The material usage [m^3] for the original design and the optimized design*

	Original design	Optimized design	Difference [%]
Main beams	1x0.415	1x0.521	+16
Edge beams	2x0.451	4x0.052	-77
Main columns short side	1x0.084	1x0.058	-31
Main columns long side	1x0.115	1x0.058	-50
Gable columns	0x0	2x0.052	-
Corner columns short side	2x0.084	2x0.047	-44
Corner columns short side	2x0.115	2x0.047	-59
Total	**1.950**	**1.137**	**-42**

4.3 Choice of Roof System

The results from the additional feature in the tool concerning the effect on the total carbon dioxide equivalents from the roof structure, timber roof or steel roof, are presented below. The results are based on arbitrary building dimensions and loading circumstances according to Table 4.9.

Table 4.9: *Input values for an arbitrary building used in the evaluation of roof structure*

Geometry/dimensions	Width [m]	8
	Length [m]	20
	Height [m]	4
	Roof angle [°]	5
Structural system	Column spacing [m]	3.3
	Beam type [-]	1
Loading circumstances	Terrain category [-]	2
	Service class [-]	2
	Characteristic snow value [kN/m^2]	2.5
	Basic wind velocity [m/s]	24
	Approximate roof weight [kg/m^2]	60
	Exposure [-]	Normal
	Intended use of building [-]	Industry
Maximum utilization rates	ULS [%]	100
	SLS [%]	100
	Compression perpendicular to the grain [%]	100
Other	Include effect of roof type [-]	Timber & Steel
	View model [-]	Yes

In Table 4.10, the results from the comparison between sizing optimization and topology optimization are shown, when the steel roof is chosen.

Table 4.10: *Comparison between sizing optimization and topology optimization for steel roof construction*

	Sizing optimization	Topology optimization
Volume glulam, $[m^3]$	4.4	4.6
$co_{2,eq}$, $[\frac{kg}{m^2}]$	25.5	22.9
Spacing, [m]	3.3	2.0
Beam type, [-]	1	2
Product	T70-57L-1058	T70-57L-1058
Plate thickness, [mm]	0.8	0.7

In Table 4.11, the results from the comparison between sizing optimization and topology optimization are shown, when the timber roof is chosen.

Table 4.11: *Comparison between sizing optimization and topology optimization for timber roof construction*

	Sizing optimization	Topology optimization
Volume glulam, $[m^3]$	4.4	3.9
$co_{2,eq}$, $[\frac{kg}{m^2}]$	4.63	4.61
Spacing, [m]	3.3	4.0
Beam type, [-]	1	1
Purlin, bxh [m]	0.10x0.20	
Plywood thickness, [m]	0.015	0.015

4.4 Verification

The results from the verification of the structural system are displayed in the following subchapters.

4.4.1 Load Effects and Resistances

In the following subchapters the result of the verification of the load effects and resistances in the form of utilization rates are displayed. Extracts of the calculation results from FEM-design can be found in Appendix F.

4.4.1.1 Beam with Constant Cross Section

In Table 4.12 the utilization rates for the main beam with constant cross section can be seen. These beams have the dimensions 190x1125 mm.

Table 4.12: *Utilization rates from the tool and FEM-design - beam constant cross section*

	FEM-design	The tool	Difference
Bending moment up (Not restrained for LT)	60%	61%	1 percentage unit
Shear force	43%	43%	0 percentage units
Bending moment down (Restrained for LT)	69%	69%	0 percentage units
Instantaneous deflection	93%	91%	2 percentage units
Final deflection	90%	89%	1 percentage unit

4.4.1.2 Tapered Beam

In Table 4.13 the utilization rates for the tapered main beam can be seen. These beams have the dimensions 215x810-1187 mm.

Table 4.13: *Utilization rates from the tool and FEM-design - tapered beam*

	FEM-design	The tool	Difference
Bending moment down, critical section (restrained for LT)	67%	67%	0 percentage units
Bending moment up, critical (Not restrained for LT)	46%	49%	3 percentage units
Shear force	57%	57%	0 percentage units
Instantaneous deflection	95%	96%	1 percentage unit
Final deflection	94%	94%	0 percentage units

4.4.1.3 Edge Beam

In Table 4.14 the utilization rates for the edge beams can be seen. These beams have the dimensions 66x450 mm.

Table 4.14: *Utilization rates from the tool and FEM-design - edge beam*

	FEM-design	The tool	Difference
Bending moment (restrained for LT)	76%	76%	0 percentage units
Shear force	58%	58%	0 percentage units
Instantaneous deflection	82%	79%	3 percentage units
Final deflection	75%	74%	1 percentage unit

4.4.1.4 Columns

In Table 4.15 the utilization rates for the main columns can be seen. These columns have the dimensions 190x405 mm.

Table 4.15: *Utilization rates from the tool and FEM-design - main column*

	FEM-design	The tool	Difference
Bending (Restrained for buckling)	52%	53%	1 percentage unit
Shear force	31%	31%	0 percentage units
Torsional buckling	62%	62%	0 percentage units
Combined bending and axial compression	62%	63%	1 percentage unit

In Table 4.16 the utilization rates for the main columns can be seen. These columns have the dimensions 165x405 mm.

Table 4.16: *Utilization rates from the tool and FEM-design - gable column*

	FEM-design	The tool	Difference
Bending (Restrained for buckling)	72%	72%	0 percentage units
Shear force	39%	39%	0 percentage units
Torsional buckling	73%	73%	0 percentage units
Combined bending and axial compression	77%	77%	0 percentage units

In Table 4.17 the utilization rates for the main columns can be seen. These columns have the dimensions 215x405 mm.

Table 4.17: *Utilization rates from the tool and FEM-design - corner column*

	FEM-design	The tool	Difference
Normal force	1.4%	1.4%	0 percentage units
Shear force	27%	27%	0 percentage units
Combined bending and axial compression, y-axis	81%	81%	0 percentage units
Combined bending and axial compression, z-axis	94%	94%	0 percentage units

4.4.2 Applied Loads

Table 4.18 and 4.19 shows the verification of the applied loads. A few values in the verification differ significantly, the reason to which is discussed in Chapter 5.3.2.

Table 4.18: *Applied loads [kN/m] from reference project 1 and the tool*

		Reference project	The tool	Difference [%]
Main beam	Snow, right side	12.28	12.16	-1.0
	Snow, left side	11.0	12.16	+10.5
	Wind, zone 1	-0.8	1.40	+249.9
	Wind, zone 2	-4.82	1.40	+129
	Self weight roof	3.43	3.49	+0.9
	Self weight beam	0.73	0.817	+11.79
Edge beam	Snow	6.14	6.01	-2.1
	Wind, zone 1	0.08	0.699	+733.8
	Wind, zone 2	0.08	0.699	+733.8
	Self weight roof	1.716	1.760	+2.6
	Self weight beam	0.30	0.33	+9.3
Main columns	Point load	105.51	166.02	+52.6
	Wind	4.42	4.29	-2.9
Gable columns	Point load	215.9	125	-42.1
	Wind	4.66	4.58	-1.7
Corner columns	Point load	29.38	28.90	-1.6
	Wind, z-direction	2.210	2.145	-2.9
	Wind, y-direction	2.568	3.077	+19.8

Table 4.19: *Applied loads [kN/m] from reference project 2 and the tool*

		Reference project	tool	Difference [%]
Main beam	Snow	11.6	11.6	0
	Wind, zone 1	0.30	1.264	+321.3
	Wind, zone 2	0.30	1.264	+321.3
	Self weight roof	3.62	3.70	+2.2
	Self weight beam	0.289	0.310	+7.3
Edge beam	Snow	6.0	5.8	-3.3
	Wind, zone 1	0.156	0.632	+305.1
	Wind, zone 2	0.156	0.632	+305.1
	Self weight roof	1.87	1.85	+1.1
	Self weight beam	0.29	0.31	+7.3
Main columns	Point load	52.03	58.82	+13.0
	Wind	3.315	3.336	+0.6
Corner columns	Point load	30.4	36.66	+20.6
	Wind, z-direction	1.657	1.668	+0.7
	Wind, y-direction	1.872	2.213	+18.2

5
Discussion

A discussion of the results from the case studies is conducted in this chapter. Moreover, the results from the verification is discussed together with the limitations and the usability of the tool.

5.1 Case Studies

From the case studies the efficiency of the tool can be evaluated. What can be observed is that the material usage in both reference projects can be lowered significantly both with and without the optional topology optimization. As mentioned in Chapter 2.1.3 The Smart Built Environment estimates a possibility of a 40 percent reduction of the environmental footprint through digital development. By performing only sizing optimization and sizing optimization combined with topology optimization for the two reference projects the material usage, and hence the carbon dioxide equivalents per square meter building, for the structural systems could be reduced with between 27 and 42 percent. Worth noting is that these case studies only treat the environmental footprint of the basic structural system which is only part of the elements and factors that affect the environmental footprint of a complete building. It is consequently hard to make a direct comparison of the numeric values of the reduction that The Smart Built Environment estimates and what is achieved in these case studies. However, it can be confirmed that the usage of digital tools is an efficient method in lowering the carbon dioxide emissions in the construction industry and developing sustainable buildings. Generally speaking, the tool chooses elements with a high value for the relation between width and height of the cross sections. Another observation is that a higher spacing generally gives a smaller glulam volume.

5.1.1 Sizing Optimization

When performing only sizing optimization the material usage could be lowered with 27 percent for reference project 1 and 32 percent for reference project 2. One factor that is important to have in mind when making these kinds of comparisons is the utilization rates used in the reference project and the corresponding utilization rates used in the tool. If the utilization rate is much lower in the original reference project it is not surprising that the system can be made with a lower amount of material by simply increasing the utilization rates. To ensure that the tool lowers the material usage by choosing efficient cross sections and not only increasing the

utilization rates the maximum utilization rates were matched. This was done by using the maximum utilization rate for any element in the reference projects as input for the tool. The reference projects have a utilization rate of around 80 percent as maximum for the entire project, but both projects also include several elements with lower utilization rates. A summary of the maximum utilization rates for each element can be found in Appendix C. The tool uses the highest utilization rate as a limit for all elements, making the optimized structure more utilized for several structural elements. The efficiency of the tool in choosing a more material efficient option whilst still preserving the same utilization rate can however still be validated by comparing the material usage for only the main beams. These members have corresponding maximum utilization rates. For reference project 1 the material usage for the main beams can be decreased by 25 percent and for reference project 2 the reduction is 20 percent for these beams. The outcome of the optimization of the main beams shows that a high utilization rate does not always guarantee the most material efficient option and that the tool manages to perform a successful sizing optimization.

The results of the case studies show that the material usage can be reduced for most of the rest of the structural elements as well. The conclusion that this is not only due to the fact that the utilization rates are increased in the tool can however not be drawn. Concerning utilization rates the tool does provide rapid results of which cross sections are efficiently utilized, which is an important factor to consider when designing sustainable building structures.

5.1.2 Topology Optimization

The topology optimization is made with regard to the column spacing as well as the beam type. Both reference projects could be optimized further when adding this type of optimization, proving the significance of evaluating different structural systems. For reference project 1 the corner columns in the topology optimized design resulted in a higher material usage than the original design, even though the cross sections are the same size. The reason for this is that the main beams are higher in the optimized design, which results in higher corner columns. All the other elements in the optimized design did however result in lower material amounts making the total sum lower for the optimized design. For reference project 2 all the structural elements could be optimized individually to reduce the material usage.

For reference project 1 the additional material reduction could be achieved by changing the spacing of the columns from 5.5 meter to 7.33 meters. This gives two main beams instead of the original three. Even though this optimized design has a 33 percent higher spacing, and hence higher load per beam, the main beams can still be optimized and chosen to dimensions that result in a 3 percent reduction in material for each main beam. This shows the importance in choosing the relation between height and width of the beam attentively.

The material usage in reference project 2 could be further lowered compared to the original design by exchanging the beam with constant cross section for a tapered beam. This system requires gable columns which is not part of the original design. In this case the volume of the main beam is increased by 16 percent compared to the original reference project. This means that despite adding two structural elements and choosing a main beam with larger volume the topology optimized structural system has a smaller material volume. This is due to the reduction of material for all the remaining elements. The edge beams can be reduced since the spans are reduced to half and the added gable columns help reduce the load on the corner columns. The main columns are also shorter on one side of the building for the topology optimized system, making the moment from the wind on the wall smaller which in turn gives smaller dimensions.

Another interesting comparison is between the systems produced from only sizing optimization and the systems produced from both sizing optimization and topology optimization. For reference project 1 it can be observed that the total amount of material for the main beams can be reduced by an additional 13 percent when applying topology optimization. The material usage for the structural system was reduced with 6 percent by applying topology optimization on top of the sizing optimization. This shows that a combination of choosing the cross sections attentively and adjusting the spacing and beam type is favourable from a material usage point of view.

One thing that should be considered for a case where tapered beams gives a lower volume than beams with constant cross sections is how the tapered beams are manufactured. One way to produce tapered beams is to first produce a straight beam and then form the tapered edge by sawing away material. The waste is in this case used for district heating. Tapered beams can also be produced by gluing together lamellas of different lengths. The lamellas get shorter and shorter towards the apex. The edge is then sawn according to the angle of the beam. The later method is preferable if the change to a tapered beam should be justified from a material efficiency perspective. The available production methods means that even though the waste is as low as possible by using the second method it is slightly higher when producing tapered beams than beams with constant cross section. Hence, if the tapered beam only gives a slightly smaller volume it may be favourable to choose the beam with constant cross section due to the extra material waste at production for tapered beams. Nevertheless, if the tapered beams give a significantly smaller volume the production waste will not play an as significant role.

5.2 Choice of roof system

In section 4.3 the environmental effect of the type of roof structure can be seen. Table 4.9 demonstrates the effect of the roof structure for an arbitrary building. In Table 4.10 and 4.11, a significant deviation in the carbon dioxide equivalents can be observed between the steel roof and the timber roof. The steel roof has 23-26 kg/m^2 carbon dioxide equivalents whilst the timber roof has 5 kg/m^2. This indicates that

the timber roof is more beneficial from an environmental perspective.

After topology optimization was performed for the steel roof, the results of which is shown in Table 4.10, it can be seen that the tool generates a system with a lower spacing and the smallest steel plate, T70-57L-1058, with the plate thickness of 0.7 millimeter. Since steel has a relatively high value of carbon dioxide equivalents per volume material, 2.6 kg/m^3, compared to glulam, 0.133 kg/m^3, a significant influence on the environmental footprint is expected when using steel products. In Table 4.11 it can however be observed that for the timber roof a greater spacing results in a slightly lower carbon dioxide equivalents. Generally, it can be seen in the case studies that a greater spacing results in a lower volume and hence a lower carbon footprint. However, in the evaluation of the timber roof the possible spans of the structural timber used for the purlins is circumscribed to about 4 meters due to the elements not being able to withstand higher load effects. If a greater spacing was possible in the timber alternative an even greater reduction could have been achievable. This could be attainable if glulam elements could be used in the dimensioning of the purlins.

Noteworthy is that when considering which structural system is the most environmentally beneficial it is of great importance to account for the complete structural system. Moreover, it is crucial to be aware of how the material choices affect the environmental emissions when considering the whole life-cycle, from cradle to grave. For instance, a timber construction is not necessarily beneficial from an environmental point of view if not a sustainable timber production is used, including re-planting of trees.

5.3 Verification

In order to demonstrate the accuracy of the tool two verifications were made. Firstly, the verification of the calculated load effects and resistances are verified. Secondly, a verification of the applied loads was made, which is based on a compassion of two case studies.

5.3.1 Load Effects and Resistances

In Chapter 4.4.1, the results from the verification of the calculated load effects and resistances can be seen for each structural element. The utilization rates for each constraint from FEM-deign and the tool are clearly stated. In general, it can be seen that the results from FEM-design and the results from the tool correspond well. The utilization rates regarding the three columns types have a negligible difference of maximum one percentage unit, which can be seen in Tables 4.15, 4.16 and 4.17. Otherwise, the results show a maximum difference of ± 3 percentage units. However, all checks that are required for designing a tapered beam is not possible to perform in the FEM software. Thus, the verification of tension stresses perpendicular to the grain at the apex is not verified in the software. The check in the tool is however carried out according to the regulation according to Eurocode and EKS 11 and is

deemed reasonable.

In Table 4.12 and Table 4.13 a minor difference in the check for bending moment that is not restrained against lateral torsional buckling can be observed, both in the beam with constant cross section and the tapered beam. The difference is one respectively three percentage units. Important to note is that the calculations of torsional moment of inertia is based on a linear interpolation between set data points, which can be a minor cause of error. Furthermore, the assumption of the effective length can be an additional cause of error when assuming a uniformly distributed load.

In the Tables 4.12 and 4.14 a slight difference in the utilization rates for deflection can be spotted for the main beam with constant cross section and the edge beams. In the design in serviceability limit state a few simplifications have been made for beams with constant cross section such as an assumption of a uniformly distributed load. The structural model in FEM-design is modelled according to Figure 3.6, which can have a slight effect on the results.

5.3.2 Applied Loads

In Chapter 4.4.2, the results from the verification of the applied loads in the tool can be seen. The verification is made based on a comparison between the tool and two reference projects, in order to ensure that the applied loads generated by the tool are reasonable. However, the reference projects are not necessarily considered as the unambiguous correct answer due to the possibilities in diversity of design choices from the designer. Therefore a certain disparity is expected and accepted in the results. Nevertheless, it is considered as an adequate method to see if the result are reasonable. In Table 4.18 the comparison of reference project 1 can be seen and in the Table 4.19 the comparison regarding reference project 2 can be seen.

A significant distinction can be spotted when analysing the wind load on the beams in both the reference projects. This difference spans from about 130 to 734 percent. In reference project 1 the wind load on the main beam is applied upwards whilst the applied wind load in the tool is acting downwards, to the roof surface. Hence, this wind load is not compatible. The wind load applied on the edge beam in reference project 1 differs significantly with 734 percent. Noteworthy is that the references projects do not have an applied internal wind pressure on the beams, which in this case is the cause of the significant difference. If the tool neglects the internal wind pressure the difference is an increase of maximum 5 percent related to the reference project, which is considered as a minor difference. These value, without the internal wind pressure, can be found in Appendix D. Nevertheless, the choice of retaining the internal wind pressure integrated in the tool is considered to be justifiable since the design is according to Eurocode and EKS 11.

Regarding the wind load applied on the columns in both reference projects minor difference can be spotted to the loads in the tool, especially for the main columns

and the gable columns. In the same way as for the main beams the internal wind pressure is integrated in the calculation in the tool but not the reference projects, causing the difference. A substantial difference can be seen in the corner columns for the applied load in the y-direction. The reference project does not include the effect of internal wind pressure on the corner columns, which is the cause of error. When excluding the internal pressure in the tool a maximum difference of 3 percent is obtained. The wind load applied in the z-direction on the corner column does however have a minor difference. Important to note is that the tool evaluates the worst case of the internal wind pressure together with the external wind pressure, which can result in a favourable effect in one of the directions, in this case z-direction.

Furthermore, another significant difference that can be spotted in Table 4.18 is in the point load, both for the main and gable columns where the difference is about ± 50 percent. The calculations in the tool is based on the fact that four cross braces is located, one in each wall, which in this case results in an additional point load on the gable columns and main columns. The reference project has introduced an additional point load on the gable column due to the wind load but not on the main columns, which can be a reason of the increased point load on the main columns in the tool. Regarding the point load on the gable columns it is in the reference project considered to be unjustifiably large. However, the point load can be an effect of a design choice due to some specific loading circumstances that is not apparent in the provided documentation. In reference project 2, Table 4.19, regarding the point load a similar reasoning as in reference project 1 for the main column can be applied.

Moreover, in reference project 1, where the structural system consist of tapered beams, a difference in the self-weight of the beam of 11.8 percent and the snow load on left side of 10.5 percent can be seen in Table 4.18. In the design of the tapered beam in the tool some simplification have been made which may have an impact on the results. For instance, uniformed distributed load is assumed, both for the self-weight and the snow load. Whilst in the reference project the snow load is different for the different roof sides, according to duo pitched roof design, and the self-weight is not uniformed distributed. The tool chooses the maximum snow load and uses that load along the whole beam, which results in an adequate match on the snow load on the right side and slightly over dimensioning of the snow load on the left side.

In general, a deviation of about ± 10 percent is considered as an acceptable difference. Nevertheless, if a reason of a more significant deviation can be found and explained it is considered to be a justifiable result.

5.4 Limitations in the Tool

There are no distinct bounds to the development of a parametric tool. Due to the limited time frame for this master thesis the tool includes several limitations.

The structural system that can be produced has certain limitations. The columns always have to be spaced equally, making the possibility of using the tool for specific

projects with a certain varying spacing limited. No possibility of placing columns somewhere other than along the outer walls exists. The system is limited to beams simply supported on columns and frames are not implementable. There is hence currently no possibility to investigate if a framed system could be more material efficient than a simply supported one. The beams are limited to two types. The implemented beam types are admittedly two common ones and are in many cases chosen. It is however a limitation that it is not possible to investigate how they compare to more unusual beam types.

Cross bracing is always assumed and no other methods of horizontal stabilization are possible to evaluate. The cross braces are not dimensioned nor included in the calculation of material volume and carbon dioxide equivalents. As discussed in Chapter 5.2, the whole structural system affect the carbon dioxide equivalents of the building. Even though the bracing has a small volume it will give a slightly larger environmental footprint to include them as well.

The evaluation of the connections is superficially treated in the tool. This is something which needs post-processing to ensure that the structural system will work as intended. The environmental impacts of the material used for the connections is not included, which may be a limitation since the size and amount of connections may differ between different cases. All chosen structural elements originate in a list of standard dimensions and no other dimensions can be chosen. This limits the possibility to optimize the structure fully since there is a step between all dimensions. It is however practical from a production point of view to only use standard dimensions. It also saves computational power to limit the amount of options to evaluate.

The steel roof is implemented using rough estimations as described in Chapter 3.2.4.2. This means that further calculations may be necessary to ensure that the correct dimension is chosen. Three different steel sheet roofs are implemented, making the optimization somewhat limited. The purlins have a predefined spacing of 1200 mm and are always made of structural timber, both of which limit the possible spans of the purlins. These are all important factors to have in mind when optimizing the structure with the effect of the roof type included.

5.5 Usability of the Tool

The aim of the tool is to produce a first draft of an optimized load-bearing structure with regard to material volume. This, in order to give the structural designer an indication of which design choice is more beneficial in an environmental point of view, already at an early stage. In an early design stage there are greater possibilities for evaluation of several solutions and their consequences. Hence, this kind of early evaluation mitigates the risk of changes in a later stage. Generally, it is time consuming and expensive to make changes in a later stage, which also make multiple iteration in an early stage beneficial from an economical perspective. The results of the implementation of a parametric optimization tool show a possible reduction of

the carbon dioxide equivalents per square meter gross area. Hence, a parametric tool can be beneficial in terms of lowering the environmental footprint of a load-bearing structure.

A parametric tool for structural dimensioning is most convenient when it is used for designing structural systems that are frequently requested. The time that it takes to implement the parametric set-up should be less than the aggregated time of doing the same work manually. If a very specific structural system should be optimized it may be more efficient to optimize only that system and not set up a general parametric optimization tool that can be used for several other cases as well. The industrial building in glulam is requested often enough to make the time that it takes to implement a parametric tool worthwhile and can therefore also be beneficial from an economical point of view when it saves time spent in the projects. Hence, it is justifiable to set up a tool applicable for this specific type of building.

The sole purpose of the optimization is to minimize the carbon dioxide equivalents per square meter building. This means that other aspects can be overlooked. A decision that is advantageous from an environmental point of view may be disadvantageous in other aspects. Slim structural elements proves to be an efficient method for lowering the material usage, but can however introduce difficulties in assembling the structure. Before bracing is provided a high beam poses a risk of wobbling or tipping over. More care also has to be taken in transportation and how the lifting device is fastened in the element. Furthermore, unconventional solutions can lead to increasing costs due to more special solutions. Besides this, the tapered beam is usually more expensive to manufacture than the beam with constant cross section. Because of this, the environmental advantages have to be weighed against practical disadvantages as well as economical disadvantages. Moreover, slender elements may lead to special solutions for connections and may result in greater costs due to special method at the construction site. Hence, it is of importance to be aware of and handle the consequences different solutions may give. A way to take more aspects into consideration is to implement a multi-objective optimization. As the regulations for the environmental impacts of new buildings get stricter the carbon dioxide equivalents of a building may however play a more significant role in the weighing of aspects.

Since the tool is developed in commercial software certain prior knowledge is required to use the tool. Firstly, the user has to be able to open and download Rhino and Grasshopper. No further knowledge is required in Rhino but the user has to be able to navigate to the user-defined input section in the Grasshopper file. Some components used in the Grasshopper scripting are plug-ins which means that they are not included in the standard version of Grasshopper and have to be downloaded. They are free and Grasshopper will automatically ask the used to download the required plug-ins, but some prior experience of how plug-ins work is beneficial. The topology optimization is performed by an existing component i Grasshopper called Galapagos. To run this optimization the user has to be able to open the component, apply the correct settings and start the optimization. How the tool is supposed to

be used and how everything works is described in a user manual which can be found in Appendix A.

6
Conclusion

The implemented tool functions as intended and has for the two reference projects proven that the material usage can be lowered with up to 42 percent by evaluating alternative solutions for the structural system. It contributes to reducing the tender period for structural designers. For reoccurring building types a parametric tool could certainly be useful. The time it takes to implement the tool is most likely earned in the time that is saved in the individual projects. Especially in the early design stages it is a valuable asset to have a parametric tool to use for quick iterations and evaluations.

The tool is user friendly and efficient. After providing the required input data a material optimized structural system is instantly generated and perspicuous data with information about the system is displayed. The results can be used as a foundation for the project and an early indication of which structural system would suit the project. By changing the input data different structural systems and dimensions of the building can be evaluated efficiently. The tool makes environmentally sustainable buildings more achievable without requiring more generous time frames. As discussed in Chapter 5.5 the user has to have certain knowledge to use the tool. However, non of the knowledge has to be acquired prior to using the tool and all the necessary information is provided in the user manual.

One objective of the thesis was to investigate what structural system is the most environmentally beneficial. In the results it can be seen that the tool generally chooses high and slender elements. Furthermore, it can be seen that a greater spacing leads to a reduction of the material usage. However, this conclusion is made with a prerequisite that the effect of the roof type is not included or that a timber roof construction is used. If a steel roof is used instead it is more environmentally beneficial to minimize the amount of steel and hence choose the smallest steel plate combined with the maximum spacing that is achievable. The tool also evaluates which beam type is the best alternative in the topology optimization. A general conclusion regarding which beam type is the most beneficial can not be made since the chosen solution varies from case to case. Noteworthy is that the results of the thesis are based on a comparison of two case studies. Thus, conclusions cannot be guaranteed with certainty, but it can be seen in this thesis that a reduction of material usage and a reduction of emissions carbon dioxide equivalents is possible in these cases.

An important aspect to consider is if the results are practically feasible and if there

are any difficulties regarding the output solutions from the tool. The fact remains that there are other aspect to consider when designing structural systems, such as economical and practical aspects. Hence, there is an importance of awareness from the designer to account for these difficulties. However, the tool can be considered as an encouragement to the construction industry to challenge today's way of building. The near future will come with several regulations regarding the environmental footprint of buildings, making new methods for sustainable construction more desirable. This thesis is aimed particularly towards structural engineers and designers and their possibilities to contribute to a more sustainable future.

6.1 Further Work

The tool is currently fully functional. More features can however with advantage be implemented. To extend the usability of the tool more beam types, such as curved beams, boomerang beams and truss beams, continuous beams as well as frames could be added. Other building materials for the load-bearing structure, such as steel, could also be implemented and evaluated. The bracing elements could be further treated and be dimensioned to withstand the horizontal forces. The dimensioning of the structural elements could be extended to include loads applied during lifts at the construction site. The total amount of carbon dioxide equivalents would be more telling if the effect of more elements were included. The cross bracing, internal and external walls, connection details and foundation are examples of such elements. One click LCA can be integrated in the tool to get more extensive calculations of the emissions during the building's life-cycle as well as to get access to a updated climate database and eventual product specific data. Further developments could also be made to the choice of roof system, as it currently is quite superficially treated. An additional feature that could add value to the tool is to implement a generation of a FEM-model that easily can be exported to FEM-design for further calculations. To take the more aspects into consideration, such as economical and practical, a multi-objective optimization could be integrated.

Bibliography

[1] NASA's Jet Propulsion Laboratory. Carbon Dioxide [Internet]. California Institute of Technology; [Updated: January 25, 2023; cited January 26, 2023]. URL: https://climate.nasa.gov/vital-signs/carbon-dioxide/

[2] Boverket. Utsläpp av växthusgaser från bygg- och fastighetssektorn [Internet]. Boverket; [Updated: 9 januari 2023; cited January 24, 2023]. URL: https://www.boverket.se/sv/byggande/hallbart-byggande-och-forvaltning/miljoindikatorer—aktuell-status/vaxthusgaser/

[3] Boberg P. Utsläpp av växthusgaser till år 2045 [Internet]. Sveriges Miljömål; [Updated Mars 21, 2023; Cited: January 26, 2023]. URL: https://www.sverigesmiljomal.se/etappmalen/utslapp-av-vaxthusgaser-till-ar-2045/

[4] Boverket. Utveckling av regler om klimatdeklaration av byggnader [Internet]. Karlskrona: Boverket; 2020. [Cited: January 26, 2023]. URL: https://www.boverket.se/globalassets/publikationer/dokument/2020/utveckling-av-regler-om-klimatdeklaration-av-byggnader.pdf

[5] Naturvårdsverket. Klimatet och bygg- och fastighetssektorn [Internet]. Naturvårdsverket; [Cited: January 26, 2023]. URL: https://www.naturvardsverket.se/amnesomraden/klimatomstallningen/omraden/klimatet-och-bygg–och-fastighetssektorn/

[6] Malmqvist T, et al. *Design and construction strategies for reducing embodied impacts from buildings – Case study analysis*. Elsevier; 2018.

[7] Boverket. Mer om miljövarudeklaration för byggprodukter (EPD) [Internet]. Boverket; [Updated: February 20, 2019; cited February 02, 2023]. URL: https://www.boverket.se/sv/byggande/hallbart-byggande-och-forvaltning/livscykelanalys/miljodata-och-lca-verktyg/miljovarudeklaration-for-byggprodukter-epd/

[8] Boverket. Byggnaders klimatpåverkan utifrån ett livscykelperspektiv[Internet]. Karlskrona: Boverket; 2015. [Cited: February 06, 2023]. URL: https://www.boverket.se/globalassets/publikationer/dokument/2015/byggnaders-klimatpaverkan-utifran-ett-livscykelperspektiv.pdf/

[9] Boverket. Referensvärden för klimatpåverkan vid uppförande av byggnader [Internet]. Boverket; 2023 [Cited: May 17, 2023]. URL: https://www.boverket.se/sv/byggande/hallbart-byggande-och-forvaltning/referensvarden-for-byggandets-klimatpaverkan/

[10] Boverket. Vägledning om LCA för byggnader [Internet]. Boverket; 2019. [Cited: February 06, 2023]. URL: https://forvaltarforum.se/wp-content/uploads/2019/02/Vagledning-om-LCA-för-byggnader.pdf/

[11] Hamil S. What is Building Information Modelling (BIM)? [Internet]. NBS; 2021 [Updated: September 9, 2021; Cited: April 05, 2023]. URL: https://www.thenbs.com/knowledge/what-is-building-information-modelling-bim

[12] Savic D. Single-objective vs. Multiobjective Optimisation for Integrated Decision Support. Exeter: Centre for Water Systems, Department of Engineering School of Engineering and Computer Science, University of Exeter; 2002.

[13] Christensen P, Klarbring A. *An Introduction to Structural Optimization*. Linköping: Springer.

[14] Srivastava P K, et al. Structural Optimization Methods: A General Review. *International Journal of Innovative Research in Science, Engineering and Technology*. 2017; 6(9): 88-92.

[15] López J, et al. Structural shape optimization using Bézier triangles and a CAD-compatible boundary representation. *Engineering with Computers*; 2020: 1657–1672.

[16] Risberg M. Topologioptimering av gjutgods. Jönköping: Swerea SWECAST AB; 2010.

[17] Bendsøe M P, Sigmund O. *Topology Optimization*. 2 ed. Berlin: Springer-Verlag Berlin Heidelberg; 2004.

[18] Sarker R. Evolutionary Optimization (Evopt): A Brief Review And Analysis. *International Journal of Computational Intelligence and Applications;* 2003.

[19] Encyclopædia Britannica, Inc. Stochastic process [Internet]. Encyclopædia Britannica, Inc; [Updated: February 15, 2023; Cited: February 17, 2023]. URL: https://www.britannica.com/science/stochastic-process

[20] Eberhard P, et al. Some advantages of stochastic methods in multicriteria optimization of multibody systems. *Archive of Applied Mechanics*. 1999; (69): 543-554.

[21] Erdinç O. *Optimization in renewable energy systems : recent perspectives*. Kidlington; Butterworth-Heinemann; 2017

[22] Jabi W. Parametric Design for Architecture. London; Laurence King Student & Professional; 2013

[23] Feng F. *Design and Analysis of Tall and Complex Structures*. Kidlington; Butterworth-Heinemann; 2018.

[24] Holzer D. Parametric Design and Structural Optimisation for Early Design Exploration. *International journal of architectural computing;* 2007

[25] Rhino3d. Features. [Internet]. Robert McNeel & Associates. URL: https://www.rhino3d.com/features/

[26] Rhino3d. What are NURBS? [Internet]. Robert McNeel & Associates. URL: https://www.rhino3d.com/features/nurbs/

[27] TOI-Pedia [Internet]. 2021 -. Galapagos Optimization; [Updated: June 17, 2021; Cited Februari 9, 2023]. URL: http://wiki.bk.tudelft.nl/toi-pedia/Galapagos_Optimization

[28] Trä Och Träindustrin - Världens Sjätte Största Producent [Internet]. Stockholm: Föreningen Skogen, [Cited: April 28, 2023]. URL: https://www.skogen.se/portal/tra-och-traindustrin-varldens-sjatte-storsta-producent/

[29] Trä i byggprocessen [Internet]. Svenskt Trä; [Cited: March 10, 2023]. URL: https://www.svenskttra.se/bygg-med-tra/byggande/bygga-i-tra/
[30] Swedish Wood. Design of timber structures volume 1. Stockholm; 2019.
[31] Träguiden. Träets styrka och styvhet [Internet]. Svenskt Trä; [Cited: May 22, 2023]. URL: https://www.traguiden.se/om-tra/materialet-tra/traets-egenskaper-och-kvalitet/mekaniska-egenskaper1/traets-styrka-och-styvhet/
[32] Träguiden. Brandsäkerhet [Internet]. Svenskt Trä; [Updated: December 1, 2021; Cited: March 10, 2023]. URL: https://www.traguiden.se/om-tra/brandsakerhet/
[33] Swedish Wood. Wood construction cuts climate footprint [Internet]. Swedish Wood; [Cited April 4, 2023]. URL: https://www.swedishwood.com/wood-facts/about-wood/wood-and-sustainability/wood-construction-cuts-climate-footprint/
[34] Hawkins W. Timber and carbon sequestration [Internet]. The Structural Engineer. January 2021; Volume 99, issue 1: pages 18-20. URL: https://www.istructe.org/IStructE/media/Public/TSE-Archive/2021/Timber-and-carbon-sequestration.pdf
[35] Svenskt Trä. Limträhandboken del 2. Stockholm; 2016.
[36] Svenskt Trä. Limträhandboken del 1. Stockholm; 2016.
[37] About glulam [Internet]. Swedish Wood; [Cited: March 6, 2023]. URL: https://www.swedishwood.com/building-with-wood/about-glulam/R27
[38] Träguiden. Konstruktionssystem [Internet]. Svenskt Trä; [Cited: May 03, 2023]. URL: https://www.traguiden.se/konstruktion/limtrakonstruktioner/fakta-om-limtra/projektering/konstruktionssystem/inledning/
[39] Hansson T. Hallkonstruktioner. Träinformation. 1999: 1/99; p. 11 - 15.
[40] SS-EN 1991-1-3. Eurocode 1 – Actions on structures – Part 1-3: General actions – Snow loads.
[41] SS-EN 1991-1-1. Eurocode 1: Actions on structures - Part 1-1: General actions - Densities, self-weight, imposed loads for buildings.
[42] EN 1991-1-4:2005. Eurocode 1: Actions on structures – Part 1–4: General actions – Wind actions.
[43] Ramboll. Fenix tuo rakennesuunnittelun tulevaisuuden tähän päivään [Internet]. [Cited: May 17, 2023]. URL: https://c.ramboll.com/fi/fenix-by-ramboll
[44] Svenskt Trä. Limträhandboken del 3. Stockholm; 2016.

A

User Manual

The following sections provides a guide of how the tool should be used.

A.1 Before Using the Tool

To use the tool an installation of Rhinoceros 3D is required. As the tool is implemented in Rhino 7 this is the recommended version of the program. Rhino 7 includes Grasshopper and hence no separate installation of Grasshopper is required.

A.2 Getting Started

Opening the Grasshopper file *Optimization_Tool_Industrial_Building* will initiate the tool. Double clicking the file will prompt Rhino as well as Grasshopper to start. The Grasshopper file contains two custom components, *plug-ins*, which are not included in the standard version of Grasshopper and have to be installed separately. Grasshopper will point out which components are missing and prompt the user to install these. They are installed by clicking *download and install*, as illustrated in Figure A.1. The required plug-ins are listed below.

- Human
- Sasquatch

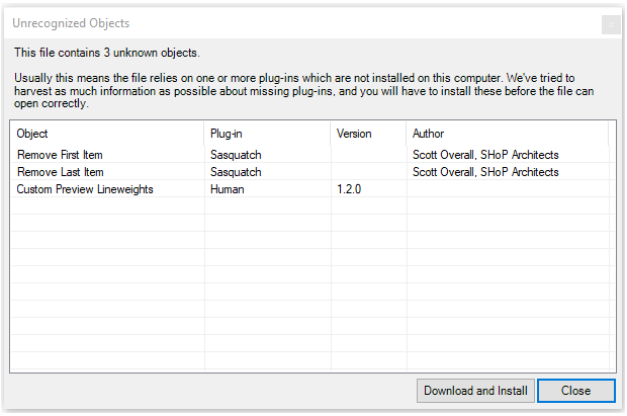

Figure A.1: Pop-up window for missing plug-ins.

When the installation is finished the window shown in Figure A.2 will be displayed. Both open pop-up windows can now be closed. After the relevant plug-ins are installed Rhino and Grasshopper have to be **restarted** and the file re-opened.

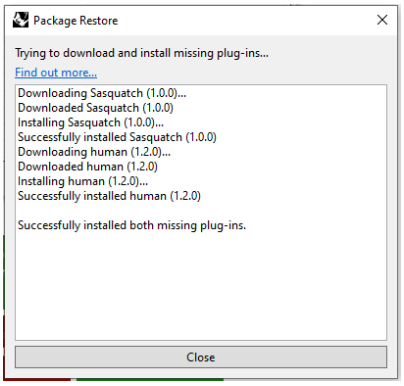

Figure A.2: Pop-up window displayed when the missing plug-ins are installed.

A.3 Orientation in the Tool

Two windows are now opened. Rhino is used only to display the results. No actions has to be taken in this window other than navigating in the view window. Information about how Rhino is operated can be found at *https://docs.mcneel.com/rhino/6/usersguide/en-us/index.htm*.

All the user-defined input can be found in the upper left corner in the Grasshopper file, see figure A.3.

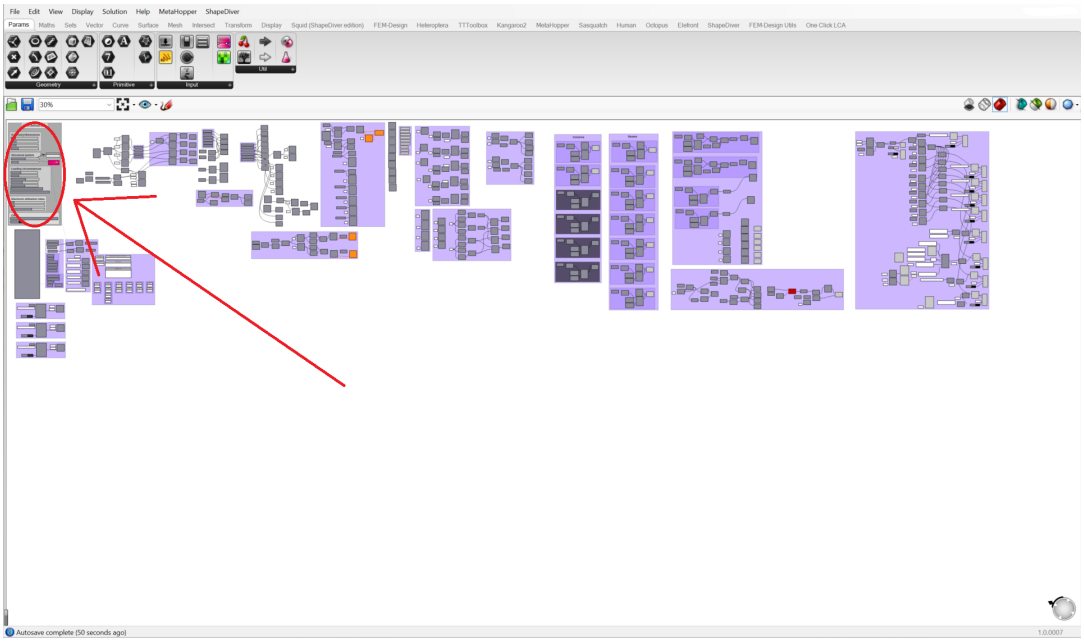

Figure A.3: The grasshopper file with the user-defined data marked.

The user defined data is controlled mainly by sliders with preset maximum and minimum values. Some input is adjusted with drop-down menus and the model is turned on and off using a button. The input section is seen in Figure A.4.

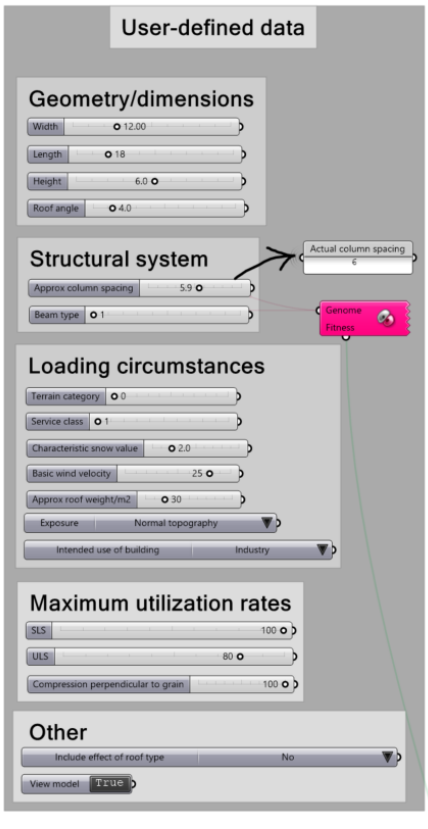

Figure A.4: The input section of the tool.

All values in this section can be altered by the user according to the specific project at hand. The input is explained below.

- **Width** - Width of the building [m]. Defined from column center to column center.
- **Length** - Length of the building [m]. Defined from column center to column center.
- **Height** - Height of the building [m]. Defined as the lowest free height indoors.
- **Roof angle** - Angle of the roof [°]. For the tapered beam the value can change by ±2 degrees to find the most material effective solution.
- **Approx. column spacing** - Approximate center-to-center distance [m] of the columns along the length of the building, i.e. between the main columns. The columns are always spaced evenly, which means that if the building length is not a multiple of the specified spacing another spacing will be chosen by the tool. This new spacing is based on the specified spacing but will be adjusted to the closest value which provides equal gaps between the columns.
- **Beam type** - Beam type for the main beams. 1 = beams with constant cross section, 2 = tapered beams.

- **Terrain category** - The terrain category at the site, according to SS-EN 1991-1-4, A1.
- **Service class** - The service class, according to SS-EN-1995-1-1, 2.3.1.3.
- **Characteristic snow value** - Value for the characteristic snow [kN/m^2]. Values can be found in EKS 11.
- **Basic wind velocity** - Value for the basic wind velocity [m/s]. Values can be found in EKS 11.
- **Approx. roof weight/m^2** - Approximation of what the roof construction weighs [kg].
- **Exposure** - The wind exposure at the building site. Choose the most suitable of windswept topography, normal topography or sheltered topography. For further explanation see SS-EN 1991-1-3, 5.2.
- **Intended use of building** - The intended area of usage for the building. Choose the most suitable of industry, school/store etc, animal stable or machine hall.
- **SLS** - Maximum allowed utilization rate in serviceability limit state.
- **ULS** - Maximum allowed utilization rate in ultimate limit state.
- **Compression perpendicular to grain** - Maximum allowed utilization rate for compression perpendicular to the grain.
- **Include effect of roof type** - Controls if the carbon dioxide equivalents for the roof construction should be included in the total carbon dioxide equivalents or not. Choose between no, only steel roof, only timber roof or both steel and timber roof. If *both steel and timber roof* is chosen the tool will pick the option that provides the lowest carbon dioxide equivalents. The steel roof works for larger spans than the timber roof. If the roof type cannot fulfil the requirements of the specified building the only output will be the that no structural system fulfils the requirements. In the case where both roof types are included and only one roof type can fulfil the requirements the tool will automatically choose this one. The *effect* of roof type hence only refers to the carbon dioxide equivalents and not the weight of the roof construction. The weight is regulated in the input *Approx. roof weight/m^2*.
- **View model** - Choose to view the structural elements in the model or not. The model should preferably be turned off when topology optimization is performed. This is altered by double clicking the button.

The sliders can be altered by either sliding the dot or bubble clicking it, typing in the value and pressing the green tick, as seen in Figure A.5.

Figure A.5: Adjusting the input sliders.

The input controlled by drop-down menus is altered by clicking the black arrow and choosing the desired alternative. An example of this is shown in Figure A.6.

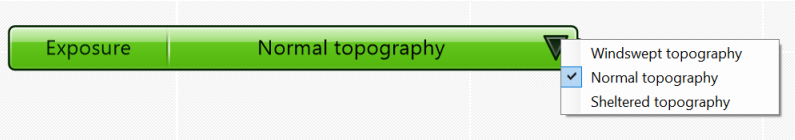

Figure A.6: Adjusting the drop-down menus.

A.4 Performing the optimization

The sizing optimization does not need to be initiated. When all input is provided a sizing optimized structural system will automatically be provided. If the user wishes to optimize the structure further a topology optimization can be performed by allowing the tool to change the the column spacing and beam type. This is performed using the component *Galapagos*. This component characterized by its pink colour and can be found by the user-defined data. Double clicking the component will prompt an editor window to open. This window can be seen in Figure A.7.

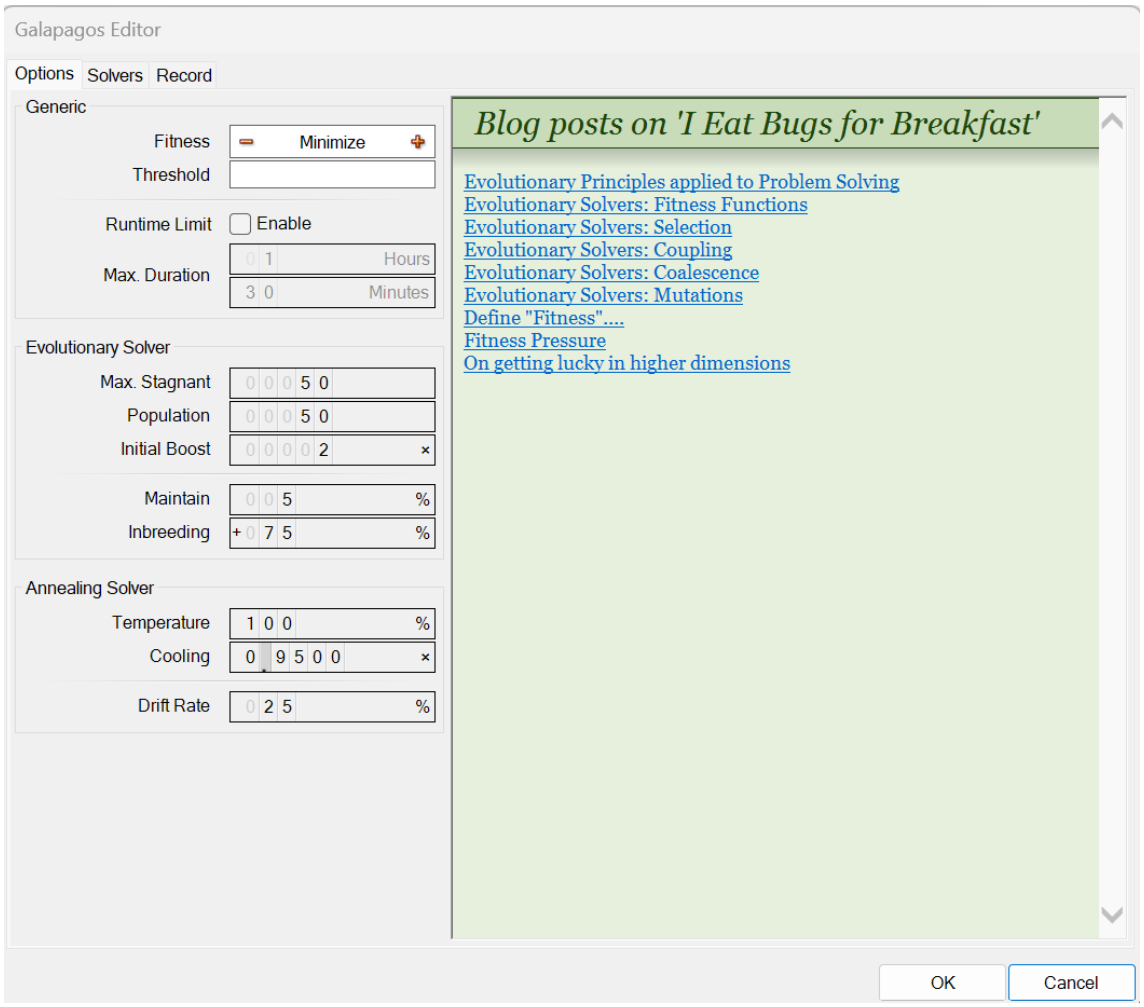

Figure A.7: The Galapagos editor.

Here, the user should fill in the information in the section *Generic* and *Evolutionary solver*. The fitness should be set to *Minimize*. The standard settings can generally be used, but the settings can also be altered. The threshold should be left blank. A run-time limit can be applied. This limit causes the optimization to stop if it consumes to much time without finalizing. The max stagnant controls how many generations that can be generated without gaining a better solution before the solver stops. Population is the amount of options that are tested before the optimization moves on to the next generation. The initial boost controls the size of the population in the first generation of solutions. Inbreeding is a freedom factor which manages the similarity of the genes that are bred. A positive value means similar genes whilst a negative value will give different genes. Lastly, maintain governs how many cross-overs that should be done in each generation.

When the input is set the algorithm is stated by navigating to the *solvers* tab. Choose the evolutionary solver by clicking the symbol marked in Figure A.8. Turn the model of before starting the optimization. Start the optimization by clicking *Start Solver*.

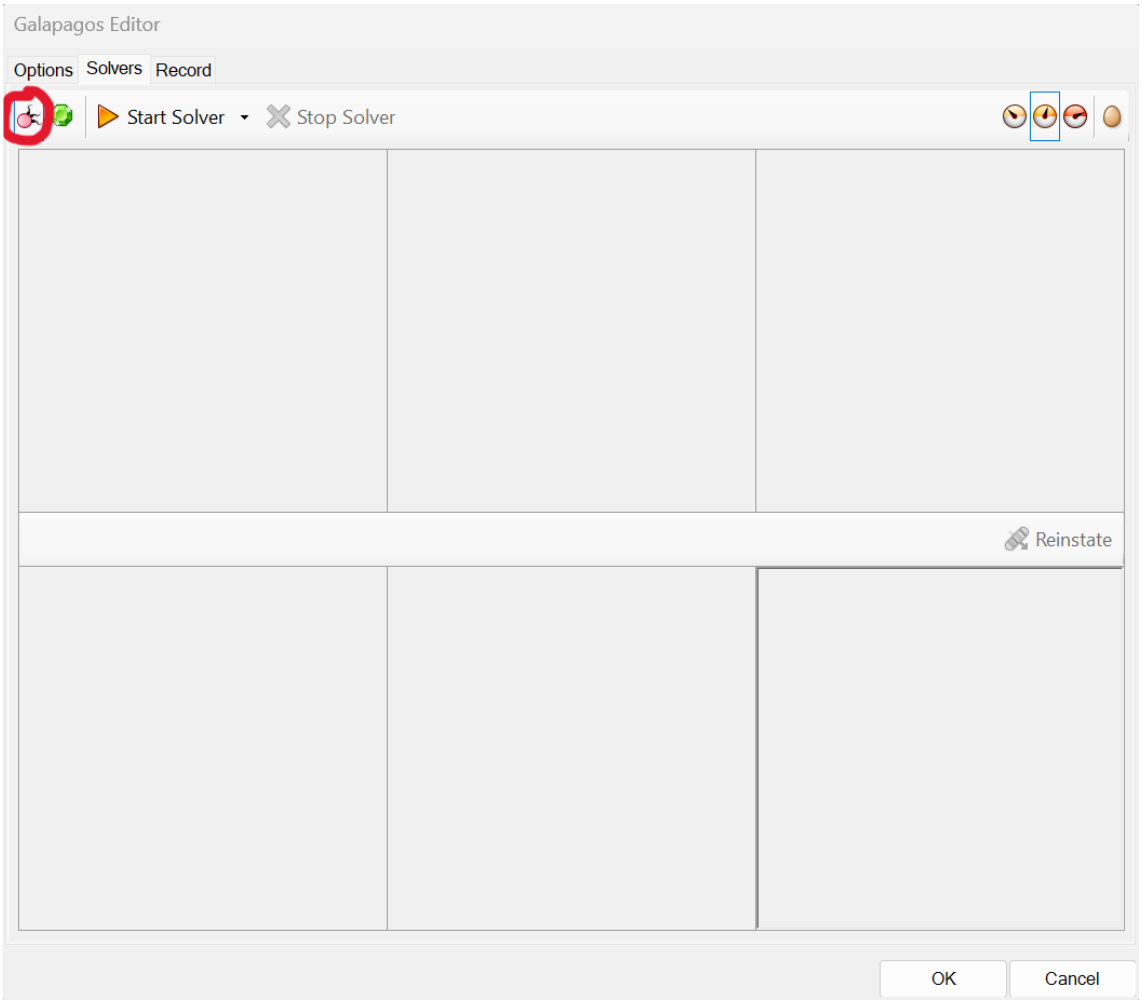

Figure A.8: The solver window in Galapagos.

Sometimes the algorithm keeps running for a while after an optimized solution has been found. When the values marked by a red circle in Figure A.9 converges the solver can be stopped by pressing *Stop Solver*.

Figure A.9: The solver window while the optimization is run. Here the values have converged.

A.5 Results

The results are displayed in the form of a wire frame model, a model containing the structural elements and an information panel. An example of the output is illustrated in Figure A.10.

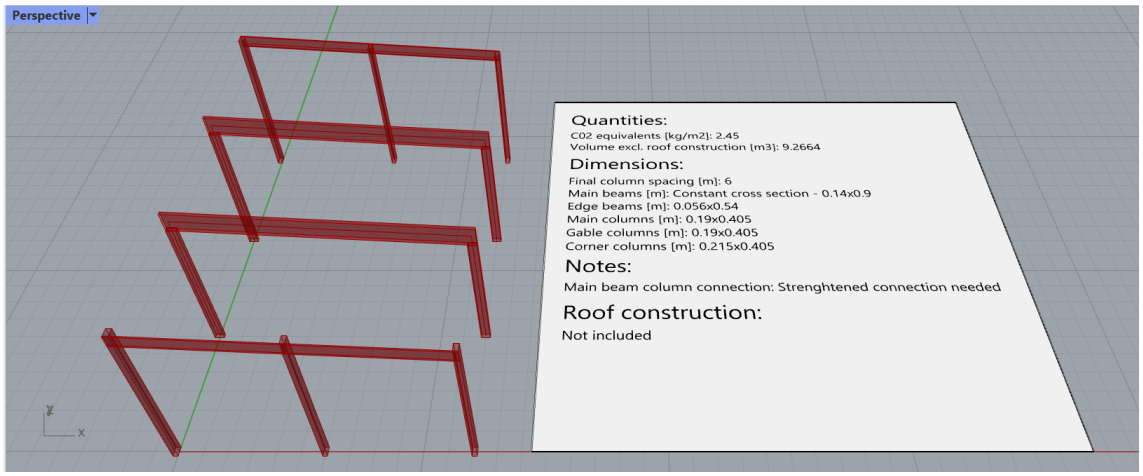

Figure A.10: Example of the output from the tool.

If no system fulfils the structural requirements the output in Figure A.11 will be shown. The user then needs to alter the input to gain a functioning structural system.

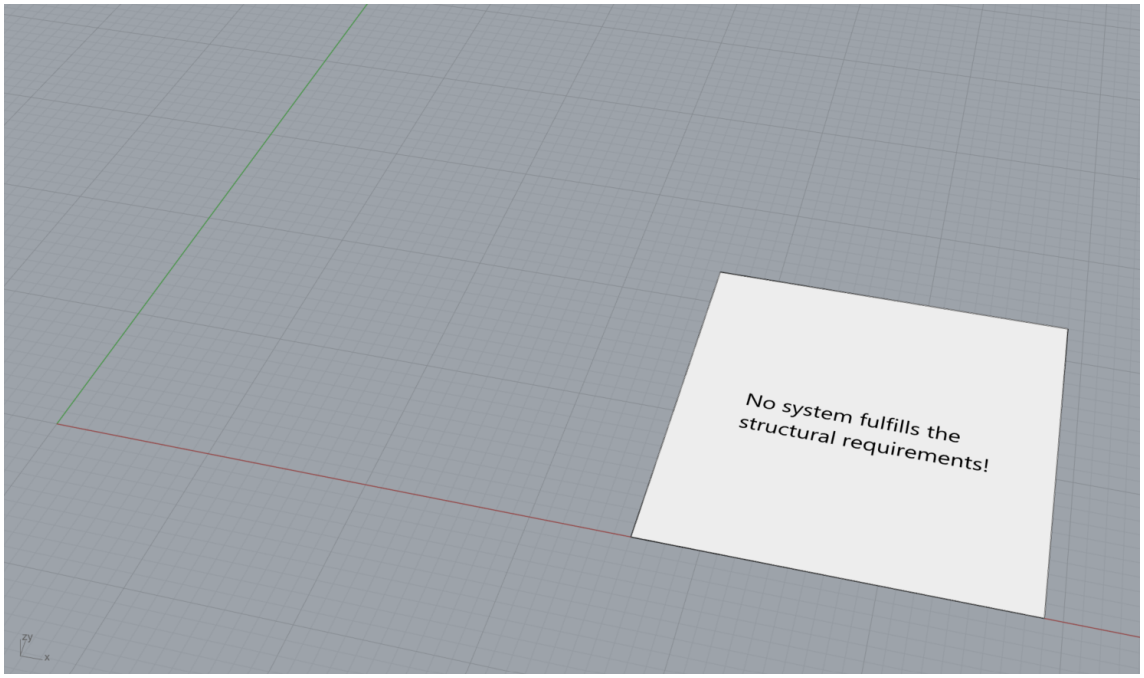

Figure A.11: Output when no system can be created.

Important to note is that the roof construction only is a rough estimation which has to be taken into account for a final design. The dimensioning of the roof is made to get a rough estimation of the carbon dioxide equivalents it will add. Furthermore the connections between the elements are not treated which means that they also requires post-processing before reaching a final design. The calculation of the strengthening of the connection between the main columns and main beams is made only with regard to if it is feasible or not. The calculation of how the strengthening is actually made has to be performed manually. If the output shows

that a strengthened connection is needed the user should be aware of the compression perpendicular to the grain of the main beams. Moreover, the design assumes cross bracing in all four walls but the actual dimensioning of these elements is not performed in the tool and has to be supplemented.

B

Input

In this appendix the internalized input data used in tool is shown.

B.1 Excel Sheet Standard Glulam Dimensions

Figure B.1 shows an extract of the excel sheet used to import information about glulam standard dimensions to the tool.

b	h	Class	f_{vk}	f_{mk}	E_{0mean}	ρ_{mean}	f_{c0k}	E_{005}	f_{c90k}	G_{005}	G_{mean}	ρ_k	f_{t90k}
42	90	GL28hs	3500000	28000000	1,31E+10	480	28000000	1,05E+10	2500000	5,4E+08	6,5E+08	430	500000
42	135	GL28hs	3500000	28000000	1,31E+10	480	28000000	1,05E+10	2500000	5,4E+08	6,5E+08	430	500000
42	180	GL28cs	3500000	28000000	1,25E+10	430	24000000	1,04E+10	2500000	5,4E+08	6,5E+08	390	500000
42	225	GL28cs	3500000	28000000	1,25E+10	430	24000000	1,04E+10	2500000	5,4E+08	6,5E+08	390	500000
42	270	GL28cs	3500000	28000000	1,25E+10	430	24000000	1,04E+10	2500000	5,4E+08	6,5E+08	390	500000
42	315	GL28cs	3500000	28000000	1,25E+10	430	24000000	1,04E+10	2500000	5,4E+08	6,5E+08	390	500000
42	360	GL28cs	3500000	28000000	1,25E+10	430	24000000	1,04E+10	2500000	5,4E+08	6,5E+08	390	500000
42	405	GL28cs	3500000	28000000	1,25E+10	430	24000000	1,04E+10	2500000	5,4E+08	6,5E+08	390	500000
56	90	GL28hs	3500000	28000000	1,31E+10	480	28000000	1,05E+10	2500000	5,4E+08	6,5E+08	430	500000
56	135	GL28hs	3500000	28000000	1,31E+10	480	28000000	1,05E+10	2500000	5,4E+08	6,5E+08	430	500000
56	180	GL28cs	3500000	28000000	1,25E+10	430	24000000	1,04E+10	2500000	5,4E+08	6,5E+08	390	500000
56	225	GL28cs	3500000	28000000	1,25E+10	430	24000000	1,04E+10	2500000	5,4E+08	6,5E+08	390	500000
56	270	GL28cs	3500000	28000000	1,25E+10	430	24000000	1,04E+10	2500000	5,4E+08	6,5E+08	390	500000
56	315	GL28cs	3500000	28000000	1,25E+10	430	24000000	1,04E+10	2500000	5,4E+08	6,5E+08	390	500000
56	360	GL28cs	3500000	28000000	1,25E+10	430	24000000	1,04E+10	2500000	5,4E+08	6,5E+08	390	500000
56	405	GL28cs	3500000	28000000	1,25E+10	430	24000000	1,04E+10	2500000	5,4E+08	6,5E+08	390	500000
56	450	GL28cs	3500000	28000000	1,25E+10	430	24000000	1,04E+10	2500000	5,4E+08	6,5E+08	390	500000
56	495	GL28cs	3500000	28000000	1,25E+10	430	24000000	1,04E+10	2500000	5,4E+08	6,5E+08	390	500000
56	540	GL28cs	3500000	28000000	1,25E+10	430	24000000	1,04E+10	2500000	5,4E+08	6,5E+08	390	500000
66	90	GL28hs	3500000	28000000	1,31E+10	480	28000000	1,05E+10	2500000	5,4E+08	6,5E+08	430	500000
66	135	GL28hs	3500000	28000000	1,31E+10	480	28000000	1,05E+10	2500000	5,4E+08	6,5E+08	430	500000
66	180	GL28cs	3500000	28000000	1,25E+10	430	24000000	1,04E+10	2500000	5,4E+08	6,5E+08	390	500000
66	225	GL28cs	3500000	28000000	1,25E+10	430	24000000	1,04E+10	2500000	5,4E+08	6,5E+08	390	500000
66	270	GL28cs	3500000	28000000	1,25E+10	430	24000000	1,04E+10	2500000	5,4E+08	6,5E+08	390	500000
66	315	GL28cs	3500000	28000000	1,25E+10	430	24000000	1,04E+10	2500000	5,4E+08	6,5E+08	390	500000
66	360	GL28cs	3500000	28000000	1,25E+10	430	24000000	1,04E+10	2500000	5,4E+08	6,5E+08	390	500000
66	405	GL28cs	3500000	28000000	1,25E+10	430	24000000	1,04E+10	2500000	5,4E+08	6,5E+08	390	500000
66	450	GL28cs	3500000	28000000	1,25E+10	430	24000000	1,04E+10	2500000	5,4E+08	6,5E+08	390	500000
66	495	GL28cs	3500000	28000000	1,25E+10	430	24000000	1,04E+10	2500000	5,4E+08	6,5E+08	390	500000
66	540	GL28cs	3500000	28000000	1,25E+10	430	24000000	1,04E+10	2500000	5,4E+08	6,5E+08	390	500000

Figure B.1: Extract of the input data of the glulam standard dimensions.

B.2 Excel Sheet Timber Roof

Figure B.2 shows an extract of the excel sheet used to import information about standard dimensions of structural timber to the tool.

b	h
12	48
19	75
19	100
19	125
22	75
22	100
22	125
22	150
22	175
22	200
25	23
25	36
25	48
25	75
25	100
25	125
25	150
32	75
32	100
32	125
32	150
32	175
32	200
32	225
38	75
38	100
38	125
38	150
47	75
47	100

Figure B.2: Extract of the input data of the standard dimensions of structural timber.

B.3 Excel Sheet Steel Roof

Figure B.3 shows an extract of the excel sheet used to import information about maximum spans for different steel roof structures to the tool.

S_k=1 kN/m^2				S_k=1,5 kN/m^2				S_k=2 kN/m^2			
Span	Plate	t	Weight	Span	Plate	t	Weight	Span	Plate	t	Weight
5	T70	0,7	8,14664	4,2	T70	0,7	8,14664	3,6	T70	0,7	8,14664
5,6	T70	0,8	9,164969	4,7	T70	0,8	9,164969	4,1	T70	0,8	9,164969
6,2	T130	0,7	9,164969	5,1	T130	0,7	9,164969	4,4	T130	0,7	9,164969
7,2	T130	0,8	10,1833	6	T130	0,8	10,1833	4,5	T70	0,9	10,1833
8,1	T130	0,9	11,20163	6,8	T130	0,9	11,20163	5,2	T130	0,8	10,1833
8,8	T130	1	13,23829	7,5	T130	1	13,23829	5,9	T130	0,9	11,20163
9,3	T153	1	14,25662	7,9	T153	1	14,25662	6,5	T130	1	13,23829
9,6	T130	1,2	15,27495	8,9	T130	1,2	15,27495	6,9	T153	1	14,25662
9,6	T130	1,2	15,27495	9,1	T153	1,2	17,31161	7,8	T130	1,2	15,27495
9,6	T130	1,2	15,27495	9,6	T130	1,5	19,34827	8	T153	1,2	17,31161
9,6	T130	1,2	15,27495	9,6	T130	1,5	19,34827	9,6	T130	1,5	19,34827

S_k=2,5 kN/m^2				S_k=3 kN/m^2				S_k=4 kN/m^2			
Span	Plate	t	Weight	Span	Plate	t	Weight	Span	Plate	t	Weight
3,3	T70	0,7	8,14664	2,9	T70	0,7	8,14664	2,5	T70	0,7	8,14664
3,7	T70	0,8	9,164969	3,4	T70	0,8	9,164969	2,9	T70	0,8	9,164969
3,9	T130	0,7	9,164969	3,5	T130	0,7	9,164969	3,2	T70	0,9	10,1833
4,1	T70	0,9	10,1833	3,7	T70	0,9	10,1833	3,5	T130	0,8	10,1833
4,6	T130	0,8	10,1833	4,2	T130	0,8	10,1833	4	T130	0,9	11,20163
5,3	T130	0,9	11,20163	4,8	T130	0,9	11,20163	4,5	T130	1	13,23829
5,8	T130	1	13,23829	5,3	T130	1	13,23829	4,8	T153	1	14,25662
6,2	T153	1	14,25662	5,6	T153	1	14,25662	5,5	T130	1,2	15,27495
7	T130	1,2	15,27495	6,4	T130	1,2	15,27495	5,7	T153	1,2	17,31161
7,2	T153	1,2	17,31161	6,6	T153	1,2	17,31161	6,9	T130	1,5	19,34827
8,7	T130	1,5	19,34827	8	T130	1,5	19,34827	6,9	T130	1,5	19,34827

Figure B.3: Extract of the input data of the glulam standard dimensions.

The excel sheets show in Figure B.3 are based on data retrieved from product specific load tables. These are products by Ruukki Construction and the tables are collected from
https://www.ruukki.com/swe/building-envelope/service-support/load-bearing-sheet-and-purlin-support/lasttabell.

C
Reference Projects

The maximum utilization rates for each element is presented in this appendix. The provided documentation for the reference projects is also presented.

C.1 Maximum Utilization Rates

Table C.1 shows the maximum utilization rate for all elements in reference project 1 and Table C.2 shows the maximum utilization rate for all elements in reference project 2.

Table C.1: *The maximum utilization rates for reference project 1*

Main beams	87%
Edge beams	51%
Main columns	46%
Gable columns	73%
Corner columns	53%

Table C.2: *The maximum utilization rates for reference project 2*

Main beams	77%
Edge beams	40%
Main columns	44%
Corner columns	39%

C.2 Provided Documentation - Reference Project 1

Structural drawings for reference project 1 can be seen in Figure C.1 and Figure C.2. The calculation data for the project was provided in Swedish and the document is appended below the figures.

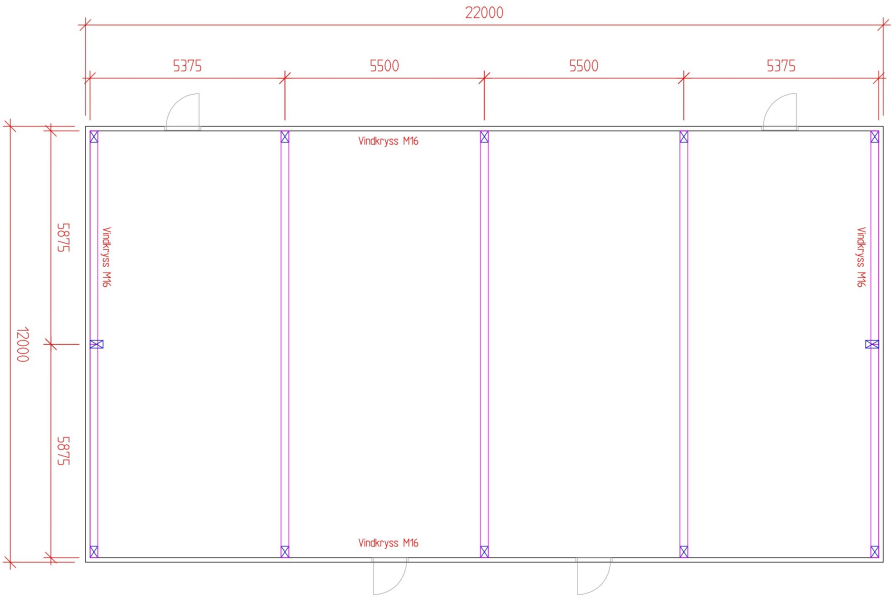

Figure C.1: Plan view for reference project 1.

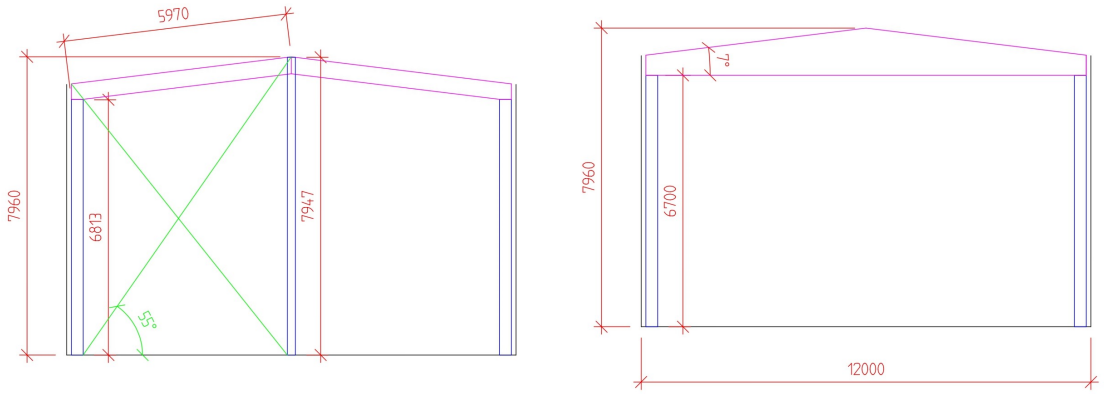

(a) Section 2. **(b)** Section 1.

Figure C.2: Sectional views for reference project 1.

KALKYLUNDERLAG

MÅTT

Bredd: 12m

Längd: 22m

Höjd: 8m

Taklutning: 7°

STOMSTABILISERING

Skrivverkan i tak: Ja

Långsida: Vindkryss

Kortsida: Vindkryss

LASTFÖRUTSÄTTNINGAR

För dimensionering och utförande gäller följande bestämmelser:

- EKS 11 (Boverkets föreskrifter om tillämpning av europeiska konstruktionsstandarder, Eurokoder)
- Boverkets byggregler, BBR 29

Säkerhetsklass: 3

Egentyngd tak: 0,65 kN/m^2

Snölast: 2,5 kN/m^2

Vindlast q_k: 0.73 kN/m^2

Terrängtyp: II

V_{ref}: 24 m/s

LIMTRÄ

Hållfasthetsklass: GL30c

Klimatklass: 2

STÅL

Hållfasthetsklass: S355

Korrosivitetsklass: C2

Utförandeklass: EXC2

BRANDKLASS

R30

C.3 Reference Project 2 - Beams with Constant Cross Section

Structural drawings for reference project 2 can be seen in Figure C.3 and Figure C.4. The calculation data for the project was provided in Swedish and the document is appended below the figures.

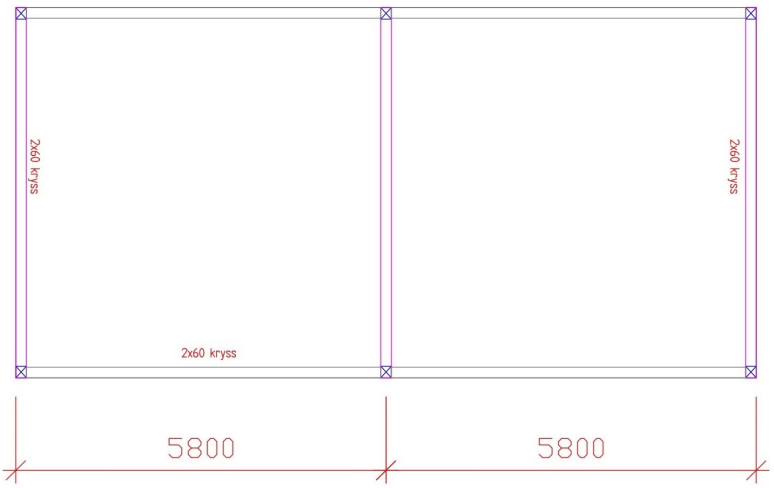

Figure C.3: Plan view for reference project 2.

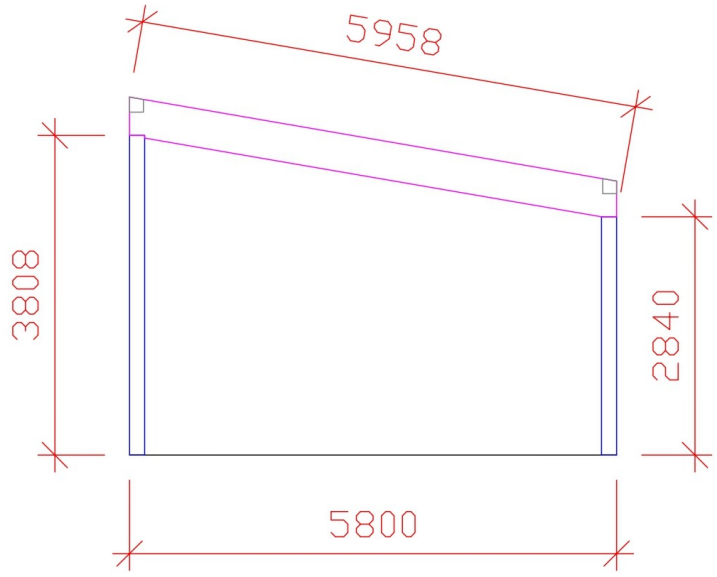

Figure C.4: Sectional view for reference project 2.

KALKYLUNDERLAG

MÅTT

Bredd:	6m
Längd:	12m
Höjd:	4,6m
Taklutning:	10°

STOMSTABILISERING

Tak stabiliseras genom skivverkan i takplåt.

Långsida: Vindkryss

Kortsida: Vindkryss

LASTFÖRUTSÄTTNINGAR

För dimensionering och utförande gäller följande bestämmelser:

- EKS 11 (Boverkets föreskrifter om tillämpning av europeiska konstruktionsstandarder, Eurokoder)
- Boverkets byggregler, BBR 29

Säkerhetsklass:	2
Egentyngd tak:	0,65 kN/m^2
Snölast:	2,5 kN/m^2
Vindlast q_k:	0.52 kN/m^2
Terrängtyp:	II
V_{ref}:	22 m/s

LIMTRÄ

Hållfasthetsklass:	GL30c
Klimatklass:	2

STÅL

Hållfasthetsklass:	S355
Korrosivitetsklass:	C2
Utförandeklass:	EXC2

D
Verification

In this appendix supplementary material for the verification is shown.

D.1 Adjusted Values

This section shows how the wind load from the tool compares to the applied wind loads in the reference projects if the internal wind load is excluded in the tool in the same way as it is in the reference projects. Table D.2 shows values for reference project 1 and Table D.2 shows the corresponding values for reference project 2. The values from the tool are in verification purposes adjusted to see how the loads correspond if the internal wind pressure is removed. These are hence not the loads that are actually used in the dimensioning by the tool. They are used to evaluate if the large differences seen in Tables 4.18 and 4.19 depends on different design choices, rather than errors in load application. When dimensioning the elements the tool always takes the internal wind load into account as this will provide the highest, and hence dimensioning, loads.

Table D.1: *The adjusted wind loads from the tool compared to the wind loads reference project 1 [kN/m]*

	Reference project 1	The tool	Difference [%]
Main beam, zone 1	-0.8	0.164	-120.5
Main beam, zone 2	-4.82	0.164	-103.4
Edge beams, zone 1	0.08	0.082	+2.5
Edge beams, zone 2	0.08	0.082	+2.5
Corner columns, y-direction	2.568	2.64	+2.8

Table D.2: *The adjusted wind loads from the tool compared to the wind loads reference project 2 [kN/m]*

	Reference project 2	The tool	Difference [%]
Main beam, zone 1	0.3	0.316	+5.3
Main beam, zone 2	0.3	0.316	+5.3
Edge beams, zone 1	0.156	0.158	+1.3
Edge beams, zone 2	0.156	0.158	+1.3
Corner columns, y-direction	1.872	1.897	+1.3

E

Calculation data

E.1 Torsional Moment of Inertia

Figure E.1 shows an illustration of how the torsional moment of inertia, I_T, can be calculated based on the relationship between the height and width of a rectangular cross section.

Tabla 3.A3.1 Piezas solicitadas a torsión uniforme

Pieza de sección rectangular

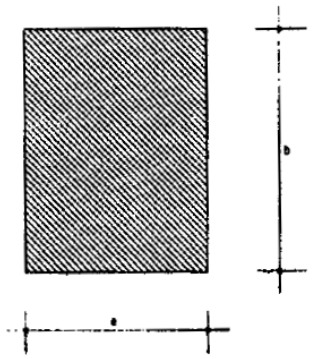

$$\tau^*_{max} = \frac{M^*_T}{W_T} = \frac{\theta_i G I_T}{W_T}$$

$I_T = \beta b e^3$

$W_T = \mu b e^2$

$$\tau^* = \frac{M^*_T}{W_T}$$

La τ^*_{max} se presenta en el centro del lado mayor. En el centro del lado menor, la τ^*_e tiene el valor

$$\tau^*_e = \tau^*_{max}\frac{e}{b}$$

β, μ = coeficientes
b = lado mayor
e = lado menor

m = b/e	μ	β
1.0	0.208	0.141
1.5	0.238	0.196
2.0	0.256	0.229
2.5	0.269	0.249
3.0	0.278	0.263
4.0	0.290	0.281
5.0	0.298	0.291
6.0	0.303	0.299
7.0	0.307	0.303
8.0	0.310	0.307
9.0	0.312	0.310
10.0	0.314	0.313
>10.0	0.333	0.333

Figure E.1: Data for calculation of torsional moment of inertia for a rectangular cross section.

The data from Figure E.1 was linearly interpolated to find values for the torsional moment of inertia for intermediate values of β.

F

Calculation Results FEM-design

In this appendix extracts of the calculation results from FEM-design can be found.

F.1 Main Beam - Constant Cross Section

B.1.1
Maximum of load combinations

GL 30c
(Glued laminated), Service class 1

$E_{0,05}$	=	10800 N/mm^2	$f_{t,90,k}$	=	0.50 N/mm^2
$G_{0,05}$	=	540 N/mm^2	$f_{c,0,k}$	=	24.50 N/mm^2
γ_M	=	1.25	$f_{c,90,k}$	=	2.50 N/mm^2
$\gamma_{M,acc./seis.}$	=	1.00	$f_{v,k}$	=	3.50 N/mm^2
k_{sys}	=	1.00			

Rectangle 190x1125

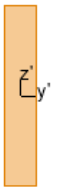

A	=	213750 mm^2	$f_{t,0,k}$	=	19.50 N/mm^2
W_1	=	4.008e+07 mm^3	$f_{m,1,k}$	=	30.00 N/mm^2
W_2	=	6.769e+06 mm^3	$f_{m,2,k}$	=	33.00 N/mm^2
i_1	=	325 mm			
i_2	=	55 mm			
I_2	=	6.430e+08 mm^4			
I_t	=	2.298e+09 mm^4			

Combined bending and axial tension - 6.2.3
Not relevant

Combined bending and axial compression - 6.1.4, 6.2.4
LC: 'ULS1', $k_{mod} = 0.90$, x = 8774.27 mm

$\sigma_{c,0,d} = 0.00$ N/mm^2 $\leq f_{c,0,d} = 17.64$ N/mm^2 (6.2) - OK

$$\left(\frac{\sigma_{c,0,d}}{f_{c,0,d}}\right)^2 + \frac{\sigma_{m,1,d}}{f_{m,1,d}} + k_m \frac{\sigma_{m,2,d}}{f_{m,2,d}} = \left(\frac{0.00}{17.64}\right)^2 + \frac{14.93}{21.60} + 0.70\,\frac{0.00}{23.76} = 0.69 \leq 1.00 \quad (6.19) - \text{OK}$$

$$\left(\frac{\sigma_{c,0,d}}{f_{c,0,d}}\right)^2 + k_m \frac{\sigma_{m,1,d}}{f_{m,1,d}} + \frac{\sigma_{m,2,d}}{f_{m,2,d}} = \left(\frac{0.00}{17.64}\right)^2 + 0.70\,\frac{14.93}{21.60} + \frac{0.00}{23.76} = 0.48 \leq 1.00 \quad (6.20) - \text{OK}$$

Combined shear and torsion - 6.1.7, 6.1.8
LC: 'ULS1', $k_{mod} = 0.90$, x = 0.00 mm

$\tau_d = 1.09$ N/mm^2 $\leq f_{v,d} = 2.52$ N/mm^2 (6.13) - OK

Flexural buckling around axis 1 - 6.3.2

LC: 'ULS1', $k_{mod} = 0.90$, $x = 8774.27$ mm

$\beta_c = 0.1$ (6.29)

$$\lambda_1 = \frac{l_0}{i_1} = \frac{18036}{325} = 55.54$$

$$\lambda_{rel,1} = \frac{\lambda_1}{\pi}\sqrt{\frac{f_{c,0,k}}{E_{0,05}}} = \frac{55.54}{\pi}\sqrt{\frac{24.50}{10800}} = 0.842 \quad (6.21)$$

$$k_1 = 0.5\left(1 + \beta_c\left(\lambda_{rel,1} - 0.3\right) + \lambda_{rel,1}^2\right) =$$
$$= 0.5\left(1 + 0.1\left(0.842 - 0.3\right) + 0.842^2\right) = 0.882 \quad (6.27)$$

$$k_{c,1} = \frac{1}{k_1 + \sqrt{k_1^2 - \lambda_{rel,1}^2}} = \frac{1}{0.882 + \sqrt{0.882^2 - 0.842^2}} = 0.875 \quad (6.25)$$

$$\frac{\sigma_{c,0,d}}{k_{c,1} \cdot f_{c,0,d}} + \frac{\sigma_{m,1,d}}{f_{m,1,d}} + k_m \cdot \frac{\sigma_{m,2,d}}{f_{m,2,d}} = \frac{0.00}{0.875 \cdot 17.64} + \frac{14.93}{21.60} + 0.70 \cdot \frac{0.00}{23.76} = 0.69 \le 1.00 \quad (6.23) \text{ - OK}$$

Flexural buckling around axis 2 - 6.3.2

LC: 'ULS1', $k_{mod} = 0.90$, $x = 8774.27$ mm

$\beta_c = 0.1$ (6.29)

$$\lambda_2 = \frac{l_0}{i_2} = \frac{18036}{55} = 328.83$$

$$\lambda_{rel,2} = \frac{\lambda_2}{\pi}\sqrt{\frac{f_{c,0,k}}{E_{0,05}}} = \frac{328.83}{\pi}\sqrt{\frac{24.50}{10800}} = 4.985 \quad (6.22)$$

$$k_2 = 0.5\left(1 + \beta_c\left(\lambda_{rel,2} - 0.3\right) + \lambda_{rel,2}^2\right) =$$
$$= 0.5\left(1 + 0.1\left(4.985 - 0.3\right) + 4.985^2\right) = 13.161 \quad (6.28)$$

$$k_{c,2} = \frac{1}{k_2 + \sqrt{k_2^2 - \lambda_{rel,2}^2}} = \frac{1}{13.161 + \sqrt{13.161^2 - 4.985^2}} = 0.039 \quad (6.26)$$

$$\frac{\sigma_{c,0,d}}{k_{c,2} \cdot f_{c,0,d}} + k_m \cdot \frac{\sigma_{m,1,d}}{f_{m,1,d}} + \frac{\sigma_{m,2,d}}{f_{m,2,d}} = \frac{0.00}{0.039 \cdot 17.64} + 0.70 \cdot \frac{14.93}{21.60} + \frac{0.00}{23.76} = 0.48 \le 1.00 \quad (6.24) \text{ - OK}$$

Lateral torsional buckling - 6.3.3

Not relevant

Bending at apex - 6.4.3

Not relevant

Tension at apex - 6.4.3

Not relevant

F.2 Main Beam - Tapered

B.2.1
Maximum of load combinations

GL 30c
(Glued laminated), Service class 1

$E_{0,05}$	=	10800 N/mm^2	$f_{t,90,k}$	=	0.50 N/mm^2
$G_{0,05}$	=	540 N/mm^2	$f_{c,0,k}$	=	24.50 N/mm^2
γ_M	=	1.25	$f_{c,90,k}$	=	2.50 N/mm^2
$\gamma_{M,acc./seis.}$	=	1.00	$f_{v,k}$	=	3.50 N/mm^2
k_{sys}	=	1.00			

Sections of relevant verifications
x = 0 mm, Rectangle 215x810

A	=	174150 mm^2	$f_{t,0,k}$	=	19.50 N/mm^2
W_1	=	2.351e+07 mm^3	$f_{m,1,k}$	=	30.00 N/mm^2
W_2	=	6.240e+06 mm^3	$f_{m,2,k}$	=	33.00 N/mm^2
i_1	=	234 mm			
i_2	=	62 mm			
I_2	=	6.708e+08 mm^4			
I_t	=	2.234e+09 mm^4			

x = 6000 mm, Intermediate 1

A	=	228187 mm^2	$f_{t,0,k}$	=	19.50 N/mm^2
W_1	=	4.036e+07 mm^3	$f_{m,1,k}$	=	30.00 N/mm^2
W_2	=	8.177e+06 mm^3	$f_{m,2,k}$	=	33.00 N/mm^2
i_1	=	306 mm			
i_2	=	62 mm			
I_2	=	8.790e+08 mm^4			
I_t	=	3.067e+09 mm^4			

Combined bending and axial tension - 6.2.3
LC: 'ULS', k_{mod} = 0.90, x = 6000.00 mm
α = 0.02 rad

$$k_{m,\alpha} = 1 / \sqrt{1 + \left(\frac{f_{m,1,d}}{0.75 \cdot f_{v,d}} \tan(\alpha)\right)^2 + \left(\frac{f_{m,1,d}}{f_{t,90,d}} \tan^2(\alpha)\right)^2} =$$

$$= 1 / \sqrt{1 + \left(\frac{21.60}{0.75 \cdot 2.52} \tan(0.02)\right)^2 + \left(\frac{21.60}{0.36} \tan^2(0.02)\right)^2} = 0.97 \quad (6.39)$$

$$\frac{\sigma_{t,0,d}}{f_{t,0,d}} + \frac{\sigma_{m,1,d}}{k_{m,\alpha} \cdot f_{m,1,d}} + k_m \frac{\sigma_{m,2,d}}{f_{m,2,d}} = \frac{0.00}{14.04} + \frac{14.17}{0.97 \cdot 21.60} + 0.70 \frac{0.00}{23.76} = 0.67 \leq 1.00 \quad (6.17) \text{ - OK}$$

$$\frac{\sigma_{t,0,d}}{f_{t,0,d}} + k_m \frac{\sigma_{m,1,d}}{k_{m,\alpha} \cdot f_{m,1,d}} + \frac{\sigma_{m,2,d}}{f_{m,2,d}} = \frac{0.00}{14.04} + 0.70 \frac{14.17}{0.97 \cdot 21.60} + \frac{0.00}{23.76} = 0.47 \leq 1.00 \quad (6.18) \text{ - OK}$$

Combined bending and axial compression - 6.1.4, 6.2.4

LC: "ULS", $k_{mod} = 0.90$, $x = 0.00$ mm

$\alpha = 0.02$ rad

$$k_{m,\alpha} = 1 / \sqrt{1 + \left(\frac{f_{m,1,d}}{1.50 \cdot f_{v,d}} \tan(\alpha) \right)^2 + \left(\frac{f_{m,1,d}}{f_{c,90,d}} \tan^2(\alpha) \right)^2} =$$

$$= 1 / \sqrt{1 + \left(\frac{21.60}{1.50 \cdot 2.52} \tan(0.02) \right)^2 + \left(\frac{21.60}{1.80} \tan^2(0.02) \right)^2} = 0.99 \quad (6.40)$$

$\sigma_{c,0,d} = 0.00$ N/mm^2 $\leq f_{c,0,d} = 17.64$ N/mm^2 (6.2) - OK

$$\left(\frac{\sigma_{c,0,d}}{f_{c,0,d}} \right)^2 + \frac{\sigma_{m,1,d}}{k_{m,\alpha} \cdot f_{m,1,d}} + k_m \frac{\sigma_{m,2,d}}{f_{m,2,d}} =$$

$$= \left(\frac{0.00}{17.64} \right)^2 + \frac{0.00}{0.99 \cdot 21.60} + 0.70 \frac{0.00}{23.76} = 0.00 \leq 1.00 \quad (6.19) - OK$$

$$\left(\frac{\sigma_{c,0,d}}{f_{c,0,d}} \right)^2 + k_m \frac{\sigma_{m,1,d}}{k_{m,\alpha} \cdot f_{m,1,d}} + \frac{\sigma_{m,2,d}}{f_{m,2,d}} =$$

$$= \left(\frac{0.00}{17.64} \right)^2 + 0.70 \frac{0.00}{0.99 \cdot 21.60} + \frac{0.00}{23.76} = 0.00 \leq 1.00 \quad (6.20) - OK$$

Combined shear and torsion - 6.1.7, 6.1.8

LC: "ULS", $k_{mod} = 0.90$, $x = 0.00$ mm

$\tau_d = 1.44$ N/mm^2 $\leq f_{v,d} = 2.52$ N/mm^2 (6.13) - OK

Flexural buckling around axis 1 - 6.3.2

LC: 'ULS', $k_{mod} = 0.90$, $x = 0.00$ mm

$\beta_c = 0.1$ (6.29)

$$\lambda_1 = \frac{l_0}{i^*_1} = \frac{9000}{288} = 31.22$$

$$\lambda_{rel,1} = \frac{\lambda_1}{\pi}\sqrt{\frac{f_{c,0,k}}{E_{0,05}}} = \frac{31.22}{\pi}\sqrt{\frac{24.50}{10800}} = 0.473 \quad (6.21)$$

$$k_1 = 0.5\left(1 + \beta_c\left(\lambda_{rel,1} - 0.3\right) + \lambda_{rel,1}{}^2\right) =$$

$$= 0.5\left(1 + 0.1\left(0.473 - 0.3\right) + 0.473^2\right) = 0.621 \quad (6.27)$$

$$k_{c,1} = \frac{1}{k_1 + \sqrt{k_1{}^2 - \lambda_{rel,1}{}^2}} = \frac{1}{0.621 + \sqrt{0.621^2 - 0.473^2}} = 0.978 \quad (6.25)$$

$\alpha = 0.02$ rad

$$k_{m,\alpha} = 1 / \sqrt{1 + \left(\frac{f_{m,1,d}}{1.50 \cdot f_{v,d}}\tan(\alpha)\right)^2 + \left(\frac{f_{m,1,d}}{f_{c,90,d}}\tan^2(\alpha)\right)^2} =$$

$$= 1 / \sqrt{1 + \left(\frac{21.60}{1.50 \cdot 2.52}\tan(0.02)\right)^2 + \left(\frac{21.60}{1.80}\tan^2(0.02)\right)^2} = 0.99 \quad (6.40)$$

$$\frac{\sigma_{c,0,d}}{k_{c,1} \cdot f_{c,0,d}} + \frac{\sigma_{m,1,d}}{k_{m,\alpha} \cdot f_{m,1,d}} + k_m \cdot \frac{\sigma_{m,2,d}}{f_{m,2,d}} =$$

$$= \frac{0.00}{0.978 \cdot 17.64} + \frac{0.00}{0.99 \cdot 21.60} + 0.70 \cdot \frac{0.00}{23.76} = 0.00 \leq 1.00 \quad (6.23) \text{ - OK}$$

F.3 Edge Beams

B.1.1
Maximum of load combinations

GL 28c
(Glued laminated), Service class 1

$E_{0,05}$	=	10400 N/mm^2	$f_{t,90,k}$	=	0.50 N/mm^2
$G_{0,05}$	=	540 N/mm^2	$f_{c,0,k}$	=	24.00 N/mm^2
γ_M	=	1.25	$f_{c,90,k}$	=	2.50 N/mm^2
$\gamma_{M,acc./seis.}$	=	1.00	$f_{v,k}$	=	3.50 N/mm^2
k_{sys}	=	1.00			

Rectangle 66X450

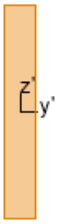

A	=	29700 mm^2	$f_{t,0,k}$	=	20.07 N/mm^2
W_1	=	2.227e+06 mm^3	$f_{m,1,k}$	=	28.82 N/mm^2
W_2	=	3.267e+05 mm^3	$f_{m,2,k}$	=	30.80 N/mm^2
i_1	=	130 mm			
i_2	=	19 mm			
I_2	=	1.078e+07 mm^4			
I_t	=	3.914e+07 mm^4			

Combined bending and axial tension - 6.2.3
Not relevant

Combined bending and axial compression - 6.1.4, 6.2.4
LC: 'ULS_up_90', k_{mod} = 0.90, x = 2774.77 mm

$\sigma_{c,0,d}$ = 0.00 N/mm^2 ≤ $f_{c,0,d}$ = 17.28 N/mm^2 (6.2) - OK

$$\left(\frac{\sigma_{c,0,d}}{f_{c,0,d}}\right)^2 + \frac{\sigma_{m,1,d}}{f_{m,1,d}} + k_m \frac{\sigma_{m,2,d}}{f_{m,2,d}} = \left(\frac{0.00}{17.28}\right)^2 + \frac{15.84}{20.75} + 0.70\,\frac{0.00}{22.18} = 0.76 \le 1.00 \quad (6.19) - OK$$

$$\left(\frac{\sigma_{c,0,d}}{f_{c,0,d}}\right)^2 + k_m \frac{\sigma_{m,1,d}}{f_{m,1,d}} + \frac{\sigma_{m,2,d}}{f_{m,2,d}} = \left(\frac{0.00}{17.28}\right)^2 + 0.70\,\frac{15.84}{20.75} + \frac{0.00}{22.18} = 0.53 \le 1.00 \quad (6.20) - OK$$

Combined shear and torsion - 6.1.7, 6.1.8
LC: 'ULS_up_90', k_{mod} = 0.90, x = 0.00 mm

τ_d = 1.46 N/mm^2 ≤ $f_{v,d}$ = 2.52 N/mm^2 (6.13) - OK

Flexural buckling around axis 1 - 6.3.2

LC: 'ULS_up_90', $k_{mod} = 0.90$, x = 2774.77 mm

$\beta_c = 0.1$ (6.29)

$$\lambda_1 = \frac{l_0}{i_1} = \frac{6012}{130} = 46.28$$

$$\lambda_{rel,1} = \frac{\lambda_1}{\pi}\sqrt{\frac{f_{c,0,k}}{E_{0,05}}} = \frac{46.28}{\pi}\sqrt{\frac{24.00}{10400}} = 0.708 \quad (6.21)$$

$$k_1 = 0.5\left(1 + \beta_c\left(\lambda_{rel,1} - 0.3\right) + \lambda_{rel,1}^2\right) =$$
$$= 0.5\left(1 + 0.1\left(0.708 - 0.3\right) + 0.708^2\right) = 0.771 \quad (6.27)$$

$$k_{c,1} = \frac{1}{k_1 + \sqrt{k_1^2 - \lambda_{rel,1}^2}} = \frac{1}{0.771 + \sqrt{0.771^2 - 0.708^2}} = 0.929 \quad (6.25)$$

$$\frac{\sigma_{c,0,d}}{k_{c,1} \cdot f_{c,0,d}} + \frac{\sigma_{m,1,d}}{f_{m,1,d}} + k_m \cdot \frac{\sigma_{m,2,d}}{f_{m,2,d}} = \frac{0.00}{0.929 \cdot 17.28} + \frac{15.84}{20.75} + 0.70 \cdot \frac{0.00}{22.18} = 0.76 \leq 1.00 \quad (6.23) \text{ - OK}$$

Flexural buckling around axis 2 - 6.3.2

LC: 'ULS_up_90', $k_{mod} = 0.90$, x = 2774.77 mm

$\beta_c = 0.1$ (6.29)

$$\lambda_2 = \frac{l_0}{i_2} = \frac{6012}{19} = 315.55$$

$$\lambda_{rel,2} = \frac{\lambda_2}{\pi}\sqrt{\frac{f_{c,0,k}}{E_{0,05}}} = \frac{315.55}{\pi}\sqrt{\frac{24.00}{10400}} = 4.825 \quad (6.22)$$

$$k_2 = 0.5\left(1 + \beta_c\left(\lambda_{rel,2} - 0.3\right) + \lambda_{rel,2}^2\right) =$$
$$= 0.5\left(1 + 0.1\left(4.825 - 0.3\right) + 4.825^2\right) = 12.367 \quad (6.28)$$

$$k_{c,2} = \frac{1}{k_2 + \sqrt{k_2^2 - \lambda_{rel,2}^2}} = \frac{1}{12.367 + \sqrt{12.367^2 - 4.825^2}} = 0.042 \quad (6.26)$$

$$\frac{\sigma_{c,0,d}}{k_{c,2} \cdot f_{c,0,d}} + k_m \cdot \frac{\sigma_{m,1,d}}{f_{m,1,d}} + \frac{\sigma_{m,2,d}}{f_{m,2,d}} = \frac{0.00}{0.042 \cdot 17.28} + 0.70 \cdot \frac{15.84}{20.75} + \frac{0.00}{22.18} = 0.53 \leq 1.00 \quad (6.24) \text{ - OK}$$

Lateral torsional buckling - 6.3.3

Not relevant

Bending at apex - 6.4.3

Not relevant

Tension at apex - 6.4.3

Not relevant

F.4 Main Columns

C.1.1
Maximum of load combinations

GL 30c
(Glued laminated), Service class 1

$E_{0,05}$	= 10800 N/mm²		$f_{t,90,k}$	= 0.50 N/mm²
$G_{0,05}$	= 540 N/mm²		$f_{c,0,k}$	= 24.50 N/mm²
γ_M	= 1.25		$f_{c,90,k}$	= 2.50 N/mm²
$\gamma_{M,acc./seis.}$	= 1.00		$f_{v,k}$	= 3.50 N/mm²
k_{sys}	= 1.00			

Glulam 190x405

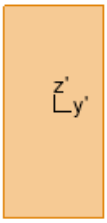

A	= 76950 mm²		$f_{t,0,k}$	= 20.28 N/mm²
W_1	= 5.194e+06 mm³		$f_{m,1,k}$	= 31.20 N/mm²
W_2	= 2.437e+06 mm³		$f_{m,2,k}$	= 33.00 N/mm²
i_1	= 117 mm			
i_2	= 55 mm			
I_2	= 2.315e+08 mm⁴			
I_t	= 6.529e+08 mm⁴			

Combined bending and axial tension - 6.2.3
Not relevant

Combined bending and axial compression - 6.1.4, 6.2.4
LC: 'ULS2', k_{mod} = 0.90, x = 3802.67 mm

$\sigma_{c,0,d} = 1.49 \text{ N/mm}^2 \le f_{c,0,d} = 17.64 \text{ N/mm}^2$ (6.2) - OK

$$\left(\frac{\sigma_{c,0,d}}{f_{c,0,d}}\right)^2 + \frac{\sigma_{m,1,d}}{f_{m,1,d}} + k_m \frac{\sigma_{m,2,d}}{f_{m,2,d}} = \left(\frac{1.49}{17.64}\right)^2 + \frac{11.74}{22.47} + 0.70\,\frac{0.00}{23.76} = 0.53 \le 1.00 \quad (6.19) \text{ - OK}$$

$$\left(\frac{\sigma_{c,0,d}}{f_{c,0,d}}\right)^2 + k_m \frac{\sigma_{m,1,d}}{f_{m,1,d}} + \frac{\sigma_{m,2,d}}{f_{m,2,d}} = \left(\frac{1.49}{17.64}\right)^2 + 0.70\,\frac{11.74}{22.47} + \frac{0.00}{23.76} = 0.37 \le 1.00 \quad (6.20) \text{ - OK}$$

Combined shear and torsion - 6.1.7, 6.1.8
LC: 'ULS2', k_{mod} = 0.90, x = 7130.00 mm

$\tau_d = 0.78 \text{ N/mm}^2 \le f_{v,d} = 2.52 \text{ N/mm}^2$ (6.13) - OK

Flexural buckling around axis 1 - 6.3.2

LC: 'ULS2', $k_{mod} = 0.90$, $x = 3802.67$ mm

$\beta_c = 0.1$ (6.29)

$$\lambda_1 = \frac{l_0}{i_1} = \frac{7130}{117} = 60.99$$

$$\lambda_{rel,1} = \frac{\lambda_1}{\pi}\sqrt{\frac{f_{c,0,k}}{E_{0,05}}} = \frac{60.99}{\pi}\sqrt{\frac{24.50}{10800}} = 0.925 \quad (6.21)$$

$$k_1 = 0.5\left(1 + \beta_c\left(\lambda_{rel,1} - 0.3\right) + \lambda_{rel,1}{}^2\right) =$$
$$= 0.5\left(1 + 0.1\left(0.925 - 0.3\right) + 0.925^2\right) = 0.959 \quad (6.27)$$

$$k_{c,1} = \frac{1}{k_1 + \sqrt{k_1{}^2 - \lambda_{rel,1}{}^2}} = \frac{1}{0.959 + \sqrt{0.959^2 - 0.925^2}} = 0.825 \quad (6.25)$$

$$\frac{\sigma_{c,0,d}}{k_{c,1} \cdot f_{c,0,d}} + \frac{\sigma_{m,1,d}}{f_{m,1,d}} + k_m \cdot \frac{\sigma_{m,2,d}}{f_{m,2,d}} = \frac{1.49}{0.825 \cdot 17.64} + \frac{11.74}{22.47} + 0.70 \cdot \frac{0.00}{23.76} = 0.62 \le 1.00 \quad (6.23) \text{ - OK}$$

Flexural buckling around axis 2 - 6.3.2

LC: 'ULS2', $k_{mod} = 0.90$, $x = 3802.67$ mm

$\beta_c = 0.1$ (6.29)

$$\lambda_2 = \frac{l_0}{i_2} = \frac{7130}{55} = 129.99$$

$$\lambda_{rel,2} = \frac{\lambda_2}{\pi}\sqrt{\frac{f_{c,0,k}}{E_{0,05}}} = \frac{129.99}{\pi}\sqrt{\frac{24.50}{10800}} = 1.971 \quad (6.22)$$

$$k_2 = 0.5\left(1 + \beta_c\left(\lambda_{rel,2} - 0.3\right) + \lambda_{rel,2}{}^2\right) =$$
$$= 0.5\left(1 + 0.1\left(1.971 - 0.3\right) + 1.971^2\right) = 2.526 \quad (6.28)$$

$$k_{c,2} = \frac{1}{k_2 + \sqrt{k_2{}^2 - \lambda_{rel,2}{}^2}} = \frac{1}{2.526 + \sqrt{2.526^2 - 1.971^2}} = 0.244 \quad (6.26)$$

$$\frac{\sigma_{c,0,d}}{k_{c,2} \cdot f_{c,0,d}} + k_m \cdot \frac{\sigma_{m,1,d}}{f_{m,1,d}} + \frac{\sigma_{m,2,d}}{f_{m,2,d}} = \frac{1.49}{0.244 \cdot 17.64} + 0.70 \cdot \frac{11.74}{22.47} + \frac{0.00}{23.76} = 0.71 \le 1.00 \quad (6.24) \text{ - OK}$$

F.5 Gable Columns

C.1.1
Maximum of load combinations

GL 30c
(Glued laminated), Service class 1

$E_{0,05}$	=	10800 N/mm^2	$f_{t,90,k}$	=	0.50 N/mm^2
$G_{0,05}$	=	540 N/mm^2	$f_{c,0,k}$	=	24.50 N/mm^2
γ_M	=	1.25	$f_{c,90,k}$	=	2.50 N/mm^2
$\gamma_{M,acc./seis.}$	=	1.00	$f_{v,k}$	=	3.50 N/mm^2
k_{sys}	=	1.00			

Glulam 165x405

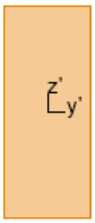

A	=	66825 mm^2	$f_{t,0,k}$	=	20.28 N/mm^2
W_1	=	4.511e+06 mm^3	$f_{m,1,k}$	=	31.20 N/mm^2
W_2	=	1.838e+06 mm^3	$f_{m,2,k}$	=	33.00 N/mm^2
i_1	=	117 mm			
i_2	=	48 mm			
I_2	=	1.516e+08 mm^4			
I_t	=	4.509e+08 mm^4			

Combined bending and axial tension - 6.2.3
Not relevant

Combined bending and axial compression - 6.1.4, 6.2.4
LC: 'ULS2', k_{mod} = 0.90, x = 3900.00 mm

$\sigma_{c,0,d} = 0.56$ N/mm^2 $\leq f_{c,0,d} = 17.64$ N/mm^2 (6.2) - OK

$$\left(\frac{\sigma_{c,0,d}}{f_{c,0,d}}\right)^2 + \frac{\sigma_{m,1,d}}{f_{m,1,d}} + k_m \frac{\sigma_{m,2,d}}{f_{m,2,d}} = \left(\frac{0.56}{17.64}\right)^2 + \frac{16.25}{22.47} + 0.70\,\frac{0.00}{23.76} = 0.72 \leq 1.00 \quad \text{(6.19) - OK}$$

$$\left(\frac{\sigma_{c,0,d}}{f_{c,0,d}}\right)^2 + k_m \frac{\sigma_{m,1,d}}{f_{m,1,d}} + \frac{\sigma_{m,2,d}}{f_{m,2,d}} = \left(\frac{0.56}{17.64}\right)^2 + 0.70\,\frac{16.25}{22.47} + \frac{0.00}{23.76} = 0.51 \leq 1.00 \quad \text{(6.20) - OK}$$

Combined shear and torsion - 6.1.7, 6.1.8
LC: 'ULS2', k_{mod} = 0.90, x = 0.00 mm

$\tau_d = 0.98$ N/mm^2 $\leq f_{v,d} = 2.52$ N/mm^2 (6.13) - OK

Flexural buckling around axis 1 - 6.3.2

LC: 'ULS2', $k_{mod} = 0.90$, $x = 3900.00$ mm

$\beta_c = 0.1$ (6.29)

$$\lambda_1 = \frac{l_0}{i_1} = \frac{7800}{117} = 66.72$$

$$\lambda_{rel,1} = \frac{\lambda_1}{\pi}\sqrt{\frac{f_{c,0,k}}{E_{0,05}}} = \frac{66.72}{\pi}\sqrt{\frac{24.50}{10800}} = 1.011 \quad (6.21)$$

$$k_1 = 0.5\left(1 + \beta_c\left(\lambda_{rel,1} - 0.3\right) + \lambda_{rel,1}^2\right) =$$
$$= 0.5\left(1 + 0.1\left(1.011 - 0.3\right) + 1.011^2\right) = 1.047 \quad (6.27)$$

$$k_{c,1} = \frac{1}{k_1 + \sqrt{k_1^2 - \lambda_{rel,1}^2}} = \frac{1}{1.047 + \sqrt{1.047^2 - 1.011^2}} = 0.759 \quad (6.25)$$

$$\frac{\sigma_{c,0,d}}{k_{c,1} \cdot f_{c,0,d}} + \frac{\sigma_{m,1,d}}{f_{m,1,d}} + k_m \cdot \frac{\sigma_{m,2,d}}{f_{m,2,d}} = \frac{0.56}{0.759 \cdot 17.64} + \frac{16.25}{22.47} + 0.70 \cdot \frac{0.00}{23.76} = 0.77 \leq 1.00 \quad (6.23) \text{ - OK}$$

Flexural buckling around axis 2 - 6.3.2

LC: 'ULS2', $k_{mod} = 0.90$, $x = 3900.00$ mm

$\beta_c = 0.1$ (6.29)

$$\lambda_2 = \frac{l_0}{i_2} = \frac{7800}{48} = 163.76$$

$$\lambda_{rel,2} = \frac{\lambda_2}{\pi}\sqrt{\frac{f_{c,0,k}}{E_{0,05}}} = \frac{163.76}{\pi}\sqrt{\frac{24.50}{10800}} = 2.483 \quad (6.22)$$

$$k_2 = 0.5\left(1 + \beta_c\left(\lambda_{rel,2} - 0.3\right) + \lambda_{rel,2}^2\right) =$$
$$= 0.5\left(1 + 0.1\left(2.483 - 0.3\right) + 2.483^2\right) = 3.691 \quad (6.28)$$

$$k_{c,2} = \frac{1}{k_2 + \sqrt{k_2^2 - \lambda_{rel,2}^2}} = \frac{1}{3.691 + \sqrt{3.691^2 - 2.483^2}} = 0.156 \quad (6.26)$$

$$\frac{\sigma_{c,0,d}}{k_{c,2} \cdot f_{c,0,d}} + k_m \cdot \frac{\sigma_{m,1,d}}{f_{m,1,d}} + \frac{\sigma_{m,2,d}}{f_{m,2,d}} = \frac{0.56}{0.156 \cdot 17.64} + 0.70 \cdot \frac{16.25}{22.47} + \frac{0.00}{23.76} = 0.71 \leq 1.00 \quad (6.24) \text{ - OK}$$

F.6 Corner Columns

C.1.1
Maximum of load combinations

GL 30c
(Glued laminated), Service class 1

$E_{0,05}$	= 10800 N/mm^2		$f_{t,90,k}$	= 0.50 N/mm^2
$G_{0,05}$	= 540 N/mm^2		$f_{c,0,k}$	= 24.50 N/mm^2
γ_M	= 1.25		$f_{c,90,k}$	= 2.50 N/mm^2
$\gamma_{M,acc./seis.}$	= 1.00		$f_{v,k}$	= 3.50 N/mm^2
k_{sys}	= 1.00			

Glulam 215x495

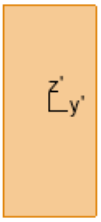

A	= 106425 mm^2		$f_{t,0,k}$	= 19.88 N/mm^2
W_1	= 8.780e+06 mm^3		$f_{m,1,k}$	= 30.58 N/mm^2
W_2	= 3.814e+06 mm^3		$f_{m,2,k}$	= 33.00 N/mm^2
i_1	= 143 mm			
i_2	= 62 mm			
I_2	= 4.100e+08 mm^4			
I_t	= 1.192e+09 mm^4			

Combined bending and axial tension - 6.2.3
Not relevant

Combined bending and axial compression - 6.1.4, 6.2.4
LC: 'ULS2_90', k_{mod} = 0.90, x = 3993.50 mm

$\sigma_{c,0,d} = 0.20$ N/mm^2 $\leq f_{c,0,d} = 17.64$ N/mm^2 (6.2) - OK

$$\left(\frac{\sigma_{c,0,d}}{f_{c,0,d}}\right)^2 + \frac{\sigma_{m,1,d}}{f_{m,1,d}} + k_m \frac{\sigma_{m,2,d}}{f_{m,2,d}} = \left(\frac{0.20}{17.64}\right)^2 + \frac{4.46}{22.02} + 0.70\,\frac{14.10}{23.76} = 0.62 \leq 1.00 \quad (6.19) \text{ - OK}$$

$$\left(\frac{\sigma_{c,0,d}}{f_{c,0,d}}\right)^2 + k_m \frac{\sigma_{m,1,d}}{f_{m,1,d}} + \frac{\sigma_{m,2,d}}{f_{m,2,d}} = \left(\frac{0.20}{17.64}\right)^2 + 0.70\,\frac{4.46}{22.02} + \frac{14.10}{23.76} = 0.74 \leq 1.00 \quad (6.20) \text{ - OK}$$

Combined shear and torsion - 6.1.7, 6.1.8
LC: 'ULS2_0', k_{mod} = 0.90, x = 7987.00 mm

$\tau_d = 0.55$ N/mm^2 $\leq f_{v,d} = 2.52$ N/mm^2 (6.13) - OK

Flexural buckling around axis 1 - 6.3.2

LC: 'ULS2_90', $k_{mod} = 0.90$, $x = 3993.50$ mm

$\beta_c = 0.1$ (6.29)

$$\lambda_1 = \frac{l_0}{i_1} = \frac{7987}{143} = 55.89$$

$$\lambda_{rel,1} = \frac{\lambda_1}{\pi}\sqrt{\frac{f_{c,0,k}}{E_{0,05}}} = \frac{55.89}{\pi}\sqrt{\frac{24.50}{10800}} = 0.847 \quad (6.21)$$

$$k_1 = 0.5\left(1 + \beta_c\left(\lambda_{rel,1} - 0.3\right) + \lambda_{rel,1}^{\ 2}\right) =$$
$$= 0.5\left(1 + 0.1\left(0.847 - 0.3\right) + 0.847^2\right) = 0.886 \quad (6.27)$$

$$k_{c,1} = \frac{1}{k_1 + \sqrt{k_1^{\ 2} - \lambda_{rel,1}^{\ 2}}} = \frac{1}{0.886 + \sqrt{0.886^2 - 0.847^2}} = 0.872 \quad (6.25)$$

$$\frac{\sigma_{c,0,d}}{k_{c,1} \cdot f_{c,0,d}} + \frac{\sigma_{m,1,d}}{f_{m,1,d}} + k_m \cdot \frac{\sigma_{m,2,d}}{f_{m,2,d}} = \frac{0.20}{0.872 \cdot 17.64} + \frac{4.46}{22.02} + 0.70 \cdot \frac{14.10}{23.76} = 0.63 \le 1.00 \quad (6.23) \text{ - OK}$$

Flexural buckling around axis 2 - 6.3.2

LC: 'ULS2_90', $k_{mod} = 0.90$, $x = 3993.50$ mm

$\beta_c = 0.1$ (6.29)

$$\lambda_2 = \frac{l_0}{i_2} = \frac{7987}{62} = 128.69$$

$$\lambda_{rel,2} = \frac{\lambda_2}{\pi}\sqrt{\frac{f_{c,0,k}}{E_{0,05}}} = \frac{128.69}{\pi}\sqrt{\frac{24.50}{10800}} = 1.951 \quad (6.22)$$

$$k_2 = 0.5\left(1 + \beta_c\left(\lambda_{rel,2} - 0.3\right) + \lambda_{rel,2}^{\ 2}\right) =$$
$$= 0.5\left(1 + 0.1\left(1.951 - 0.3\right) + 1.951^2\right) = 2.486 \quad (6.28)$$

$$k_{c,2} = \frac{1}{k_2 + \sqrt{k_2^{\ 2} - \lambda_{rel,2}^{\ 2}}} = \frac{1}{2.486 + \sqrt{2.486^2 - 1.951^2}} = 0.248 \quad (6.26)$$

$$\frac{\sigma_{c,0,d}}{k_{c,2} \cdot f_{c,0,d}} + k_m \cdot \frac{\sigma_{m,1,d}}{f_{m,1,d}} + \frac{\sigma_{m,2,d}}{f_{m,2,d}} = \frac{0.20}{0.248 \cdot 17.64} + 0.70 \cdot \frac{4.46}{22.02} + \frac{14.10}{23.76} = 0.78 \le 1.00 \quad (6.24) \text{ - OK}$$

Lateral torsional buckling - 6.3.3

Not relevant

Bending at apex - 6.4.3

Not relevant

Tension at apex - 6.4.3

Not relevant

DEPARTMENT OF ARCHITECTURE AND CIVIL ENGINEERING
CHALMERS UNIVERSITY OF TECHNOLOGY
Gothenburg, Sweden
www.chalmers.se

CHALMERS
UNIVERSITY OF TECHNOLOGY